THIXOFORGING OF ALUMINUM NANO-COMPOSITES SYNTHESIZED BY ULTRASONIC STIR CASTING

BY

MOHAMMED ABDUL AZEEM

A Thesis Presented to the
DEANSHIP OF GRADUATE STUDIES

KING FAHD UNIVERSITY OF PETROLEUM & MINERALS

DHAHRAN, SAUDI ARABIA

In Partial Fulfillment of the
Requirements for the Degree of

MASTER OF SCIENCE

In

MECHANICAL ENGINEERING

December 2013

KING FAHD UNIVERSITY OF PETROLEUM & MINERALS

DHAHRAN- 31261, SAUDI ARABIA

DEANSHIP OF GRADUATE STUDIES

This thesis, written by **MOHAMMED ABDUL AZEEM** under the direction of his thesis advisor and approved by his thesis committee, has been presented and accepted by the Dean of Graduate Studies, in partial fulfillment of the requirements for the degree of **MASTER OF SCIENCE IN MECHANICAL ENGINEERING.**

(Thesis Committee)

Dr. Numan Abu-Dheir
(Advisor)

Dr. Zuhair Gasem
Department Chairman

Dr. AbdelRahman N. Shuaib
(Member)

Dr. Salam A. Zummo
Dean of Graduate Studies

Dr. Shafique Khan
(Member)

29/1/14
Date

DEDICATION

Dedicated to my beloved Mother, Father, Brother and Sister

ACKNOWLEDGEMENTS

All praise and thanks are due to ALLAH subhanahu wa ta'ala for giving me knowledge and perseverance to complete this thesis. I am thankful to King Fahd University of Petroleum and Minerals (KFUPM) for providing me the support to pursue my graduate studies. I also acknowledge the funding provided by National Science Technology and Innovation Plan (NSTIP) for this research.

My sincere gratitude goes to my advisor Dr. Numan Abu-Dheir for his valuable guidance and constant support, especially in procuring necessary equipment that paved the way for successful completion of this research. I am also grateful to my thesis committee Dr. Shafique Khan and Dr. AbdelRahman Shuaib for their attention and expertise in evaluating this research.

Special thanks to the Mechanical Engineering Department, technical staff in ME Workshop and Material Science Laboratory for their assistance. Equally thankful to my friends at KFUPM for their encouragement and cherishing memories.

Finally, I am extremely thankful to my parents, brother and sister for their prayers, endless support and affection during my study away from home.

TABLE OF CONTENTS

LIST OF TABLES

LIST OF FIGURES

LIST OF ABBREVIATIONS

Al	Aluminum
MMCs	Metal Matrix Composites
SSM	Semi Solid Metal
SiC	Silicon Carbide
SEM	Scanning Electron Microscope
EDS	Energy Dispersive Spectroscopy
MPa	Mega Pascal
Hv	Vickers Hardness
Mins.	Minutes
wt. %	Weight Percentage
UTS	Ultimate Tensile Strength
f_s	Solid Fraction
EDX	Energy Dispersive X-ray

ABSTRACT

Full Name : Mohammed Abdul Azeem

Thesis Title : Thixoforging of Aluminum Nano-composites Synthesized by Ultrasonic Stir Casting

Major Field : Mechanical Engineering

Date of Degree : December 2013

Metal matrix composites reinforced with nanoparticles have shown great potential due to their excellent physical and mechanical properties. However incorporation of these composites in forming complex engineering parts is a great challenge. Thixoforging is an attractive technique where metal is deformed at a semi-solid temperature corresponding to higher solid fraction. Due to its inherited advantages like lesser forming load with increase in die life and reduction in forming steps, thixoforging is widely used in making complex parts of automobile and electronic industries mainly from aluminum alloys. Applying this technique to metal matrix composites provide additional advantages like improved mechanical behavior and better forming capabilities. The aim of this research is to develop aluminum based nanocomposite and subsequently thixoforged it to a required shape. In order to achieve this, aluminum alloy (A356) reinforced with SiC nanoparticles was stir casted using ultrasonic treatment as a feed stock material for thixoforging operation. The composite obtained after casting was uniformly heated using induction heating device and quickly transported to forging press for thixoforging operation at two different solid fraction of 60% and 50% using reheating holding time of 1 and 2 minutes. Different concentration of SiC was used to characterize the microstructure and mechanical properties of the composite. The microstructure characterization was carried out using optical micrograph, scanning electron microscopy (SEM) associated with energy dispersive x-ray analysis (EDX) and mechanical behavior was studied using hardness and tensile testing measurements. The results revealed that addition of SiC particles aided in refining the solidifying microstructure. Good distribution of reinforcement and better mechanical properties were observed in stir cast samples treated with 80W/cm^2 ultrasonic intensity. The microstructure changed from non-dendritic rosette to near globular morphology after induction heating. Better reheating conditions were obtained with using intermediate power of induction with holding time of 2 minutes. The microstructure of thixoforged nanocomposite showed more SiC particles agglomerated away from the center of the thixoforged part. The hardness of the nanocomposite increased with increase in amount of SiC content. Increase in ductility of nanocomposite was observed after thixoforging operation. Thixoforging at solid fraction of 50% gave complete die filling, high densification, high hardness and better tensile results.

ملخص الرسالة

الاسم الكامل: محمد عبدالعظيم
عنوان الرسالة: THIXOFORGING لسبائك الالومنيوم المؤلفه متناهية الصغر مصنعة بواسطة عملية الصب التقليبى بموجات فوق صوتية
التخصص: الهندسة الميكانيكية
تاريخ الدرجة العلمية: ديسمبر ٢٠١٣

اظهرت المواد المؤلفه بمصفوفة من المركبات معدنية معززة بجسيمات متناهية الصغر اهميه لما لها من خصائص فيزيائية وكيميائية عالية .ان دمج هذه المركبات لتشكيل اجزاء هندسية معقدة يعتبر تحدي كبير. عملية ال THIXOFORGING هي تقنية جذابه حيث يتم تشكيل المعدن عند درجة حرارة شبه- الصلابة والتي تعادل اعلى جزء للصلابة بسبب الخصائص المتاصلة فيها مثل حمل التشكيل المنخفض وزيادة عمر القالب والحد من خطوات التشكيل . ان ال THIXOFORGING تستخدم على نطاق واسع في تصنيع الاجزاء المعقدة في مصانع السيارات والالكترونيات والتي تتكون من سبائك الالومنيوم. ان تطبيق هذه التقنية في المواد المركبه ذات المصفوفية المعدنية توفر مزايا اضافية مثل تحسين السلوك الميكانيكى وقدرة افضل على التشكيل. ان الهدف من هذا البحث هو تطوير مواد مركبه الالومنيوم متناهية الصغر وTHIXOFORGING للشكل المطلوب. من اجل تحقيق ذلك تم استخدام سبائك الالومنيوم (A356) والمعززة بجزيئات متناهية الصغر من كربيد السيلكون وعمل صب له باستخدام الصب التقليبى باستخدام المعالجة بالموجات الفوق صوتية والتي استخدمت كمادة خام لعملية ال THIXOFORGING. المادة المركبة التى تم الحصول عليها بعد عملية الصب تم تسخينها بشكل منتظم باستخدام جهاز تسخين بالحث ونقلها مباشرة الى مكبس البثق باستخدام عينتين متختلفتين بنسبة ٥٠ % و ٦٠ % ويتم ايضا اعادة تسخينهما لمدة تتراوح من دقيقة الى دقيقتين. تم استخدام تراكيز مختلفة من كربيد السيلكون وذلك لاظهار الخصائص الميكانيكية للمواد المركبه. دراسة الخصائص المجهرية تمت دراستها باستخدام تقنيات متعددة مثل المجهر الضوئى والمجهر الالكترونى، وتحليل للعناصر باستخدام الاشعة السينية، اما السلوك الميكانيكي فتمت دراسته باستخدام اجهزة فحص الصلادة والشد. اظهرت النتائج ان اضافة جزيئات كربيد السيلكون تساعد في تنعيم البنية المتجمدة. كما تم ملاحظة التوزيع الجيد والتحسن في الخصائص الميكانيكية للعينات التي تمت معالجتها باستخدام الموجات الفوق صوتية بشدة بقدرة ٨٠ وات لكل سنتيمتر مربع. تغيرت البنية المجهرية من بنية غير شجرية الى بنية كروية بعد التسخين بالحث. تم الحصول على ظروف افضل لاعادة التسخين وذلك عند استخدام طاقة حث متوسطة لمدة دقيقتين. المواد المركبة باستخدام THIXOFORGING اظهرت ان نسبة كبيرة من كربيد السيلكون موجودة بعيدا عن مركز العينة . صلادة المواد المركبة متناهية الصغر زادت بزيادة كربيد السيلكون كما لوحظ زيادة مرونة المواد المركبة متناهية الصغر بعد عملية THIXOFORGING عند نسبة صلب ٥٠ % اظهرت امتلاء كامل للقالب وكثافة عالية وكذلك مقاومة شد افضل.

CHAPTER 1

INTRODUCTION

1.1 General Introduction

Considerable research is being done in the area of Metal Matrix Nano-composites (MMNC's) due to their excellent physical and mechanical properties [1-2]. Aluminum or its alloys have received much attention as the matrix element in producing these nanocomposites. This interest is based on the fact that aluminum and its alloys have considerable commercial use in various industries like automobile, electronic and aerospace [3]. The light weight and high strength combined with good ductility of the aluminum nanocomposites can replace many materials currently used in the industry for various applications.

Much research has been done in improving the properties of aluminum and its alloys by different processing routes like adding micro/nano particles [4], squeeze casting [5], secondary processing like semi-solid processing [6], extrusion, etc. However, little research has been done on studying the behavior of aluminum nanocomposites after secondary processing like thixoforging which is a semi-solid process. In this process the billets are reheated to a semi-solid temperature and shaped using forging operation [7]. The feedstock billet should be essentially produced from casting route with a non-dendritic structure for subsequent reheating and thixoforging. Feedstock production

through ultrasonic stir casting provides additional ways to synthesize nanocomposites and subsequently perform thixoforging operation [8].

1.2 Thixoforging (semi-solid processing)

The use of light weight alloys especially aluminum alloys are very much in demand especially in automobile and aviation industries [9]. Thixoforming of these alloys supplements the advantages by near net shaping [10], forming complex parts in relative short period of time by reducing forming steps, the die wear and thereby decreasing the cost involved [11-13]. However incorporation of this process to aluminum nanocomposites presents additional challenges such as the effect of reinforcement particles on the homogeneity of material during semi- solid processing.

Generally the thixoforging process is divided into three stages [14]:

- Preparation of billet: This involves fabricating a composite material through casting with appropriate grain morphology (non-dendritic)
- Reheating of billet to semi-solid state: This involves heating of the billet obtained from above step to a semi-solid state. Uniformly heated billet is necessary for having proper liquid solid fraction.
- Forging: Finally the heated billet in semi-solid state is forged in a preheated die to the required shape.

An important condition for thixoforming processing is reliable reheating of the feedstock material. To heat up the tailored slugs, mainly convective or inductive heating devices are used. The main advantage of the inductive heating process is the direct generation of heat

within the slug due to induction by eddy currents. This effect provides a heating procedure that is rapid and relatively easy to control [15].

The reheating is required to raise the temperature of the billet material between its solidus and liquidus temperature in order to ensure semi-solid state. Besides exact temperature control, homogenous temperature distribution within the slug must also be ensured to guarantee uniform flow behavior during the subsequent thixoforming process. Initially the billet must be rapidly heated in order to avoid any undesired particle growth, then after reaching semi-solid temperature, the slug is soaked at constant temperature for certain time. During this soaking (holding) period, the solid particles undergo microstructural evolutions (globular) that are the prerequisite for the thixotropic flow behavior [16]. The thixotropic globular microstructure is responsible for shear thinning of the slug under deformation; the solid globules easily slide in the liquid phase which acts as a lubricant and makes the deformation easy.

1.3 Ultrasonic Stir Casting

Metal matrix composites (MMCs) reinforced with ceramic nanoparticles offer significant advantages over pure metals or alloys. MMCs could be used to tailor the properties of matrix and reinforcing phases which is responsible for its improved performance [17]. Liquid state processing of MMCs such as stir casting have shown some special advantages compared to solid state processing route such as powder metallurgy. Stir casting process is usually cost-effective and products of complex shape can be formed directly through the melt. However particle agglomeration due to poor wettability between matrix and reinforcement is a critical issue that hinders the use of liquid state

processing for metal matrix nanocomposites [18]. Thus external forces are used to break the clusters and assist the dispersion of particles into the matrix melt.

Ultrasonic stir casting is one of the techniques used for this purpose. It is observed that the impact of transient cavitation's induced by ultrasonic vibration inside the melt is capable of breaking the clusters of particles and dispersing them uniformly in the liquid melt [19-20]. The intensity of ultrasonication and the processing time are crucial parameters involved in this technique. The difficulties like particle agglomeration, non-uniform dispersion of reinforcing nanoparticles, poor wettability and chemical reactions are always encountered in producing metal matrix composites [18]. Therefore it is required to perform composite casting in a controlled environment with proper selection of processing conditions using different techniques to overcome such difficulties.

1.4 Aluminum-SiC Nanocomposite

To further improve the properties of Aluminum and its alloys, it was commonly practiced to reinforce pure aluminum and its alloys like A356, Al-6061 with SiC particulates [21-22]. Besides its density being closer to that of aluminum, SiC reinforcement is primarily used because of its low cost and good compatibility in Silicon based aluminum alloys. The SiC reinforcement promotes an increase in the wear resistance, Young's modulus and tensile strength of the composite materials. The improved mechanical properties in SiC reinforced composites are due to transfer of shear load at the matrix/reinforcement interface, Orowan strengthening, grain refinement, mismatch in coefficient of thermal expansion between the matrix and the reinforcement particles [23]. Hence a good interfacial bonding between the matrix and reinforcement and satisfactory particle

distribution is necessary for the composite [24]. The nanocomposites are being synthesized by using nano-powders of SiC reinforcements in order to tradeoff between strength and ductility since the ductility of metal matrix composites significantly deteriorates with increase in the concentration of micro-ceramic reinforcements.

1.5 Aims/ Objectives

- To develop a processing route to produce SiC nanoparticles reinforced Aluminum A356 alloy nanocomposite by ultrasonic stir casting technique in which the SiC particles are uniformly distributed.
- To further process and deform the monolithic alloy A356 and the developed A356/SiC nanocomposite billets using semi-solid processing method i.e. thixoforging to a required shape-allowing a comparative analyses.
- Studying the effect of different weight percentage of SiC nanoparticle on the microstructure and mechanical behavior of the produced aluminum alloy nanocomposites.
- To comparatively study the effect of SiC reinforcement in the A356 alloy under ultrasonic stir casting and thixoforging conditions by gaining an understanding of the mechanisms of these processes.

CHAPTER 2

LITERATURE REVIEW

2.1 Semi-Solid Metal Processing

Semi-Solid Metal (SSM) processing is a hybrid manufacturing technique that incorporates the effects of both casting and forging [25]. It is relatively new technology which forms metals to a near net shape component with good surface finish and superior properties. Unlike conventional metal forming technologies which use either solid metals (solid state processing like forging) or liquid metals (casting) as starting materials, SSM processing deals with semisolid slurries, in which non-dendritic (globular) solid particles and liquid phases are partially present. Forming in the semisolid state requires that a metal or alloy have a roughly spherical and fine-grain microstructure before shaping in a forming die [26].

The SSM processing is divided into two routes rheocasting and thixoforming. In brief, the rheocasting process includes shearing of material during solidification to produce nondendritic semisolid slurry which is transferred directly into a mould for shaping. On the other hand, thixoforming is a two-step process in which a preformed non-dendritic material feedstock is reheated to a semi-solid temperature before shaping within a metal die. The rheocasting slurry consists of more liquid phase than solid, whereas in thixoforming the non-dendritic billet is formed when 30 to 40 per cent of the material is liquid [27].

2.1.1 Background of semi-solid forming

Semisolid metal forming is based on a discovery made at the Massachusetts Institute of Technology in the early 1970s, by Spencer [68]. During their research they found that a change in microstructure of alloys formed during solidification under agitation was responsible for a dramatic decrease in the apparent viscosity of the semi-solid slurry. This slurry when sheared also showed two-phase homogenous flow at high solid fractions. This unique property was attributed to a novel 'non-dendritic microstructure' formed under agitation. The MIT researchers then coined the term "Rheocasting" to describe the process of producing this unique microstructure by stirring alloys during solidification and injecting the slurry directly into the die for shaping [27].

The feasibility of SSM processing of various alloys for industrial production has been investigated from past 30 years. Initially, a company formed by MIT and some group of industries with name 'Rheocast Corp.' designed and built large scale rheocasters for production of aluminum and copper alloys. The semi-solid process was proved to be an effective means of reducing the heat content of the alloy production. As time passed, due to energy crisis and increasing environmental concerns since the 1980s, the lightweight high performance alloys was in demand especially in automotive sector. As a consequence, since the 1990s, SSM processing was shifted to producing parts with aluminum alloys. In later stages due to some drawbacks in rheocasting process an alternative route called thixoforming was developed in order to overcome internal defects. Thixoforging process is application of this route where in components are shaped between closed dies under application of pressure from a forging press.

2.1.2 Advantages and applications of semi-solid forming (thixoforming)

Unlike liquid metal processing which involves solidification of liquid phase into a mould, the slurries in semi-solid forming consists of partial phases of solid and liquid, leading to some technical and economic benefits.

The main advantage of the semi-solid forming process is that the forming facility can be highly automated using methods similar to those used in forging and stamping, since the working metal (slurry) is not completely liquid [28].

Particularly significant for higher-melting alloys, semisolid metal working afforded lower operating temperatures and reduced metal heat content. The lower temperature and short dwell time lead to longer die life with less thermal shock. In addition, the energy required to heat aluminum alloys for casting (ignoring losses) is 35 per cent greater than the energy required to heat the same aluminum alloy to the condition ready for semisolid forming as shown in Fig. 1.

The viscous flow behavior of the slurry during die filling leads to less gas entrapment in the formed part. Solidification shrinkage would be reduced in direct proportion to the fraction solidified within the semisolid metal working alloy, which reduces both shrinkage porosity and hot tearing tendency.

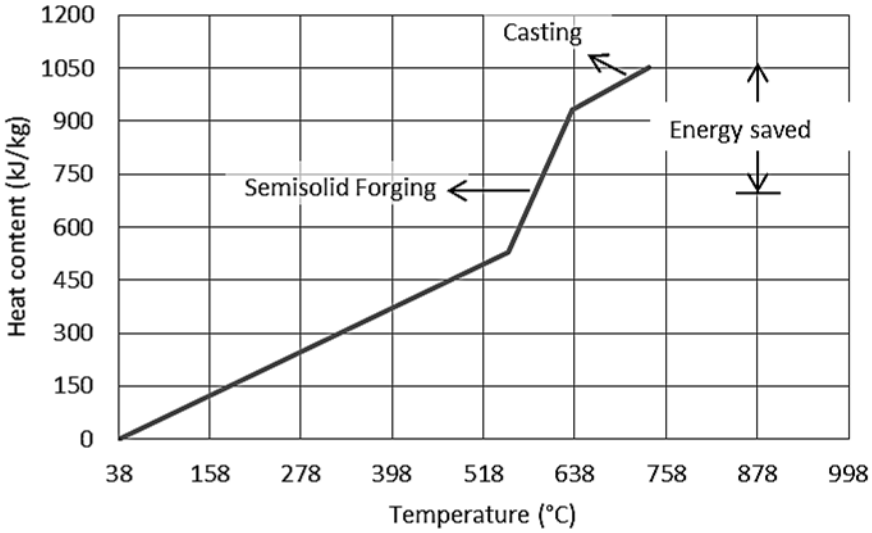

Figure 1: Heating curves showing energy savings possible in semisolid forging versus casting of A357 aluminum alloy [27]

Beside these advantages, SSM processing provides high integrity components with complex shapes and tight dimensional control. The forming stresses are lower in the semisolid state, thus able to form complex shapes, using smaller presses, and with lower finishing costs [26].

With these enabling features in mind, there are several areas where thixoforming process finds most of its applications:

• Existing permanent mould parts wherein much of the machining and finishing is avoided by near net shapes capability of SSM processing.

• High strength parts, such as suspension mounts, engine mounts, steering knuckles, alloy wheels, tie rods, control arms, master brake cylinders, fuel rails, air conditioner compressor housing etc.

2.2 Thixoforging

Thixoforging as stated earlier is a type of semi-solid process in which a partially melted non-dendritic slug is pressed and shaped inside open dies. The thixoforging is carried at solid fractions between 0.5 and 1, thus able to take advantage of both forging and semi-solid characteristics. In a typical thixoforging process the forging requires extremely low force due to low viscosity of the mushy billet. Then the punch force gradually increases till the end of the process due to shear rate dependent viscosity of the billet. The punch force during solidification of billet must provide adequate pressure inside the billet to avoid inner porosities in the thixoforged part. At the same time the punch velocity must be high enough to avoid shrinkages during material flow inside the die.

Research in thixoforging process is oriented towards processing of aluminum alloys to intricate shapes, defects analysis, and optimization of forging conditions for improved mechanical properties.

Wang et.al [30], studied the feasibility of thixoforging A356/SiC composite packaging shell. The composite was prepared using mechanical stirring at a temperature of 590^{o}C with a speed of 50-80rpm. The SiC particles and A356 alloy showed good compatibility when the particles were heated to 600^{o}C for 3hours before adding into the aluminum melt. After stirring for 10 minutes the melt was poured into a preheated die to obtain composite billets of dimensions 30mm diameter and 45mm length. These billets were reheated for thixoforging using a controlled resistance furnace at different semi-solid temperatures of 560,570,575,580 and 585^{o}C. By analyzing the microstructures, the process was optimized and one reheating condition of 580^{o}C with a soaking time of 10

minutes was selected. After this the billet was transferred to a forging press of capacity 1960kN and thixoforged in a die preheated to 300^{o}C. It was found that the SiC particle content was higher in the locations farther from the center of the thixoforged part.

Another study by Kang et.al [31], experimented the effect of forging pressure and die temperature on the microstructure and mechanical properties of the A356 and Al2024 alloys. In addition to this the filling behavior and defects in the thixoforged part was investigated. Three step inductions heating with solid fraction of 55% was used for reheating billet before thixoforging. The relationship between filling behavior and die temperature was observed by preheating the die to various temperatures like 250,300,350 and 400^{o}C. The compression velocity was maintained as 200mm/sec. The applied pressure of 100 and 150Mpa was used to determine its effect on the mechanical properties with compression holding time of 20sec. The experiments suggested to use 300oC die temperature for A356 with 150Mpa applied pressure to obtain complete die filling with dense microstructure. An increase in ultimate tensile strength, yield strength and hardness were also observed with higher applied pressure as observed in other studies [32].

Vaneetveld et.al [33], investigated the thixoformability of high performance aluminum alloy 7075 at higher solid fractions. Thixoforging was done on 5000kN hydraulic press with maximal speed of 0.315 m/s and a maximal pressure of 600 kN on a heated billet (using seven step heating cycle of 141sec.) of diameter 35mm and height 30mm. Different tool temperatures, lubricants were used to observe influences on the load and defects. Temperature of the tool is increased to slow down the cooling and avoid cracking

of the parts. By increasing temperature, punch speed has to be adapted to avoid defects due to the material flow behavior.

Another study by Kang and Jung [34] experimented die filling behavior of semi-solid A356 alloy by varying the die temperature, pressing force and pressing holding time in order to avoid liquid segregation phenomenon during thixoforming which can lead to undesirable mechanical properties. It was observed that the filling behavior into the die cavity as well as the solid grain size were the key parameters in the mechanical properties of the thixoformed part. The die temperature was varied from 200 to 300oC, the pressing forces from 64.8 to 138MPa and pressing holding time was changed from 20 to 45 seconds. Parametric study with 18 experiments were done out of which 6 complete die filling, 3 partial filling and 9 defective fillings were obtained. The die temperature of 250 with 80MPa pressing force and 45seconds holding time gave good results. The results of their experiments suggested that places of higher strain rate (generally away from the center) produce more liquid phases than solid phases. Moreover at higher pressing force the grains became denser specifically near the contact surface with the die depending on the cooling rate. Therefore it was concluded that in order to improve the thixoformability, the liquid segregation should be controlled as the multistage variation of the pressing velocity during forming.

Atkinson et.al [35], investigated thixoformability of aluminum alloy 7075 with respect to one step, two step and three step induction heating regimes. The effect of these regimes on the occurrence of defects like liquid segregation, unrecrystallised grains and porosity were discussed. Finally using a three step heating condition, the tensile properties of the thixoformed part was studied with different ram speed and die material. The results

suggested using intermediate ram velocity of 500-750mm/s with three step heating regime to give fewer defects and good mechanical properties.

Tahamtan et.al [36] investigated the microstructure, tensile properties and fracture surfaces of thixoforged A356 alloy and compares it with rheocast and gravity casted alloy. A mechanically stirred cast alloy billets were reheated to 600^{o}C using an electric muffle furnace with 10min. holding time. Then billet was transferred to the press for 50% hot deformation. The forming die, holder and billet were all heated to same temperature at the same time. The results of this study found less defects and improved tensile properties for thixoforged sample. The fracture of thixoforged alloy showed dimples. Tensile cracks were formed in the eutectic area and propagated through either trans-primary alpha phase (at 600^{o}C) or inter-primary alpha phases (eutectic silicon phases at 610^{o}C) depending on the reheating temperature.

2.3 Induction Heating

In most of the thixoforming operations commercially used, the material is delivered to the die/machines in the form of reheated billet (slugs). The dominant technology for reheating billet is the induction heating process. In this process the billet is placed around a carousel of solenoid coils connected to an induction power supply and heated using induction heating principle. This approach of reheating billet is more stable, economical and relatively straightforward to control.

For reheating billet for thixoforming, it is critically important to maintain uniform surface to center temperature profile inside the billet. The billet must also be heated quickly and homogenously throughout its length [37]. For achieving these requirements the rate of heat input supplied to the billet is the controlling factor. Too rapid heat input promotes surface melting and large temperature gradients inside the billet. Due to this the slug would not retain its shape and will create problem in transportation and in die filling during the shaping process. In induction heating this is overcome by adjusting power levels during heating as shown in Fig. 2. Initially rapid heat input is supplied until the billet remains fully solid and gradually the power is lowered near the onset of melting. This helps in holding the temperature efficiently without overshooting and achieving the required microstructure for thixoforging.

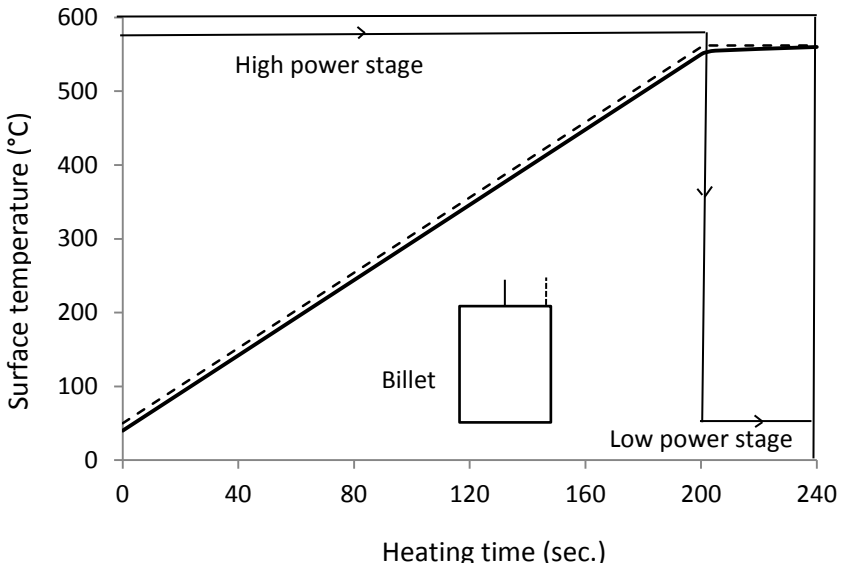

Figure 2: A typical power input profile for a two stage heating cycle and the temperature variation on the center and the edge of the billet. The heating power was lowered 205sec after the heating had started [28]

One of the essential requirements for an induction heating system is to heat the billet quickly and homogenously. H. Jung [38] extensively studied the reheating experiments on A356 alloy billet of 76mm diameter and 90mm length using an induction heating system of capacity 50kW and coil dimension of 120mm diameter and 120mm height. The optimal reheating conditions for thixoforming requirements were investigated by varying the reheating time, holding time, holding temperature, power of the induction heating system and adiabatic material size. The results of these studies showed that for a larger billet size, multi-step reheating with 2 minute final holding time is preferable in order to maintain good separation between solid and liquid phases and also to avoid coarsening of the microstructure due to cohesion of solid particles which would happen in case of reheated billets with longer holding periods [39]. It was also observed that by increasing the capacity of induction system, the temperature gradient remained less but overshooting was observed with billet getting overheated instantaneously.

Choi et.al [40] studied different heating condition and the temperature distribution inside the billet using induction heating apparatus (having the specification of 220V, 15kW and 23.5 kHz). In this study two types of step heating were used for reheating A356 billet with dimensions 75mm diameter and 100m height. In the first case the work piece was soaked after reaching to 400°C and 500°C before finally heating to the desired temperature of 583.1°C whilst maintaining 10 kW output of the induction heater. In the second case the work piece was soaked at 550°C whilst maintaining 10 kW output power before heating to the desired temperature of 583.1°C whilst maintaining the reduced output of 4.77 kW. The results of this study indicated that, in the case of heating by variation of power output, 10 and 4.77 kW, for an A356 work piece, it is seen that the time of reaching the desired temperature is shorter for 10 kW. Moreover in order to reduce the temperature gradient, step heating with 4.77kW power after first soaking is used for obtaining the desired microstructure.

Another study was based on the optimization of induction heating cycles in obtaining uniform temperature distribution and desired thixotropic microstructure. The induction heating was performed by applying 25 kW power with different heating cycles. Three different heating cycles were used: 1) single step cycle, 2) two-step cycle and 3) three-step cycle. The temperature variation between the core/center to edge/surface is observed to be 9 °C in single step, 6 °C in two steps and 2 °C in three step induction heating cycle. In order to study the microstructure obtained during various induction heating cycles, the billet was quenched after different induction cycle to freeze the microstructure obtained after induction heating. The microstructure in three step heated billet was found to be globular and the eutectic was uniformly distributed [41].

2.3.1 Principle of induction heating

The induction heating works on the principle of transferring energy via electromagnetic waves and heating of work piece by Joule effect. The induction heating setup essentially consists of an Alternating Current (AC) supply to the inductor coil which generates a magnetic field and when a metal is placed inside the inductor coil, circulating eddy currents are induced within the workpiece (Fig. 3). These currents flow against the electrical resistivity of the metal, generating precise and localized heating without any direct contact between the part and the induction coil. The magnitude of current decreases from surface to the center of the workpiece during induction heating, this phenomenon is known as skin effect. The penetration depth (thickness of layer from surface of workpiece in which 87% of the power is developed) of this current depends on the frequency of induction and characteristics of the material to be heated. Increase in frequency decreases the depth of penetration of current in the workpiece. It is preferable to use low frequency for thorough heating of the billet. Higher frequency on the other hand is used for surface heat treatments. Frequency of induction can be reduced by increasing the number of turns in the inductor coil [42].

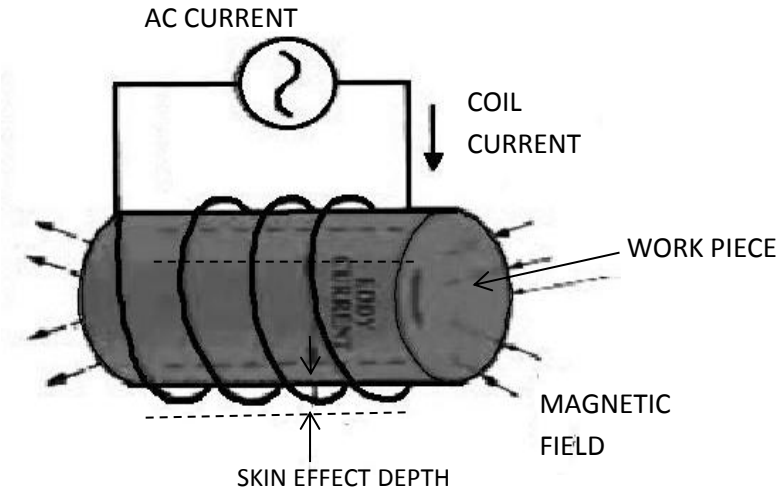

Figure 3: Principle of Induction Heating [42]

2.3.2 Induction heating of metal matrix composites

The reheating conditions for metal matrix composites differ from that of monolithic alloy. Especially when the solid fraction is concerned, the metal matrix composite shows different heating behavior due to the presence of ceramic particles. The difference in thermal conductivities of alloy and the reinforcement also contributes to the reheating variation [43]. The relationship between solid fraction and temperature can be explained by the solidifying theory of monolithic alloy. But this data cannot be applied to the metal matrix composites containing particle reinforcements.

Kang and Youn [44] proposed a method of reheating MMC's by exactly defining the relationship between temperature for predicting solid fraction and volume content rate of reinforcement. The reheating temperature for MMC's was calculated by using temperature and solid fraction data of matrix and volume percentage of reinforcements.

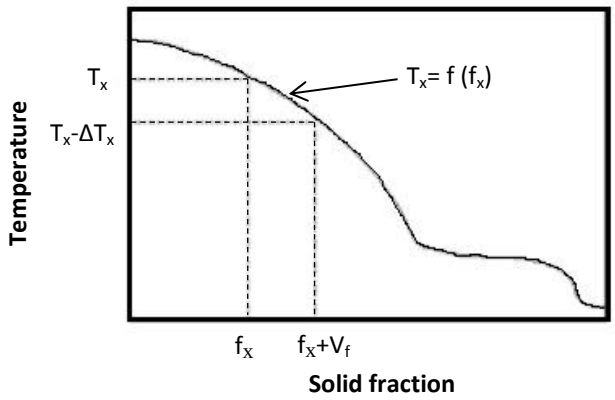

Figure 4: Relationship between the solid fraction and temperature for semi-solid aluminum alloys

As shown in Fig.4, for solid fraction of f_x if the amount of reinforcement V_f increases, solid fraction increases relatively and the temperature decreases. Therefore, reheating temperature or MMC increases within ΔT_x according to increment of the volume content rate of the reinforcement.

Kang et.al, extensively studied the effect of reheating conditions on the microstructure and mechanical behavior of particulate metal matrix composite. The effects of the dispersion state of the reinforcements on the reheating temperature and microstructural morphology were also investigated. The composite with aluminum alloy A357 and SiC particles of 14µm and 25µm size with volume fraction of 5 to 15% was prepared using mechanical stirring. Composite billets of 40mm diameter and 50mm height was reheated using 20kW induction heating system with coil dimensions of 80mm diameter and coil length of 100mm. The results suggested that in the case of composite with uniform dispersion of reinforcement, the set temperature of the final reheating step was approximately 11 °C lower than that of composite with non-uniformly dispersed

reinforcements and the total reheating time was also 3minute shorter. After reheating process the microstructure of the composite showed globular grains with uniform distribution of reinforcement [45].

2.3.3 Microstructure evolution during reheating (induction heating) process

The reheating process is very important stage in the thixoforming operation. The purpose of this process is to obtain required solid fraction inside the mushy billet along with spheroidal morphology of the solid phase. The reduction in interfacial energy between solid and liquid phases is responsible for evolution of microstructure in the semi-solid state [46]. The holding time during reheating process is very crucial to complete spheroidal transition and must be optimized in order to prevent excessive grain growth.

The mechanisms behind the microstructure evolution during reheating process are melting and combining. In the melting mechanism, due to normal ripening the root of the dendritic arm gets melted and finally evolves into spheroidal grain. These grains do not contain any entrapped liquid and its size depends on that of the initial arm fragmentation. During combining mechanism, the dendritic arms with less spacing touches and combines with some liquid phase entrapped in it. The large structure formed after combining will evolves toward spheroidal morphology with proper heating conditions. The coalescence and coarsening of grains depends on the reheating conditions like heating time, holding temperature and holding time [38-40].

The microstructural evolution during reheating and subsequent isothermal holding can characterize by the following processes:

• Partial remelting of the low melting point phase at grain boundaries

• Liquid entrapment by rapid coalescence of dendritic arms

• Spheroidization of individual particles due to atomic flux from the areas of high curvature to the areas of low curvature

• Coarsening by both dissolution of smaller particles and coalescence between particles, resulting in reduced particle density

2.3.4 Characterization of microstructure in semi-solid slurries

The flow behavior of semi-solid slurry inside the die and consequently the properties of part shaped from slurries are dependent on the fraction solid (semi-solid temperature) and size, morphology of solid particles distributed within the liquid matrix [27].

- **Fraction Solid**

The fraction solid (f_s) in the semi-solid slurry can be determined from phase diagrams for simple alloy systems or from direct measurement using metallographic techniques. One way of representing the fraction solid is by measuring the average particle size (assuming spheres of equivalent diameter 'D_{Eq}') of solid particles in the microstructure of semi-solid slurry. The fraction solid in this study is directly derived from the thermodynamic data of solid fraction and semi-solid temperature curve for A356 alloy.

- **Shape Factor**

The shape factor of spheroidized particles is an important characteristic of microstructure in the semi-solid slurry. As stated earlier the globularity of particles determines the effectiveness of thixoforming process. The shape factor is determined by measuring the

perimeter length, (P) of a particle present in the section and its surface area (A). The shape factor is then defined by Eq. (2.1).

$$S = \frac{P^2}{4\pi A} \tag{2.1}$$

Note that a shape factor of 1 represents a microstructure with perfect spheroidized particles. Whereas a convoluted perimeter would clearly produce a shape factor lower than unity.

2.4 Feedstock Production Methods for Semi-Solid Processing

The ideal feedstock material for semi-solid processing is a microstructure with fine and spherical solid phases uniformly dispersed in a liquid matrix. There are many routes for obtaining such a microstructure as described in the following sections [28, 47].

- **Mechanical stirring**

The MIT research [68] was based on producing microstructure for semi-solid processing by mechanically agitating the molten alloy vigorously during its solidification. This agitation helps in detaching the dendritic arms, resulting in formation of suspended solid phases in the liquid matrix.

- **Magneto Hydrodynamic (MHD) process**

The MHD process is most widely used technique for generating feedstock for thixoforming operation. In this process, the filtered and degassed molten metal is fed into a direct chill mould and near the freezing point the metal is vigorously stirred by dynamic electromagnetic field. The shearing action by this field and the rate of heat removal from

the mould surface can be controlled to provide the desired solidified microstructure with grain size much smaller than those obtained by mechanical stirring process.

- **Strain Induced Melt Activated (SIMA) process**

The SIMA process generally consists of four stages. In the first stage alloy is normally casted to obtain a typical dendritic microstructure. After this, the casted billet is hot worked to make the microstructure homogenous. In the third stage the billet is heavily deformed by cold working and in the final process it is partially remelted in order to obtain a fine equiaxed microstructure. The evolution of microstructure in this process is by recrystallization mechanism.

- **Spray casting**

In this process, molten metal from an induction furnace is poured through a nozzle and a jet of high pressure inert gas disintegrates this stream of molten metal into micron sized droplets. These droplet experiences gas atomization phenomenon and are collected on a substrate underneath.

- **Cooling slope casting process**

The cooling slope casting process is a relatively new technique for producing feedstock material for thixoforming. The process is similar to continuous casting except that the molten metal is poured into a mould through an inclined cooling slope plate providing a suitable superheat to the solidifying metal. The non-dendritic microstructure in this process is obtained by fragmentation of weak dendritic arms near the contact surface of cooling slope. Another reason stated by the researchers in this process is crystal separation theory. According to this theory, cooling slope is responsible for nucleation of

metal crystals which got separated by fluid motion and subsequently became granular inside the mould. Many researchers have analyzed the growth of microstructure in the cooling slope process by varying inclination, cooling temperature etc. [48].

2.4.1 Ultrasonication process

Experimentally, it is well-known that application of ultrasonic treatment to a melt at temperature just above its liquidus can produce effectively a fine and non-dendritic microstructure [49]. This microstructure is suitable for subsequent reheating and thixoforming operations which is an essential requirement for semi-solid processing. The mechanism for the formation of such fine and non-dendritic structure is related to the introduction of high power ultrasonic vibration into a liquid alloy due to two basic physical phenomena: cavitation and acoustic streaming [50-51].

The collapse of the cavitation bubbles creates shock waves to shear the clusters at high frequencies (helps in incorporating particles inside the melt). Cavitation involves the formation, growth, pulsation, and collapsing of tiny bubbles in the melt generating hydraulic waves. On the other hand the acoustic streaming tends to wash away loose individual particles (gives distribution to the particles inside the melt).

Another important effect in ultrasonic treatment is the ultrasonic degassing. This effect occurs which facilitate in avoiding porosity and oxide inclusions, since the stirring is under the surface of melt below the tip of sonotrode [52]. Too violent acoustic streaming on the melt surface exposed to air is also not desirable since the violent flow stirred by the streaming could trap gas bubbles into the melts, forming more cavities in the cast samples after solidification [53].

Han et.al [54] investigated the effect of ultrasonic vibration on the nucleation and growth of aluminum alloy A356 melt. An acoustic radiator generating ultrasonic vibrations was dipped inside the melt. The experimental results confirmed formation of globular grains when ultrasonication was performed close to liquidus temperature and subsequent cooling. Other studies also justified the effect of high-intensity ultrasonic vibration on refining both the primary aluminum phase and the eutectic silicon phase [49].

As stated earlier the application of ultrasonication to the melt at low enough temperature is recommended to optimize the grain refinement. The dominant mechanism for grain refinement was due to cavitation's induced heterogeneous nucleation. Since the cavitation developed inside the melt is proportional to the ultrasonic intensity, the degree of refinement is relative to the power of ultrasonication. The sonotrode for acoustic vibration inside the melt is not necessary be located very close to the solidification mold because the effect of ultrasonic processing on the melt remains for a certain time after the end of ultrasonication and will still influence the solidifying microstructure. With regards to the solidification time it is suggested to have higher cooling rate for getting a better ultrasonic aided grain refinement in the application of ultrasonic processing [55].

2.5 Stir Casting

The production of composites through stir casting route involves dispersing ceramic reinforcement inside the molten metal matrix. The mixing is carried out using mechanical, electromagnetic or ultrasonic means for a period of time. The processing parameters like stirring speed and time, temperature of melt, prevailing atmosphere over the melt, and nature of particles are important factors that must be monitored and accurately controlled for effective stir casting.

The addition of reinforcement particles into the molten aluminum can be done in many ways. The feeding mechanism utilized by researchers for incorporating nanoparticles inside the aluminum melt are capsulate feeding where in particles are enclosed in small capsules of metal foil(foil material is same as the metal melted). Second method is the pretreatment of the reinforcement particles before inserting it inside the melt. This method is widely used and more efficient in incorporating particles inside the melt [56]. Another method of adding nanoparticles is by making a composite powder of matrix material and reinforcement by ball milling and then incorporating this powder inside the molten metal. In some cases reinforcement is added in semi-solid melt slurry which also improved wetting [57].

2.5.1 Ultrasonic stir casting

Yang et.al., [58] studied the fabrication of Aluminum nanocomposites by ultrasonic dispersion of SiC particles inside the melt. The ultrasonic processing was done at 710^{o}C temperature with power of 80W which was found to be sufficient in a crucible dimension

of 50mm diameter and 50mm height. After 1.5 hours of ultrasonic treatment, the temperature of melt is raised to 760^{o}C for pouring due to less viscous melt obtained after ultrasonic stirring. The study suggested that the strong ultrasonic effects were able to efficiently disperse nano-particles into the melt along with enhancement in the wettability.

Another study by Li and Yang [59] tried to optimize processing temperature and ultrasonic power for a fixed 1wt% of SiC and A356 composite. The processing temperature was chosen as 650, 700 and 760^{o}C and ultrasonic power was varied from 2.5, 3 and 4kW. Processing time taken for ultrasonication was 60 minutes inside the crucible. It was found that the properties of the casted composite were dependent on the processing conditions and the maximum tensile strength of the composite was observed to be at 3kW ultrasonic power and at 700^{o}C processing temperature.

In another experiment particles were initially incorporated by stirring with a metallurgical stirrer for 3min followed by ultrasonication for 30min at 700^{o}C temperature [60]. The investigation found 1 kW power of ultrasonic transducer with 30 minutes sonication time sufficient to disperse 0.5 wt. % of reinforcement's material in 500grams of aluminum melt. From the results it was observed that with only 0.5wt% nano sized SiC, the ultimate tensile strength and yield strength of the nanocomposites were improved by 60.56% and 55.26% respectively.

Li et.al, [61] also utilized mechanical stirring for pre dispersion of SiC particles in the melt. They fabricated SiC nanoparticle reinforced ADC12 aluminum alloy composite using mechanical stirring and high intensity ultrasonic dispersion process. Preheated SiC

Nanoparticles were added into the vortex with stirring speed of 200-300 rpm and stirring time of about 1-2 minutes. Later on ultrasonication was done with 1.4kW power for 15 minutes to disperse nanoparticles homogenously.

Many researchers have emphasized the use of mechanical stirring on improving the wettability and incorporation of particles inside the melt. The wettability is more promoted when the stirring is carried out in semi-solid state of the melt [53]. The experimental work by Zhou et. al. [56] also found the wetting of SiC particle with the Al-Si alloys when the stirring is carried out in semi-solid state.

Kandemir et.al. [62] have utilized mechanical mixing using ceramic stick to disperse floating nanoparticles back into the melt during the ultrasonic processing. The nanoparticles were brought under the ultrasonic probe tip using the stick to break the clusters and incorporate nanoparticles inside the melt.

2.5.2 Challenges associated with producing MMC's by stir casting route

The challenges involved during the fabrication of metal matrix composites through stir casting route are i) difficulty in incorporating nanoparticles in the molten metal matrix ii) dispersing of particles uniformly and iii) formation of a strong interfacial bond between the reinforcement particle and the matrix [64].

The difficulty in incorporation is associated with the wettability of particles inside the molten metal. The solid ceramic particle would resist mixing due to surface tension of the liquid metal. It is more difficult to achieve complete wetting of the reinforcement as the

particle size decreases. With the nanoparticles the surface energy required for the molten metal surface to bend to a small radius is very large. Hence there is tendency of particles to agglomerate and form clusters when the particles are not wetted by the molten matrix.

The particle incorporation is hindered with two types of barriers: i) thermodynamic barrier associated with the wettability and ii) mechanical barrier which arises due to existence of gas layer on the surfaces. The second type of barrier can be overcome by vigorously stirring the melt using mechanical, electromagnetic means or by using ultrasonic particle dispersion technique. The thermodynamic barrier can be overcome by adopting measures aimed at improving wettability of particles. The wetting can be improved by either adding surfactants like magnesium in case of aluminum for reducing surface energy of the melt or by preheating particles prior to their addition in the melt.

Good Wettability between the solid ceramic particles and liquid metal is essential for generation of satisfactory bond between these two phases during casting. Heat treatment of particles before its dispersion in the melt is necessary in improving wettability by removing surface impurities, desorption of gases and a formation of an oxide layer on the surface of the particles. Several investigators have suggested preheating of SiC to (900-1000^{o}C) for improving Wettability inside aluminum melt [65].

The dispersing of particles uniformly is associated with the mixing technique used for stir casting. The mechanical stirring can introduce impurities and porosities in the cast sample. However ultrasonic dispersion technique has found to be very effective in dispersing particles by generating nonlinear effects in the liquid pool. The distribution of reinforcement is also influenced by the flow and solidification of molten matrix. The flow

and solidification characteristics depends on the pouring temperature, stirring technique and agglomeration behavior of particles before mixing, after mixing and relative density of reinforcement with respect to the liquid matrix. Therefore high density particles relative to the density of matrix, will sediment after stirring is done while low density particles would float on the surface of the liquid melt.

Molten metal and alloy matrices normally solidify dendritically during casting and the reinforcement particles are either pushed or engulfed by the solidification front depending on the interfacial energy between the particles and molten matrix. It has been reported that decrease in particle size increases the tendency of the particles to be pushed ahead of the solidification front which in turn play an active role in nucleating new grains and restricting grain growth. Segregation of particles at the grain boundaries or their engulfment depends on the velocity of the solidification front [66].

CHAPTER 3

EXPERIMENTAL PROCEDURE

3.1 Materials Preparation

The matrix material used for casting is the aluminum alloy A356 containing Si as a main alloying element and the reinforcement were beta-SiC particles of average size 40-200nm. A356 alloy is the most common aluminum alloy used in studying thixoforming process because the alloy shows good castibility and wide semi-solid temperature range. The chemical composition of aluminum alloy is shown in Table 1.

Table 1: Chemical composition in wt. % of A356 base alloy

Alloy	Si	Mg	Fe	Cu	Ti	Zn	Mn	Ni	Al
A356	6.5	0.45	0.08	0.003	0.09	0.008	0.006	0.005	93

In order to perform thixoforging at a specific solid fraction, it is very important to determine the solidus and liquidus temperature of A356 alloy. The Differential Scanning Calorimeter (DSC) technique is used for this purpose. For DSC test, 15mg mass of A356 alloy is heated to 650°C at rate of 10°K/min. The solidus and liquidus temperature of the alloy can be obtained from the DSC result as the starting and ending points of the endothermic reaction occurred during phase transformation as shown in Fig. 5.

Figure 6 shows the corresponding temperature and solid fraction curve for A356 alloy required for semi-solid processing.

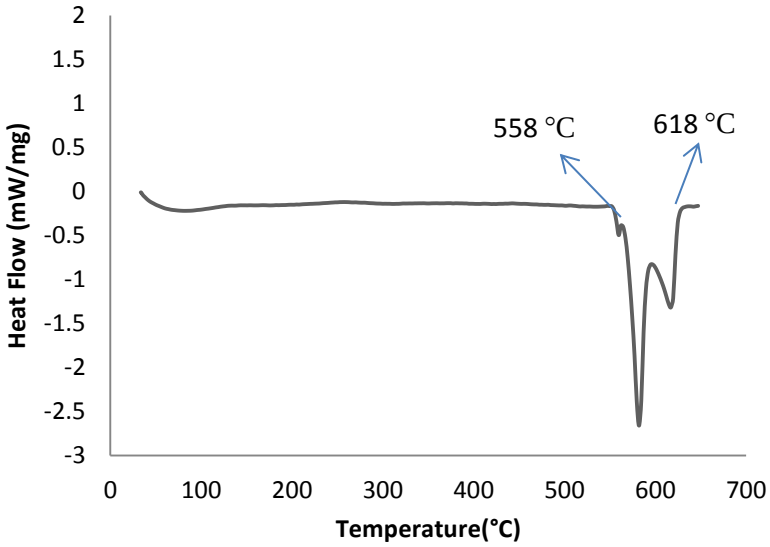

Figure 5: The DSC heating curve of the experimental alloy A356

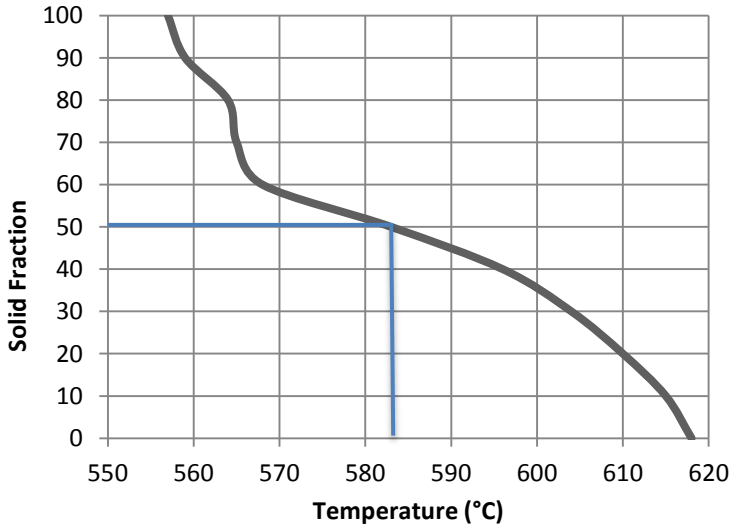

Figure 6: The volume fraction of solid phase in the experimental A356 aluminum alloy versus temperature

3.2 Ultrasonic Stir Casting Experimental Setup

As shown in Fig. 7, the experimental setup is made using a crucible furnace with an ultrasonic exciter to mix the nano particles in the aluminum alloy melt. The crucible furnace consists of an electric resistance-heating unit for melting the aluminum alloy in a SiC crucible. The ultrasonic exciter consists of a titanium alloy waveguide (sonotrode) coupled to an ultrasonic converter (transducer) for ultrasonic processing inside aluminum melt, a cooling jacket with compressed air supply is necessary to keep the transducer from overheating. The temperature of melt is monitored using a thermocouple.

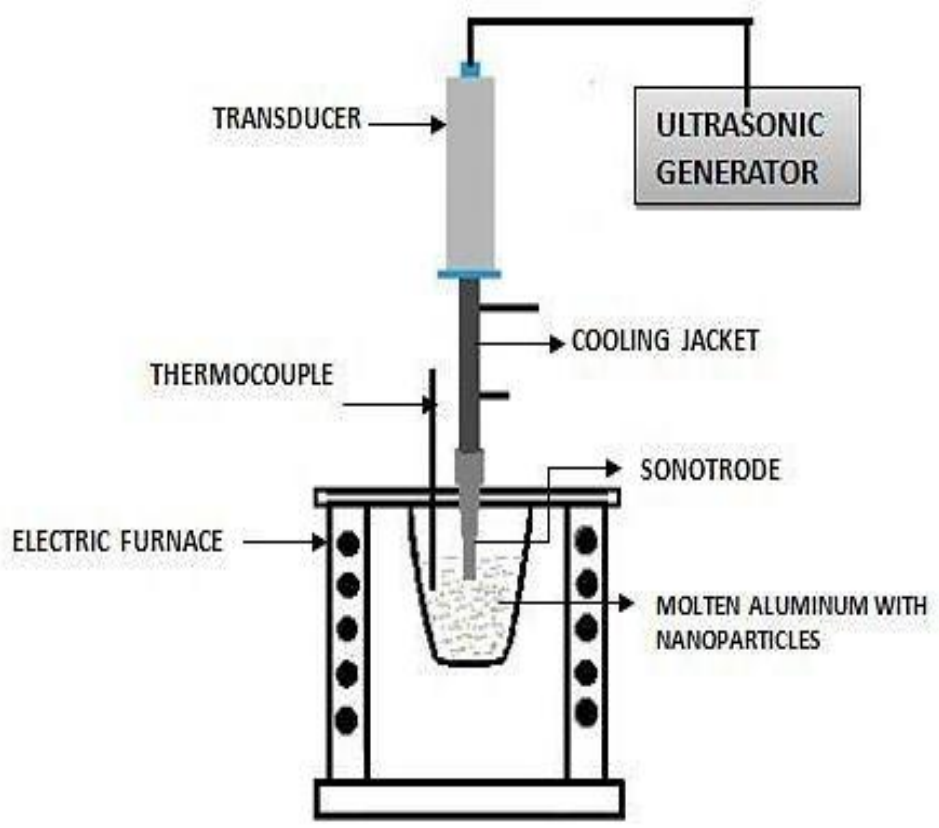

Figure 7: Schematic of Ultrasonic stir casting setup

The ultrasonic system consists of a 20 kHz generator, an air cooled converter (transducer), cooling jacket, booster and sonotrode to transmit ultrasonic vibration into aluminum melt. The effective power input to the transducer is 1.2kW depending on the sonotrode, booster combination used. The sonotrode size and frontal area defines the amplitude and intensity of stirring inside the melt. Table 2 shows two different sonotrode and corresponding intensities used for ultrasonic processing of aluminum melt.

3.3 Ultrasonic Stir Casting of A356/SiC Nanocomposite Procedure

The experimental procedure for fabricating the nanocomposite is as follows: An electrical resistance heated crucible with provision of pouring through tilting mechanism is used for melting. About 300gm of A356 alloy is placed inside the crucible and heated to 700^{o}C for complete melting of the alloy. Simultaneously, SiC nanoparticles with required weight fraction in the composite are heated to 900^{o}C in a muffle furnace. The temperature of the aluminum melt is brought down to 620^{o}C to obtain more viscous melt which helps in mixing the nanoparticles and also improves the wetting between SiC and A356 melt. Preheated SiC particles are added into the vortex generated using a mechanical stirrer inside the melt. After incorporating nanoparticles, the temperature is raised to 700^{o}C for ultrasonication. For dispersing SiC and to break agglomeration in the melt, high intensity ultrasonic wave was used. The ultrasonic sonotrode (titanium waveguide) is inserted inside the melt for 30mm depth and stirring (ultrasonic vibration) was performed for 15minutes.

Table 2: Ultrasonic intensity used for stirring inside aluminum melt

Sonotrode	Frontal area (cm^2)	Amplitude with booster (μm)	Intensity W/cm^2
BS2d22	3.8	50	80
CS2d40L2	32	32	40

After ultrasonication the melt becomes viscous, this would make it difficult for pouring inside the die due to tilt pouring mechanism. So in order to have fluidity, the melt is quickly heated to temperature of 730-750^{o}C before finally pouring it in a die preheated to 200^{o}C. Figure 8 shows the temperature and time sequence in fabricating the nanocomposites. The composite billet of dimension 30mm*30mm*100mm are obtained after each casting.

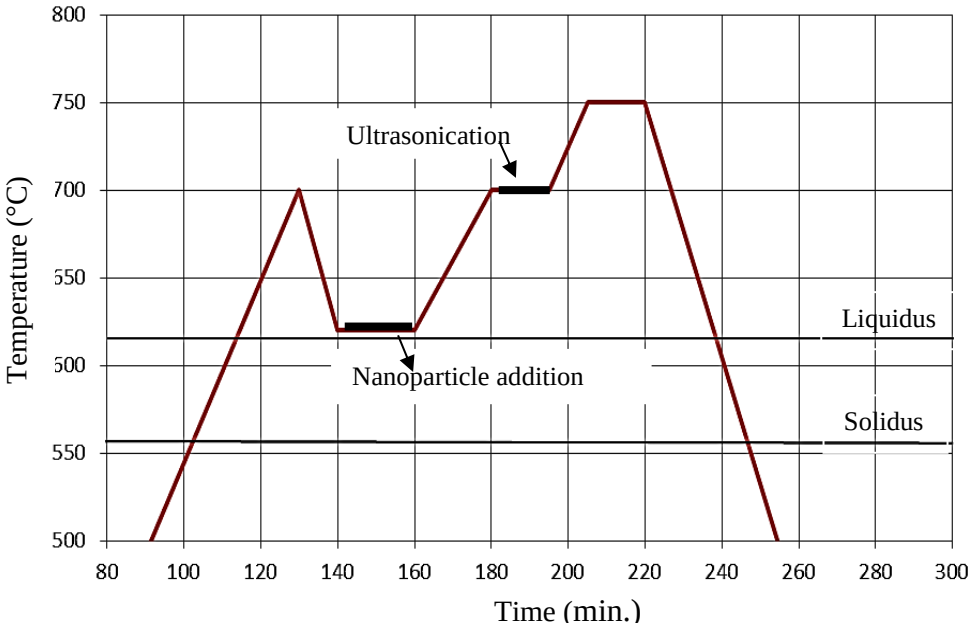

Figure 8: Schematic illustration of the temperature–time sequences during nanocomposites fabrication

3.4 Induction Heating Procedure

Induction heating study of matrix material A356 and its composites was conducted in order to study the proper heating regime for the thixoforging process. The induction heating unit consists of 100kW low frequency (1-20 kHz) power system with water cooled copper coil. The aim of induction heating study was to vary the power of induction for controlling time and temperature and obtaining a uniformly heated semi-solid billet. In order to freeze the microstructure, the billet was quickly quenched in a water bath at room temperature soon after the induction heating is completed. The schematic of induction heating experiment is shown in Fig. 9 with two thermocouples A and B positioned at the center and at the edge of the billet respectively.

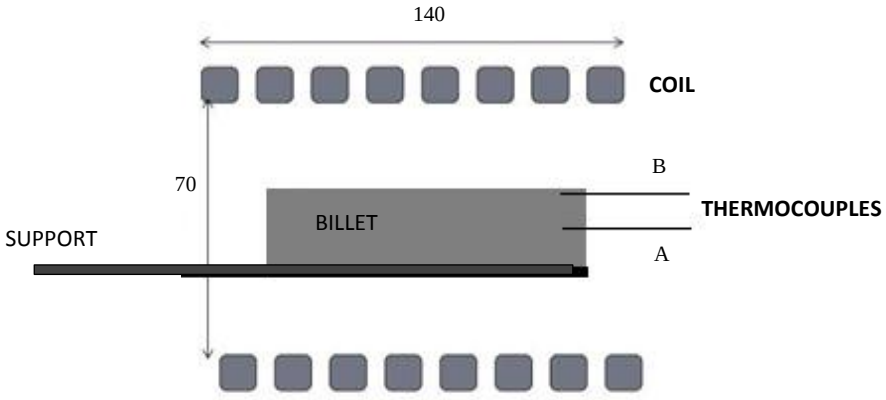

Figure 9: Schematic illustration of induction heating of A356 billet using a horizontal induction coil

For thixoforging operation the billets of A356 and its composites with dimensions 14 mm × 30 mm × 100 mm was machined for induction heating. The billet is heated on a tool steel flat plate support placed centrally inside the horizontal coil. Some portion of this

plate is outside the coil for holding and transporting the mushy billet to the die quickly. The time taken to transport the mushy billet inside the die is approximately 2 seconds. The billet was heated to two different solid fractions of 50% and 60% with two different holding (temperature soaking) times of 1 and 2 minutes for characterizing.

3.4.1 Reheating temperatures for nanocomposites

The reheating temperatures for the nanocomposite are obtained from the temperature and solid fraction curve for matrix A356 alloy and volume fraction of SiC reinforcement. For A356 alloy the semi-solid temperatures corresponding to 60% and 50% solid fraction are 568^{o}C and 583^{o}C respectively. The calculated increment in reheating temperatures for nanocomposite is shown in Fig. 10 below.

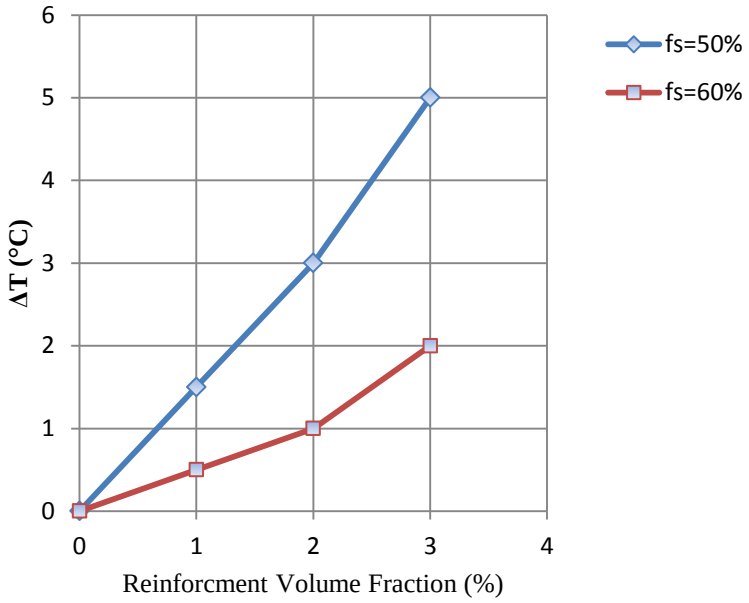

Figure 10: Relationship between reinforcement volume fraction and increment temperature to increase from the temperature-solid fraction curve of A356 to obtain reheating condition for nanocomposites

3.5 Thixoforging Experimental Procedure

After producing feedstock material from ultrasonic stir casting, the billet reheated from induction heating is quickly transferred to the die for deformation under pressure.

The thixoforging operation was carried out using a 50ton hydraulic press with ram speed of 12mm/sec. A die with dimension 30mm*45mm*120mm was manufactured according to the material flow characteristic of a rectangular semi-solid billet [Fig. 11]. The die is equipped with an extractor in the base of lower die to quickly remove the forged part after forging. An anti-seize grease containing aluminum, copper and graphite elements is applied on the walls and base of the lower and upper die in order to facilitate forging process. The grease not only helps in easy removal of the part but also assists the flow of material inside the die during forging operation. The die is uniformly heated using cartridge heaters separately placed in the upper and lower die and thermocouples are placed at different locations in the die to monitor the die temperature. The initial dimension of billet used for thixoforging was 14mm*30mm*100 mm and the dimension of part obtained after thixoforging was (6.6-7.5) mm*(44) mm*(110-120) mm. The final thickness of the component was dependent on the solid fraction in the mushy billet. That is the thickness of the component thixoforged at 60% solid fraction was more than that of 50% solid fraction.

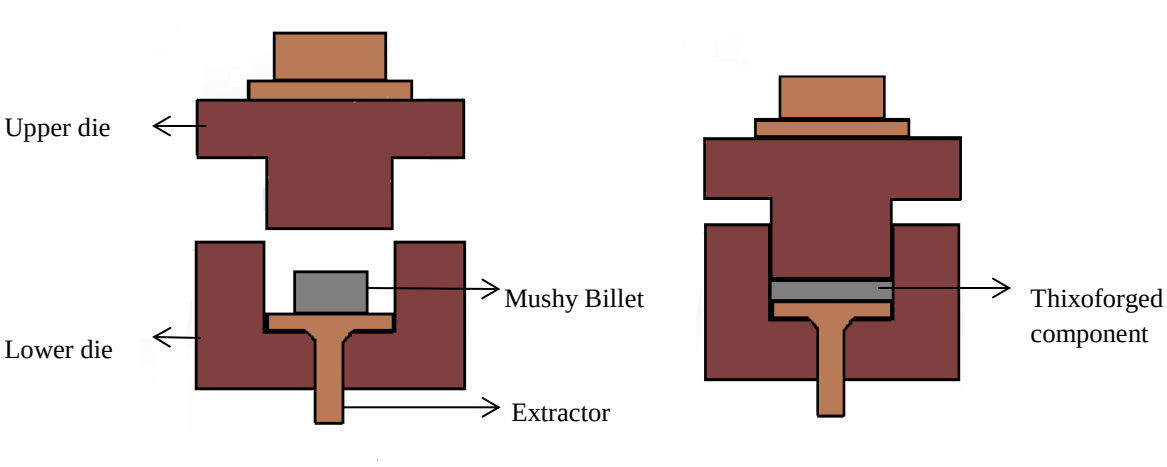

Figure 11: Schematic of thixoforging operation

3.6 Characterization of Samples

3.6.1 Microstructure analysis

For studying the microstructural features of the samples from the as-casted and thixoforged billets, samples are first mounted in a trans-optic powder sintered using Evolution, IPA 40 Remet mounting instrument. The mounted samples are grinded, polished and etched with Keller's reagent to reveal the microstructure. Keller's reagent was prepared using 2ml HF, 3ml HCl (conc.), 5ml HNO_3 and 190ml water. The optical microscope (MEIJI-Techno optical microscope, Japan) with a built in INFINITY camera driven by image analyzing software is used to inspect and characterize the microstructure. To quantify the globularization of microstructure, the area, (A) and perimeter, (P) of α-phases (primary phases) is measured using the software to evaluate the equivalent diameter and shape factor. The equivalent diameter, (D_{Eq}) is represented using Eq. (3.1).

$$D_{Eq} = \sqrt{\frac{4A}{\pi}} \tag{3.1}$$

The shape factor, S describes the circularity of the solid grains and is represented by Eq. (3.2).

$$S = \frac{P^2}{4\pi A} \tag{3.2}$$

A JEOL Scanning Electron Microscopy (SEM) model JSM 646 0 with Energy Dispersive X-ray (EDX) was used to analyze the dispersion of SiC particles, porosity and fracture surfaces of the tensile test samples.

3.6.2 Density measurements

The density of the as-casted and thixoforged samples was determined using Archimedean method of weighing flat pieces cut from the samples first in air and then in water. The theoretical density of matrix A356 and SiC are 2.68gm/cm^3 and 3.21gm/cm^3 respectively. The theoretical density of nanocomposites was calculated using the rule of mixtures according to the weight fraction of the SiC particles. Densimeter is used to determine the actual densities of samples with distilled water as an auxiliary liquid and an accurate digital balance with 0.1 mg resolution. The density of sample is measured using Eq. (3.3) and the amount of porosity in the sample can be evaluated.

$$\rho = \frac{w}{w-wo} * \rho o \tag{3.3}$$

Where ρ, ρ_o, w, w_o are density of the sample, density of water, weight of sample in air and weight of sample in water respectively.

3.6.3 Hardness measurements

The hardness of the aluminum alloy A356 and its nanocomposite obtained through different processing methods was measured using Vickers Hardness tester (Buehler MMT-3 series digital micro hardness tester, USA) with 0.1kgf of load applied for 10sec. Samples for hardness testing were made flat and polished. Hardness measurement is made at different positions on the sample. The hardness value represents the average of 6-10 readings taken at each site on the composite sample.

3.6.4 Tensile test measurements

To determine the tensile properties of the nanocomposite, tensile samples from the as-casted and thixoforged billets are machined according to ASTM E8 standard [66] (Fig. 12) and tested with a rate of 0.5mm/minute using Instron 3367 testing machine. The objective of tensile tests was to determine the yield strength, ultimate tensile strength and percentage elongation.

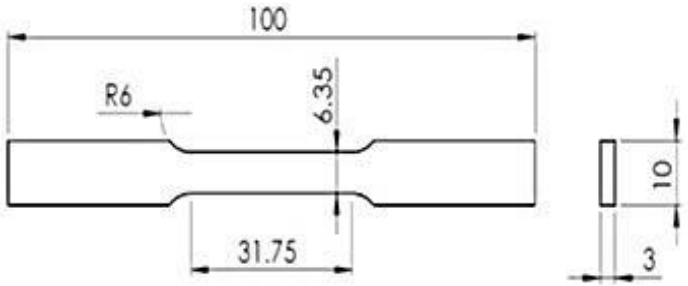

Figure 12: Sub size tensile test sample (dimensions in millimeters)

3.6.5 T6 heat treatment

The tensile tests of the composites are also performed after T6 heat treatment. This treatment is useful in homogenizing the microstructure and eliminating lattice distortion and mismatch in the composite material caused after casting process. The selected T6 heat treatment condition for A356 alloy according to ASTM B-917 standard [67] is shown in Table 3. The T6 heat treatment consists of solution hardening by isothermal heating at a specific temperature in a small resistance furnace. This is followed by rapid quenching and age hardening by again reheating to a specific temperature and holding for certain time.

Table 3: T6 heat treatment conditions for A356 alloy

Alloy	Holding temperature in solution hardening process (°C)	Holding time (hours)	Holding temperature in age hardening process (°C)	Holding time (hours)
A356	540	8	170	12

Table 4: Summary of Ultrasonic Stir Casting Experiments

Alloy (Matrix)	Reinfo.	Composition wt%	Ultrasonic Intensity ($W/cm^{2)}$	Other Processing Conditions	Characterizations
A356	SiC_p	1%, 2%, 3%	40, 80	Ultrasonication Time= 15 min. Casting temp.= 730°C, Die temp.= 200°C	SEM, Optical, Hardness, Porosity, Tensile test

Table 5: Summary of Thixoforging Experiments

Matrix	Reinforcement and composition wt. %	Induction heating conditions	Thixoforging conditions	Characterizations
A356	SiC_p 1%, 2%, 3%	Solid Fractions f_s= 60% and 50% Holding time = 1min. and 2min.	Die temp.=350°C, ram speed 12mm/sec.	SEM, Optical, Porosity, Hardness, Tensile test & Surface roughness test

CHAPTER 4

RESULTS AND DISCUSSION

4.1 Ultrasonic Stir Cast A356/SiC Nanocomposite

4.1.1 Optical micrographs of A356/SiC nanocomposite samples

The optical micrographs of nanocomposites are analyzed for change in microstructure of with addition of SiC nano particles. Figure 13 shows optical micrographs for stir casted monolithic alloy and A356 reinforced with 1, 2 and 3wt. % SiC agitated with different ultrasonic intensities of 40W/cm^2 and 80W/cm^2. The microstructure consists of α-Al primary phase surrounded by Al-Si eutectic fine platelets. In many areas in the microstructure, degenerated dendritic structure with some equiaxed and globular grains are seen. In all cases the monolithic alloy didn't show any sign of porosities with pouring temperature of 730^{o}C and die temperature of 200^{o}C. However in samples containing 2 and 3 wt. % SiC some degree of porosities are observed which also correspond to the densification data. The samples with SiC nanoparticles shows similar microstructure but with some black regions lying in the eutectic. These black regions represent the locations of nanoparticles trapped by the solidification front. Also it is observed from the micrograph that with increase in SiC content the microstructure is refined by the change in volume of primary phases. In Fig. 14, the microstructure after T6 condition shows a substantial difference in the size and shape of silicon particles, wherein the morphology of silicon particles were more spherical. The microstructure clearly reveals the change in volume of secondary phase with increase in reinforcement content.

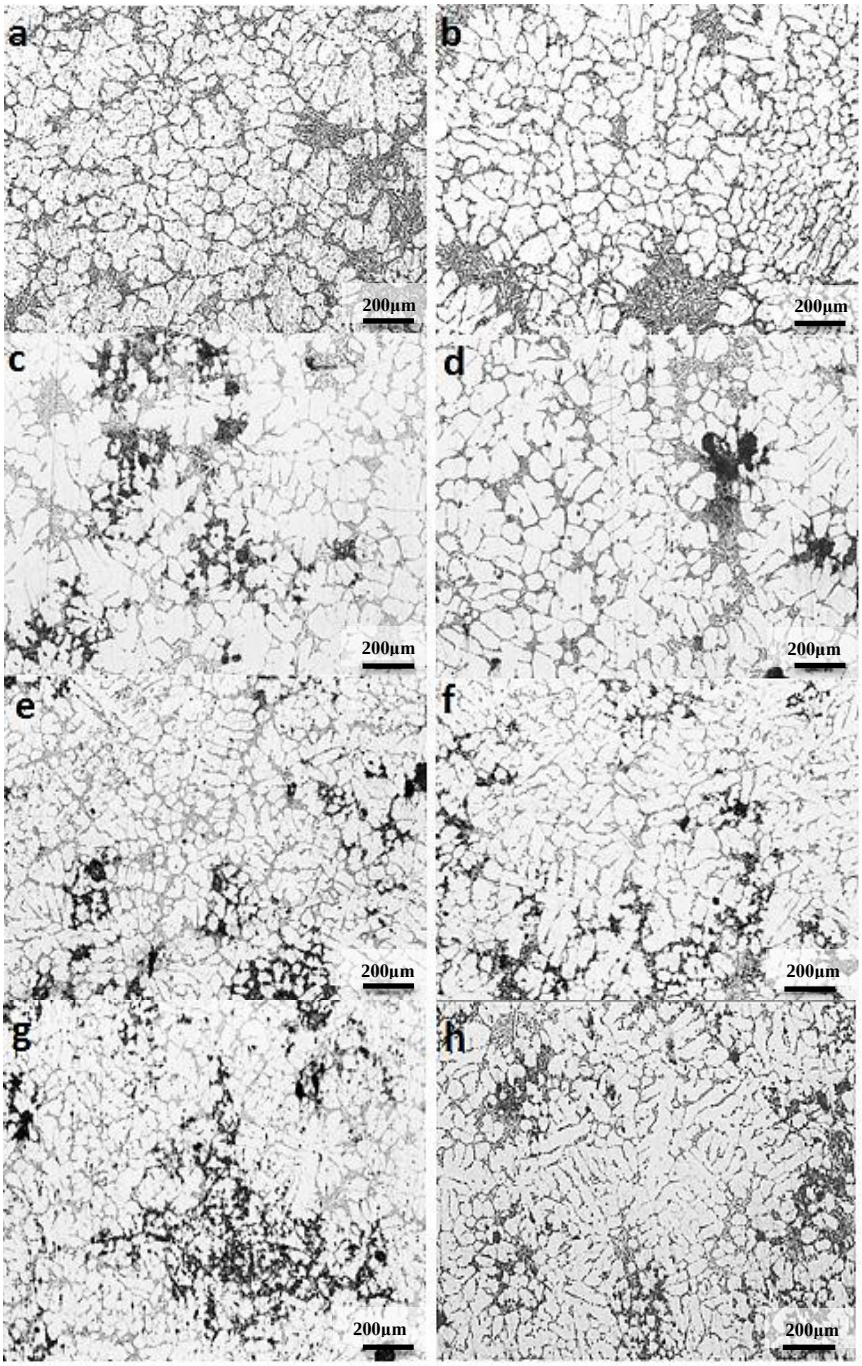

Figure 13: Optical Micrographs of stir casted A356-SiC nanocomposite treated with 40W/cm^2 intensity with a) 0wt. %, c) 1wt. %, e) 2wt. %, g) 3wt. %SiC and 80W/cm^2 intensity with b) 0wt. %, d) 1wt. %, f) 2wt. %, and h) 3wt. %SiC

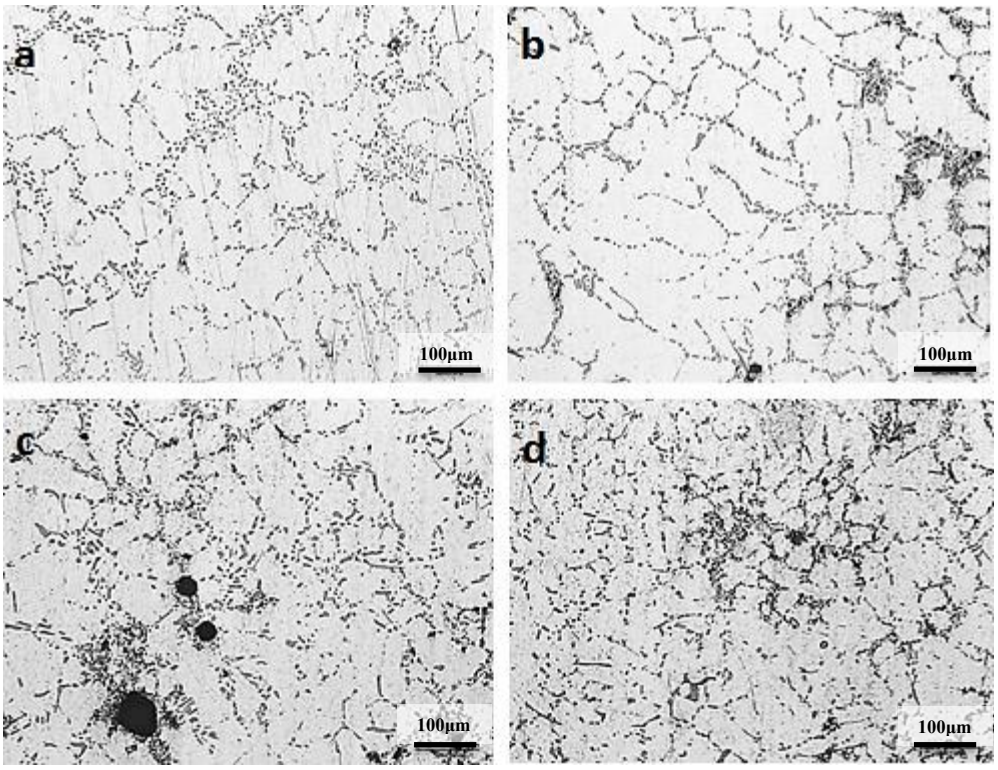

Figure 14: Optical Micrograph of T6 heat treated A356-SiC nanocomposite with a) 0wt. %, b) 1wt. %, c) 2wt. %, and d) 3wt. % SiC

4.1.2 SEM micrographs of A356/SiC nanocomposite samples

Figure 15 and 16 shows SEM micrographs for the stir casted nanocomposite samples treated with ultrasonic intensities of 40W/cm^2 and 80W/cm^2 respectively. Similar morphologies were observed in SEM micrographs as seen in optical study. It is seen from Fig. 15 that the microstructure of A356 alloy and its nanocomposites typically consists of gray colored lamellar and flake like silicon plates embedded in the relatively dark α-Al matrix. The nanocomposite additionally consists of white colored SiC particles predominantly lying at the grain boundaries. It was observed that at low ultrasonic intensity (40W/cm^2) more clusters of SiC were observed in these regions. This represents the inadequacy of low ultrasonic intensity in breaking the clusters and avoiding the

agglomeration of SiC nanoparticles at higher weight percentage. Moreover micro pores were seen in the stir casted samples with increase in reinforcement content.

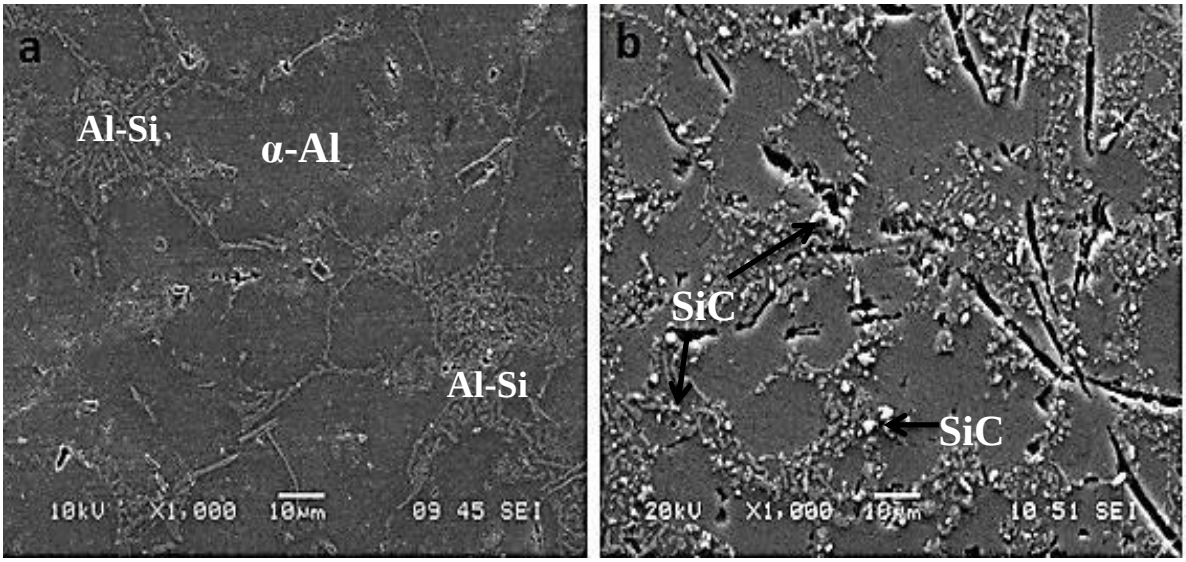

Figure 15: SEM micrographs of stir casted A356/SiC nanocomposite treated with 40W/cm^2, containing a) 0 wt. %SiC and b) 3wt. %SiC reinforcement

Figure 17 and 18 shows EDS spectrum for a stir cast nanocomposite where in reasonable amount of reinforcing phase was observed in the top and bottom region of the casting obtained after pouring inside the die. But it can be distinguished that the amount of reinforcement phase in the top region is slightly more compared to the bottom region of the cast billet. Figure 19 shows the EDS mapping of nanocomposite showing good distribution of SiC particles in the A356 matrix for the samples treated with 80W/cm^2 intensity. Whereas for the sample treated with 40W/cm^2, clear cluster of SiC is observed (Fig. 20).

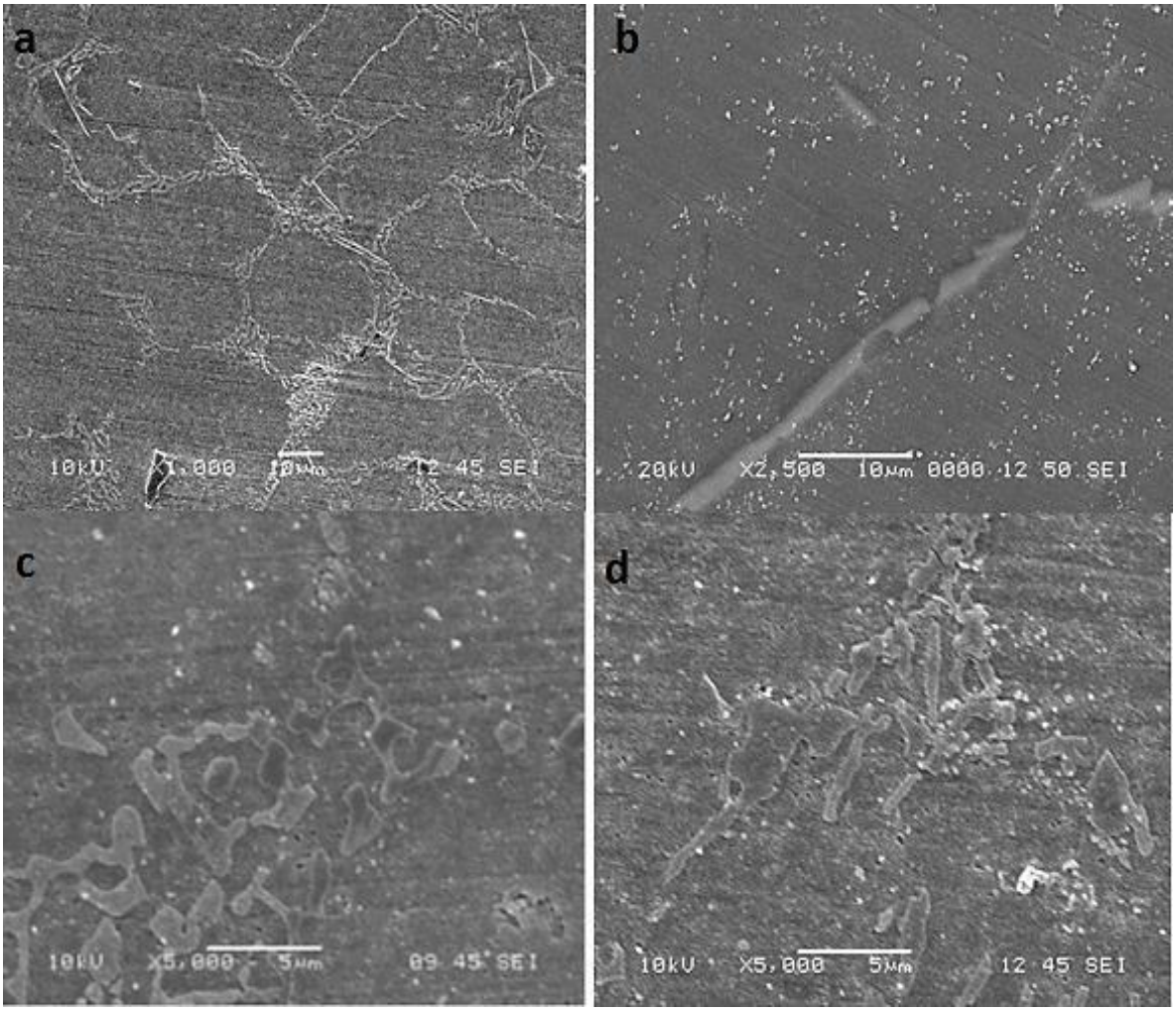

Figure 16: SEM micrographs of Stir casted A356/SiC nanocomposite treated with 80W/cm^2, containing a) 0wt. %SiC b) 1wt. %SiC c) 2wt. %SiC and b) 3wt. %SiC reinforcement

The SEM micrographs of nanocomposite treated with 80W/cm^2 showed reasonable dispersion of SiC particles (Fig. 16). However at higher weight percentage of reinforcement some particle clusters of size ranging from 200-500nm was persistent. This is far better than the samples treated with 40W/cm^2 wherein SiC clusters of up to 1micron were observed.

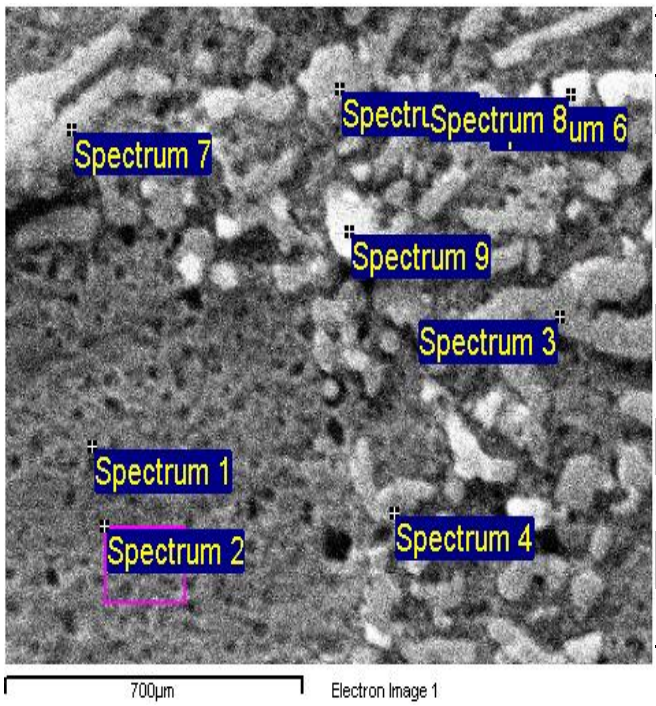

Spectrum	C	O	Al	Si
Spectrum 1	2.27	0	95.76	1.97
Spectrum 2	0	0	97.86	2.14
Spectrum 3	2.7	0	62.43	34.87
Spectrum 4	0	0	74.71	25.29
Spectrum 5	1.74	9.12	58.14	31
Spectrum 6	1.46	2.37	56.74	39.43
Spectrum 7	1.93	0	67.63	30.44
Spectrum 8	12.27	0	42.94	44.79
Spectrum 9	15.32	0	32.87	51.81

Figure 17: EDS analysis result for 2 wt. % SiC nanocomposite; Bottom of the casting

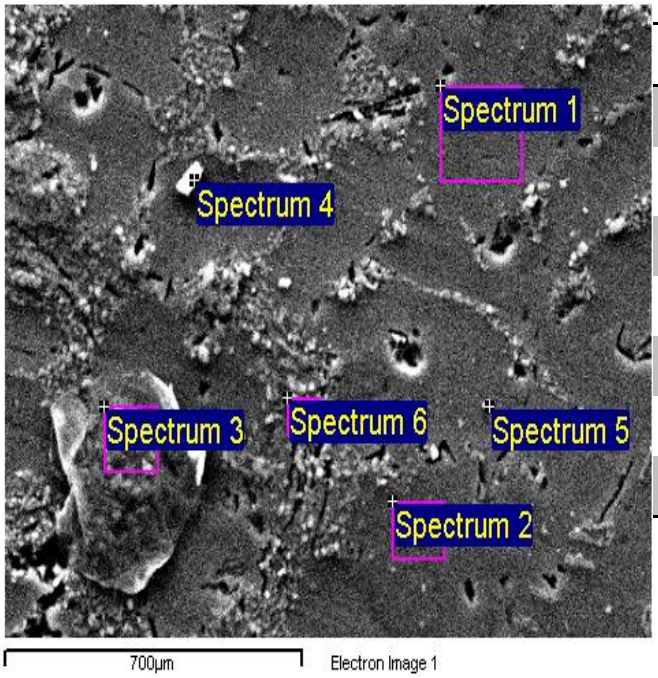

Spectrum	C	O	Al	Si
Spectrum 1	0.7	0.44	96.85	2.01
Spectrum 2	0.74	0.47	94.47	4.32
Spectrum 3	6.44	0.55	66.64	26.36
Spectrum 4	29.96	0.93	62.13	6.98
Spectrum 5	1.11	0.27	95.44	3.18
Spectrum 6	22.32	1.37	35.27	41.04

Figure 18: EDS analysis result for 2 wt. % SiC nanocomposite; Top of the casting

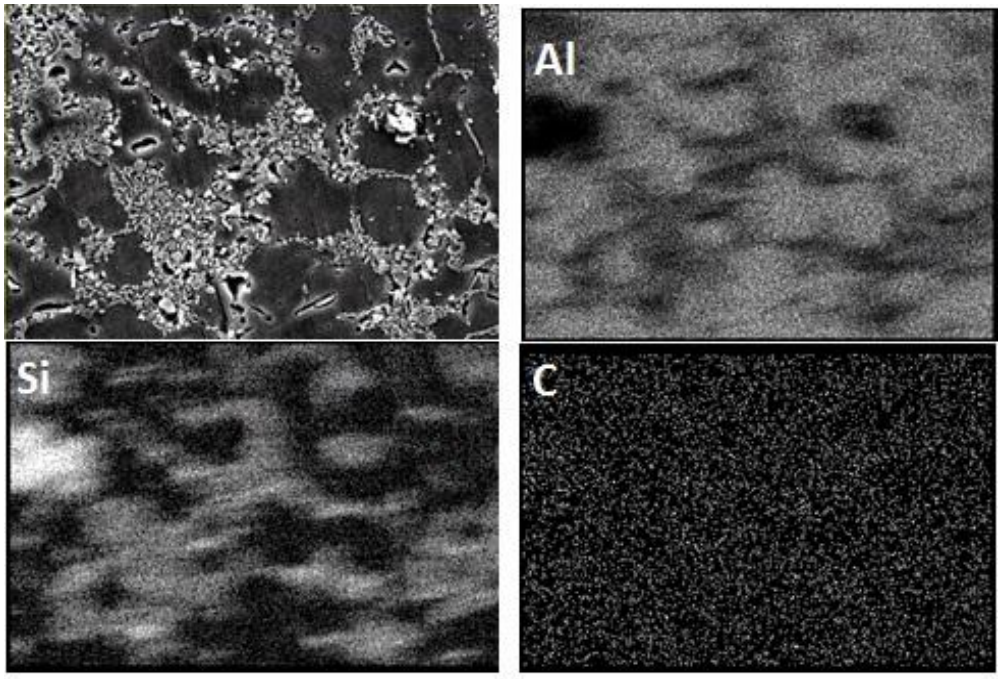

Figure 19: SEM micrograph of A356/3wt%SiC nanocomposite treated with 80W/cm^2 showing EDX mapping of Aluminum, Silicon and Carbon elements

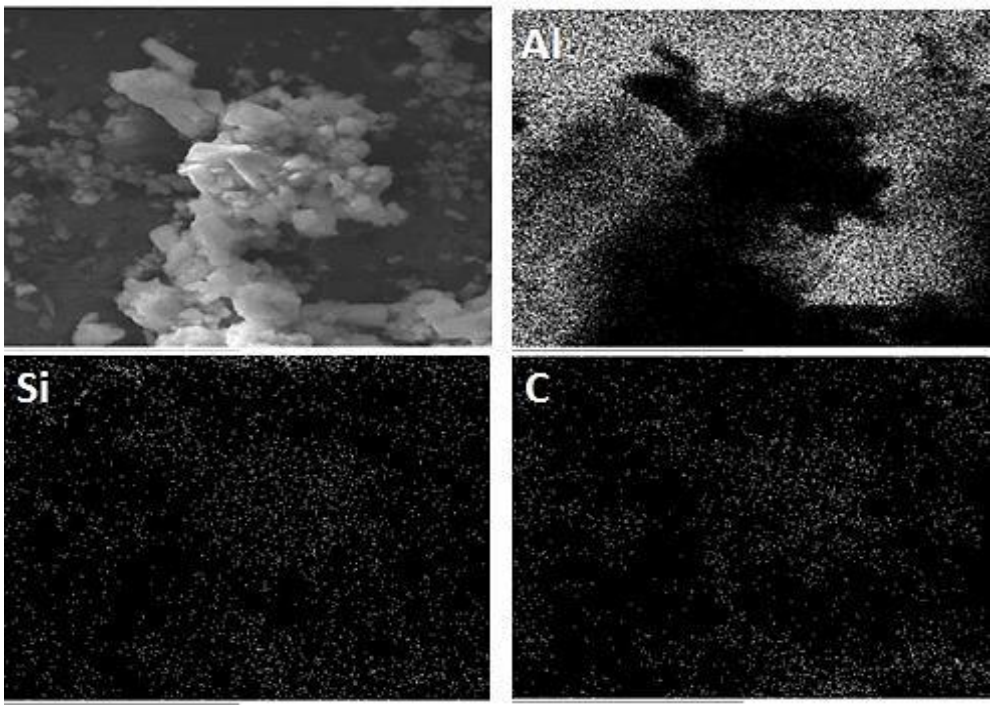

Figure 20: SEM micrograph of A356/3wt%SiC nanocomposites treated with 40W/cm^2 showing EDX mapping of Aluminum, Silicon and Carbon elements

4.1.3 Porosity and hardness of stir cast A356/SiC nanocomposite samples

The monolithic alloy and its nanocomposites treated with ultrasonication were tested for porosity and hardness after stir casting. Samples of A356/SiC nanocomposite synthesized by stir casting with pouring temperature of 730^{o}C and die temperature of 200^{o}C were used and it gave the highest densification of 99.82% for the monolithic alloy A356 after ultrasonication. As shown in Table 6, the densification results shows that with increase in SiC content there is tendency of formation of pores inside the castings. It is also seen that with increase in SiC content there is increase in hardness of the sample. However there is inconsistency in the hardness values from the center till the edge (close to the die surface) of the nanocomposite sample as seen in Fig. 21 and 22. This difference in hardness is due to the growth of grains in the die during solidification and relative distribution of reinforcement particles. More deviation in hardness values is observed in nanocomposite samples treated with ultrasonic intensity of 40W/cm^2 which is also shown in Table 7. The hardness results and standard deviation in the values also shows that the nanocomposite samples treated with 80W/cm^2 intensity gave better dispersion of nanoparticles compared to samples treated with 40W/cm^2.

Table 6: Densification (Porosity) of Stir Cast samples containing 0, 1, 2 and 3wt. % SiC with different ultrasonic intensities for A356 nanocomposite

Sample SiC wt.%	Number of samples	Densification (%)			
		40W/cm^2		80W/cm^2	
		Average	S.D	Average	S.D
0	6	99.8	0.02	99.82	0.03
1	6	98.7	0.38	99.1	0.05
2	6	97.1	2.43	98.4	0.41
3	6	96.4	1.66	97.5	0.25

Table 7: Hardness of Stir Cast samples containing 0, 1, 2 and 3wt. % SiC with different ultrasonic intensities for A356 nanocomposite

Sample SiC wt.%	Number of samples	Vickers Hardness (H_V)			
		40W/cm^2		80W/cm^2	
		Average	S.D	Average	S.D
0	3	66.5	1.91	66.8	1.78
1	3	69.8	3.60	72	3.35
2	3	76	4.33	78	3.62
3	3	77.8	4.38	81.2	4.01

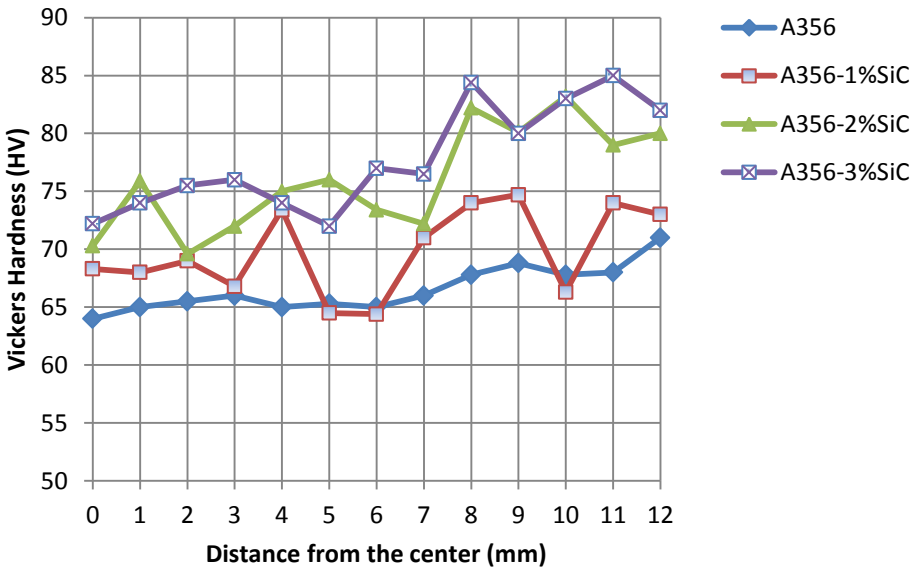

Figure 21: Hardness of A356-SiC nanocomposite synthesized with 40W/cm^2 Ultrasonic intensity

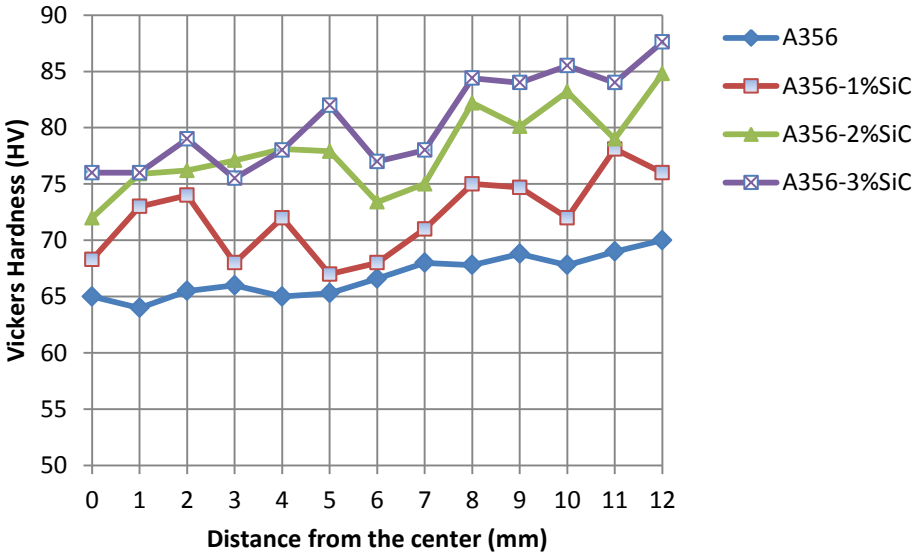

Figure 22: Hardness of A356-SiC nanocomposite synthesized with 80W/cm^2 Ultrasonic intensity

4.1.4 Tensile properties of stir cast A356/SiC nanocomposite samples

The tensile curves of nanocomposite exhibited brittle response due to the presence of SiC particles. As seen in Fig. 23 and 24 the tensile strength of nanocomposite is reduced with increase in amount of reinforcement. However the samples treated with 80W/cm^2 intensity showed higher strength and ductility compared to the samples treated with 40W/cm^2. This is attributed to better dispersion and less SiC clustering with use of higher ultrasonic intensity. Table 8, 9, 10 and 11 shows the tensile properties of nanocomposite synthesized with different stirring energy. It is observed that the samples containing SiC nanoparticles showed drastic decrease in ductility which was proportional to the amount of clustering observed.

The tensile response of T6 heat treated samples shows increase in UTS and Yield strength of nanocomposite due to the spheroidization of eutectic silicon particles and formation of Mg_2Si hardening precipitates. It is observed from Fig. 26 that the strength and ductility of nanocomposite containing 1wt. %SiC is higher compared to its monolithic alloy. This is attributed to the homogenizing of microstructure after T6 heat treatment and strengthening of alloy by the nanoparticles. However the properties remained low for samples containing 2 and 3wt. % SiC even after T6 heat treatment. Tensile response of samples treated with 40W/cm^2 followed same trend even after T6 heat treatment due to the presence of more amount of SiC clusters as seen in Fig. 23 and 25.

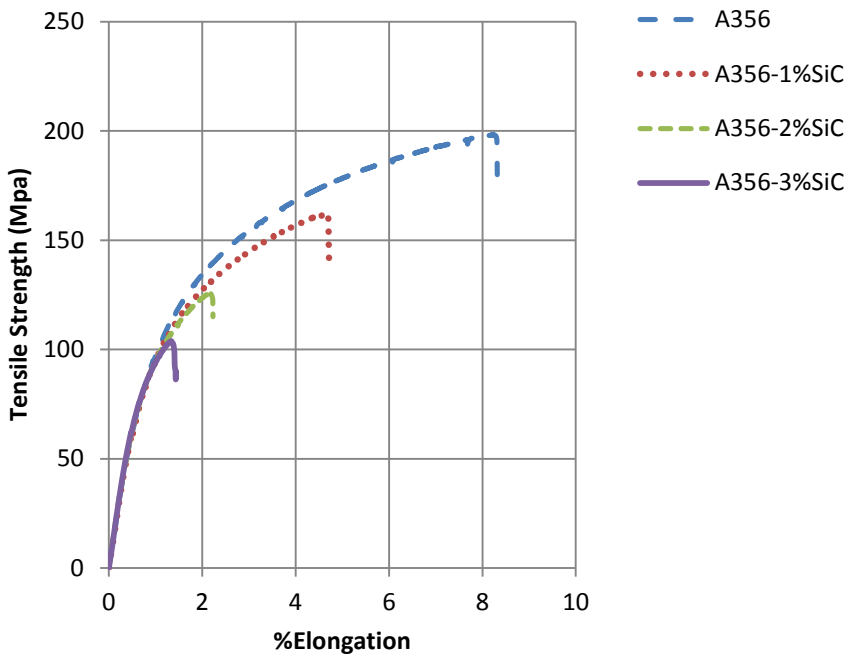

Figure 23: Stress-strain curves for A356/SiC nanocomposites after ultrasonic stir casting process using 40W/cm^2 ultrasonic intensity

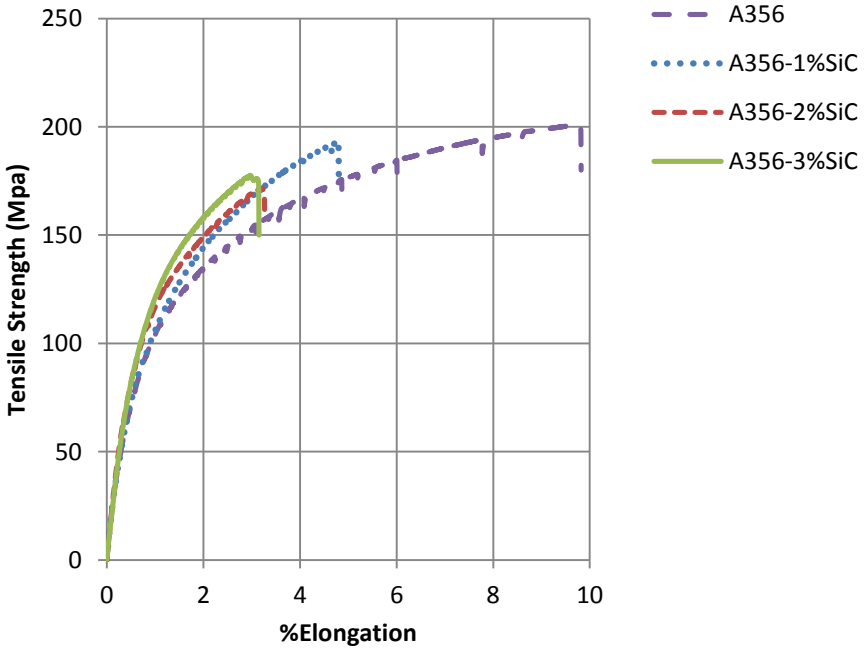

Figure 24: Stress-strain curves for A356/SiC nanocomposites after ultrasonic stir casting process using 80W/cm^2 ultrasonic intensity

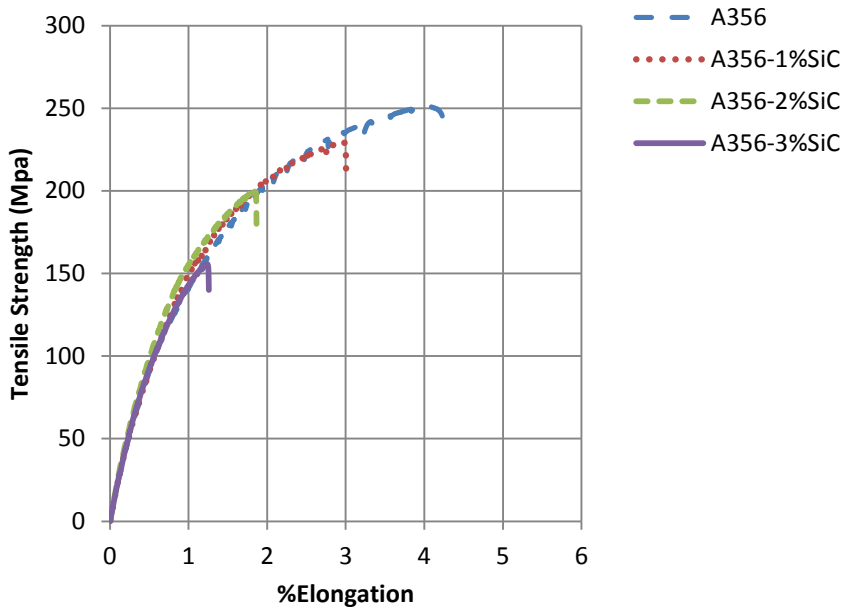

Figure 25: Stress-strain curves for A356/SiC nanocomposites after ultrasonic stir casting process using 40W/cm^2 ultrasonic intensity under T6 condition

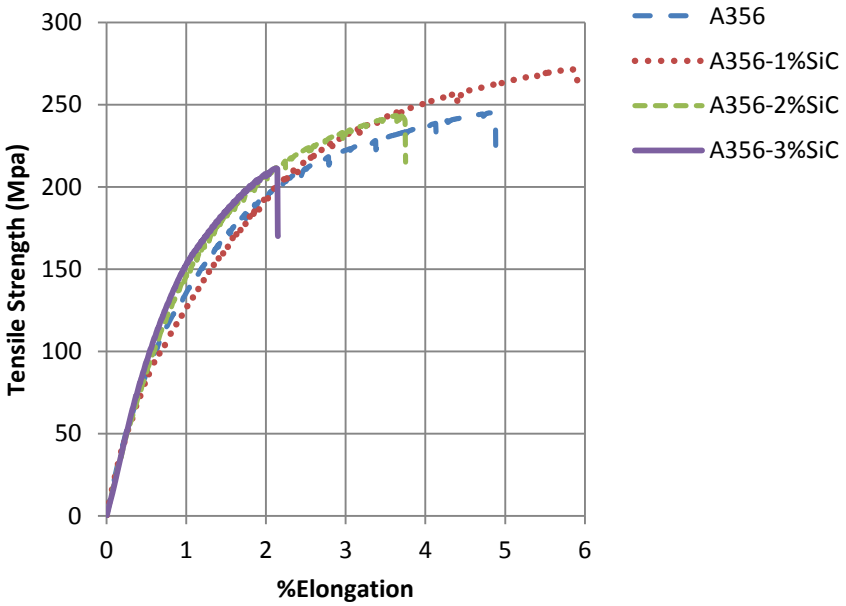

Figure 26: Stress-strain curves for A356/SiC nanocomposites after ultrasonic stir casting process using 80W/cm^2 ultrasonic intensity under T6 condition

Table 8: Tensile Test Results for Stir Casted A356/SiC nanocomposite treated with 40W/cm^2 ultrasonic intensity without T6 heat treatment

Sample	Number of Samples	UTS (MPa)		Yield Strength (MPa)		Elongation (%)	
Wt.% SiC	-	Average	SD	Average	SD	Average	SD
0	3	199.6	1.4	122.2	2.7	7.2	1.04
1	3	148.4	2.8	100.4	0.12	2.6	0.52
2	3	137.1	5.6	100.6	5.3	1.7	0.07
3	3	105.4	3.4	82.8	0.35	1.3	0.09

Table 9: Tensile Test Results for Stir Casted A356/SiC nanocomposite treated with 40W/cm^2 ultrasonic intensity with T6 heat treatment

Sample	Number of Samples	UTS (MPa)		Yield Strength (MPa)		Elongation (%)	
Wt.% SiC	-	Average	SD	Average	SD	Average	SD
0	2	234.2	17	141.8	4.8	3.4	0.84
1	2	192.5	36.6	137.4	15.6	2.1	0.87
2	2	168.2	31.3	129.9	12.8	1.4	0.43
3	2	177.6	21.8	132.2	10.5	1.5	0.3

Table 10: Tensile Test Results for Stir Casted A356/SiC nanocomposite treated with 80W/cm^2 ultrasonic intensity without T6 heat treatment

Sample	Number of Samples	UTS (MPa)		Yield Strength (MPa)		Elongation (%)	
Wt.% SiC	-	Average	SD	Average	SD	Average	SD
0	3	210.9	1.55	126.1	0.13	7.45	0.25
1	3	197.5	4.7	119.2	10.35	4.52	0.28
2	3	178.2	6.4	104.2	4.87	3.46	0.2
3	3	172.5	5.2	110.6	1.84	3.13	0.02

Table 11: Tensile Test Results for Stir Casted A356/SiC nanocomposite treated with 80W/cm^2 ultrasonic intensity with T6 heat treatment

Sample	Number of Samples	UTS (MPa)		Yield Strength (MPa)		Elongation (%)	
Wt.% SiC	-	Average	SD	Average	SD	Average	SD
0	2	237.2	7.9	149.9	3	4	1
1	2	262.7	8.7	154.9	3.9	4.8	1.1
2	2	234.1	9.1	155.6	0.9	3.3	0.4
3	2	214.9	3.7	150.2	3.6	2.3	0.2

4.1.5 Tensile fracture surfaces of stir cast A356/SiC nanocomposite

The fracture surfaces of tensile tested samples are analyzed using SEM. Figure 27 shows the tensile fracture surface of monolithic alloy and its nanocomposite treated with 40W/cm^2 ultrasonic intensity. The fracture regions of nanocomposites shows agglomerated SiC particles detached from the alloy matrix. The EDS analysis also shows the presence of SiC particles on the fracture surface in Fig. 28.

The fracture surfaces of A356/SiC nanocomposites treated with 80W/cm^2 ultrasonic intensity is shown in Fig. 29. The stir casted samples show trans-granular fracture with quasi cleavage morphology. As seen in Fig. 27a, 29a and 29c the cleavage steps or tear ridges are merged towards the direction of crack growth which is a typical mechanism for trans- granular fracture mode. The fracture surface after T6 heat treatment shows mixed morphologies including dimples, the size of these dimples were smaller with increase in amount of reinforcement (Fig. 29b, d, f and h).

Figure 29e, g illustrates the formation of large voids on the fracture surface of the A356 nanocomposites containing 2 wt. % and 3 wt. % SiC reinforcement. The large amount of SiC particles in the voids shows that the agglomeration of particulates provided sites for crack initiation and interfacial debonding resulting in reduced tensile properties of these nanocomposites.

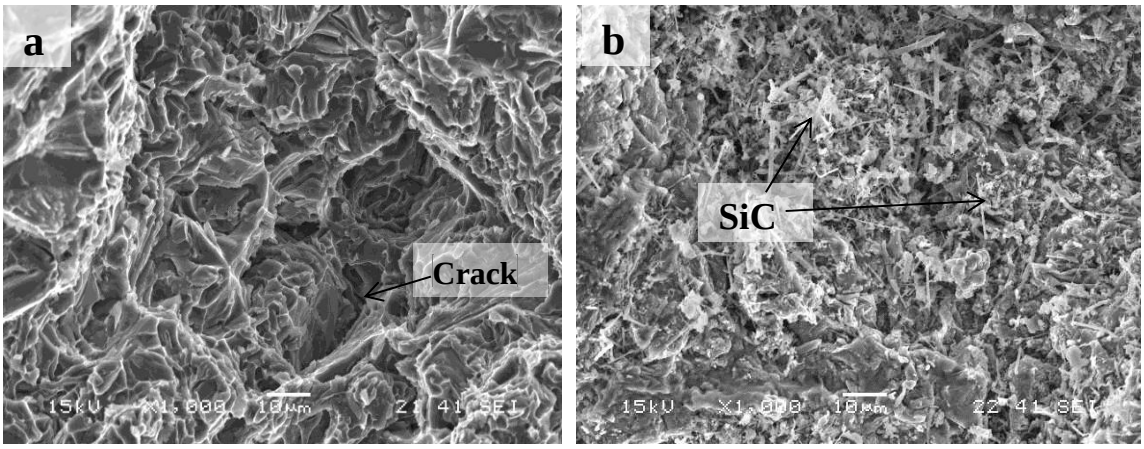

Figure 27: Tensile fracture surface of Ultrasonic stir casted A356-SiC nanocomposite treated with 40W/cm^2 intensity containing a) 0 wt. % and b) 3 wt. % SiC

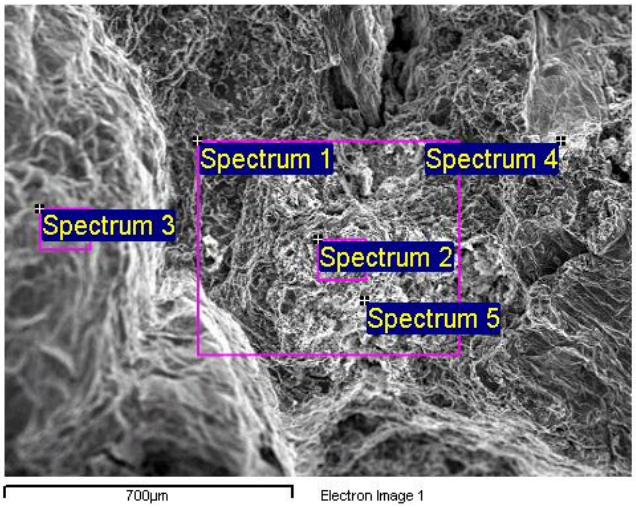

Processing option: All elements analyzed (Normalized in wt. %)

Spectrum	C	Mg	Al	Si	Fe	Total
Spectrum 1	12.15	1.51	50.64	33.40	2.30	100.00
Spectrum 2	26.25	4.73	9.16	59.87	0.00	100.00
Spectrum 3	0.52	0.71	72.89	23.86	2.01	100.00
Spectrum 4	1.42	1.74	73.09	23.35	0.41	100.00
Spectrum 5	4.42	1.43	62.70	31.46	0.00	100.00

Figure 28: EDS analysis of fracture surface of A356/SiC nanocomposite containing 3wt. % SiC reinforcement

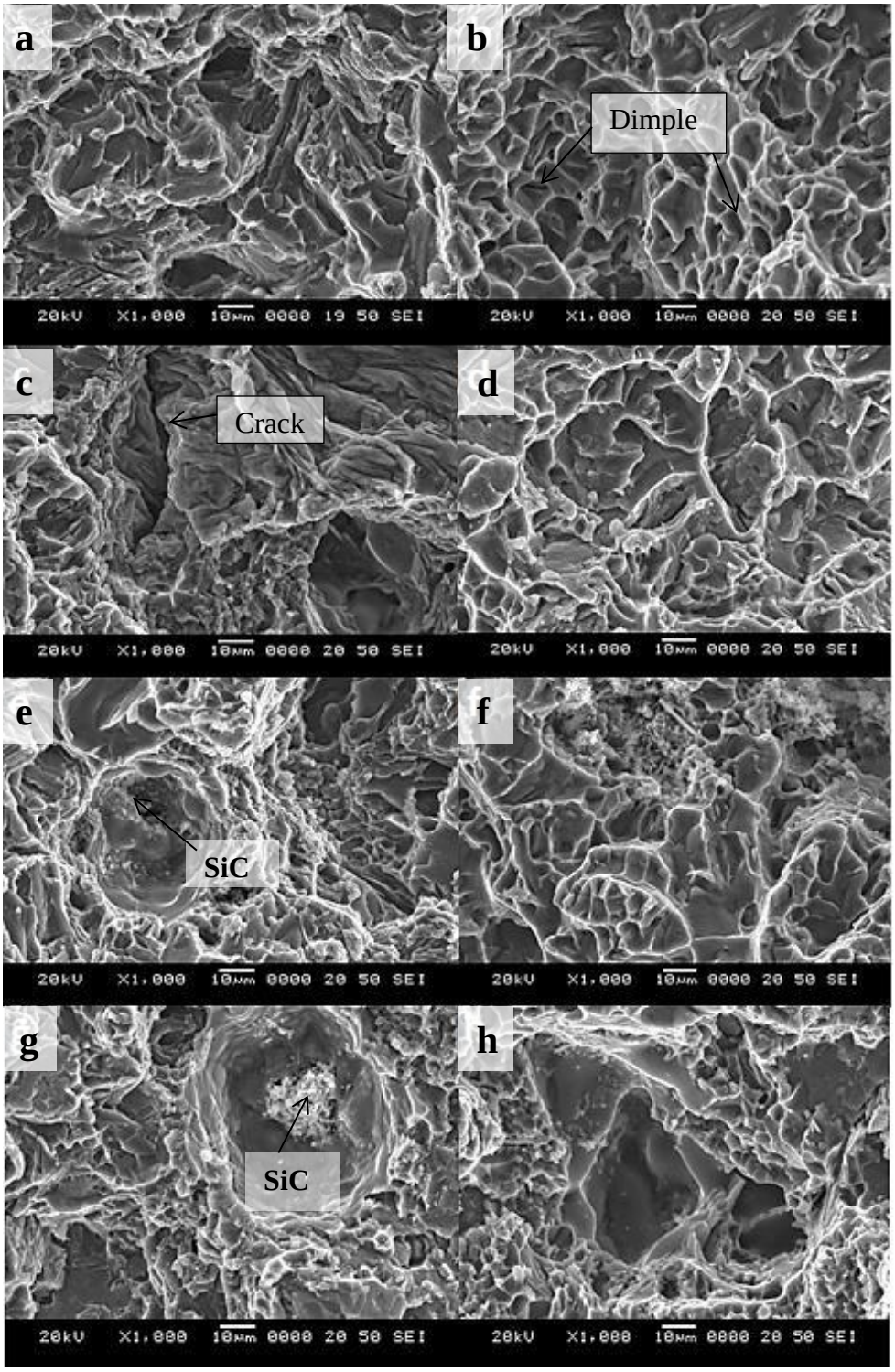

Figure 29: Tensile fracture surface of stir casted A356/SiC nanocomposite treated with 80W/cm^2 intensity containing a) 0wt. % SiC, b) 0wt. % SiC (T6), c) 1wt. % SiC, d) 1wt. % SiC (T6), e) 2wt. % SiC, f) 2wt. % SiC (T6), g) 3wt. % SiC and h) 3wt. % SiC (T6)

4.2 Induction Heating Experiment Results

4.2.1 Optimization of induction heating process

In order to satisfy the requirements of reheating, it is very important to optimize the heating of the billet with respect to the induction heating elements. The goal of these experiments was to determine a proper heating regime such that the required microstructure with uniform heating (less thermal gradient) is attained throughout the billet. Microstructure is revealed by quickly quenching the billet after induction heating is completed. Table 12 shows the induction heating parameters under investigation.

Table 12: Induction heating parameters

Semi-solid temperatures (^{o}C)	Power of induction (Watt)	Holding time (min.)
568, 577, 583	40 - 1200	0.5, 1, 2

Initially to obtain homogenous heating with less temperature gradient inside the billet, temperature readings at the center and at the edge are noted. By varying induction power, the thermal behavior of the billet is analyzed. As shown in Fig. 30, the heating time is inversely related to the power of induction. It is observed that with use of large induction power, temperature difference of more than 10^{o}C is noted. Also it is observed that the power of induction has to be gradually reduced in order to hold the billet uniformly near the semi-solid temperature. Otherwise overshooting is observed in which case it is

difficult hold the billet to a specified solid fraction. With use of intermediate power, temperature difference of less than 5^{o}C is noted.

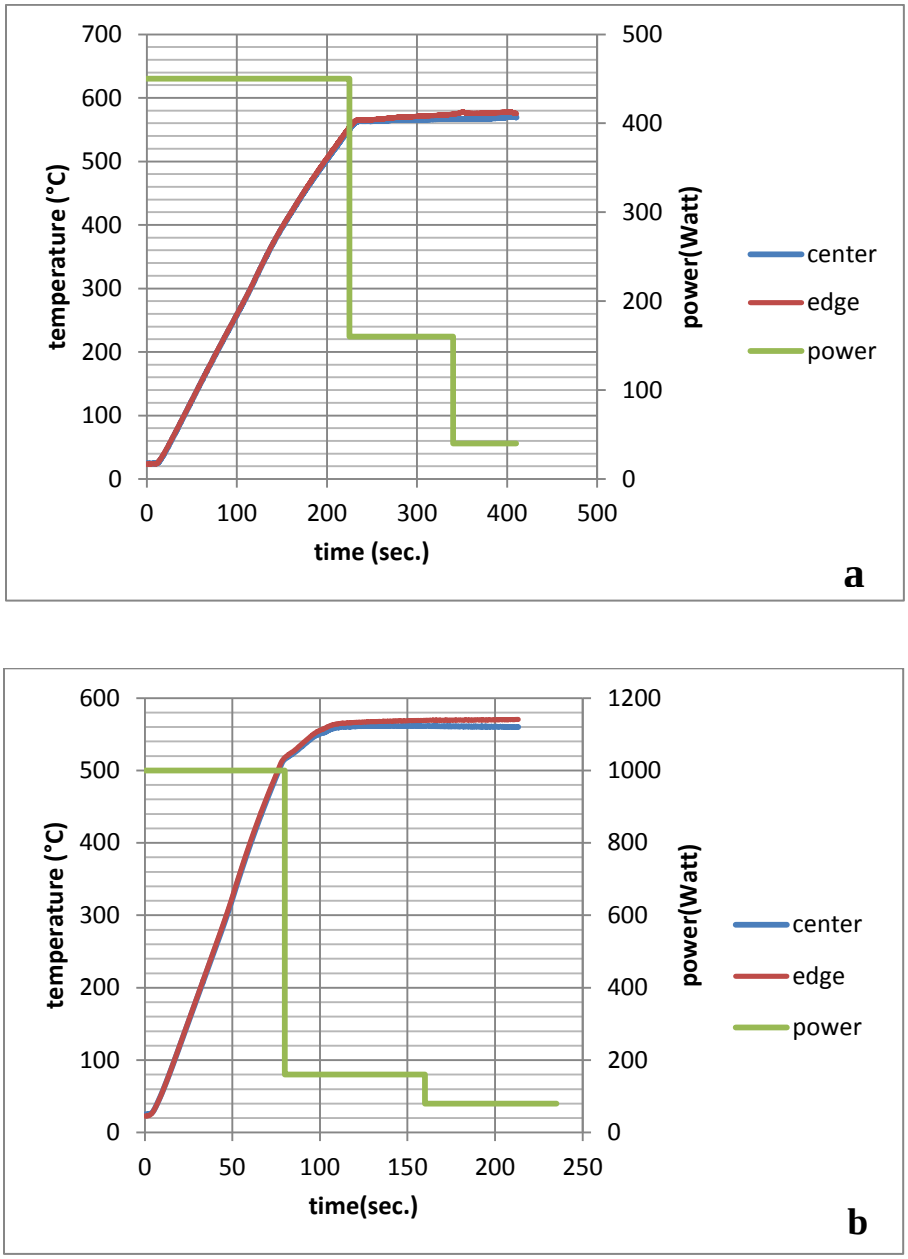

Figure 30: Temperature vs Time plot with different heating cycle lengths and the corresponding powers in reaching the temperature of 577^{o}C using a) intermediate power, b) high power

For studying the effect of holding time on the evolution of microstructure, the A356 billet is heated using intermediate induction power to a temperature of 577^{o}C and time for holding was varied from 0.5, 1 and 2 minutes. As seen in Fig. 31, at holding time of 0.5 minutes the microstructure of mushy billet was in initial stage of defragmentation, clearly majority of the primary phase couldn't develop a globular morphology. Liquid pools within solid regions can also be seen in Fig. 31a and in some regions of 31b. However with holding time of 2 minutes no liquid pool was observed and the primary phase was fully disintegrated and globularized.

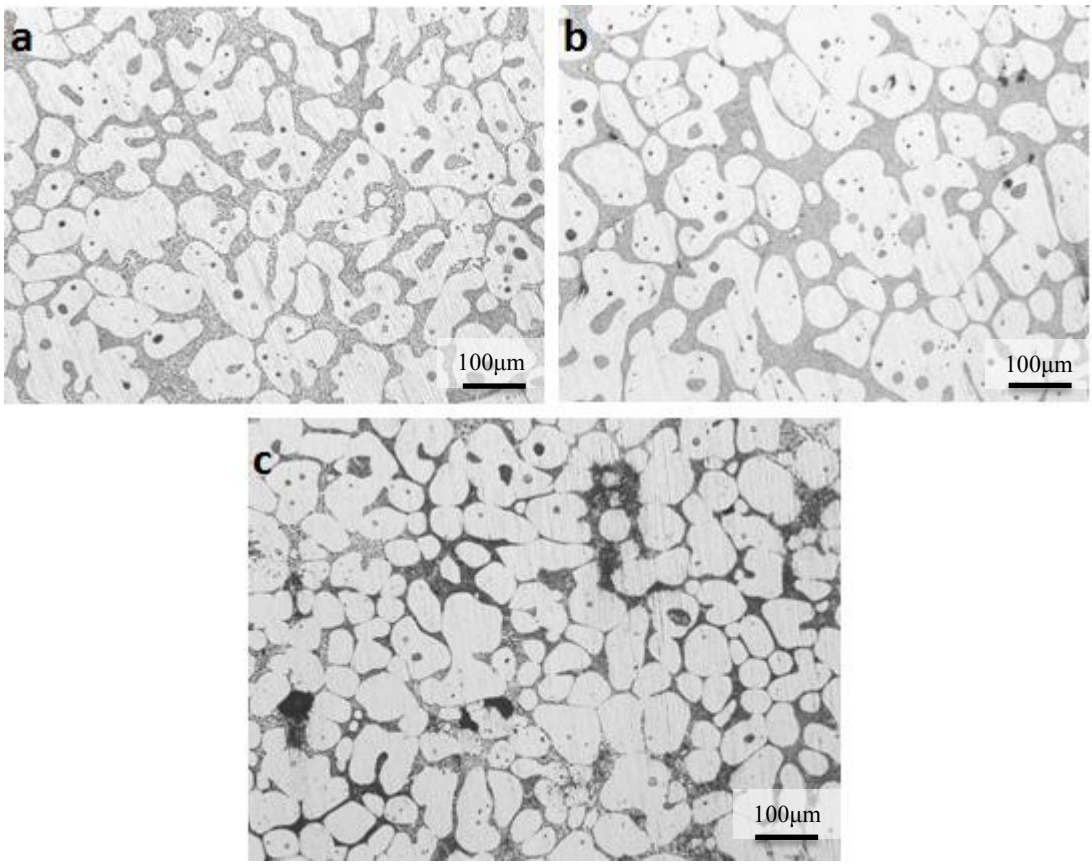

Figure 31: Optical Micrographs of induction heated A356 with different holding time of a) 0.5, b) 1, and c) 2 minutes reheated to 577^{o}C

Figure 32 shows the microstructure of semi-solid billet of A356 with increase in semi-solid temperature. The microstructure shows non-dendritic morphology at all temperatures. It is also observed that the eutectic phase is not completely melted in figure 32a due to semi-solid temperature less than 573^{o}C which is the eutectic melting temperature for A356. The mushy billet at this temperature range is more stable i.e. the billet retains its shape during soaking and can be easily transported to the die.

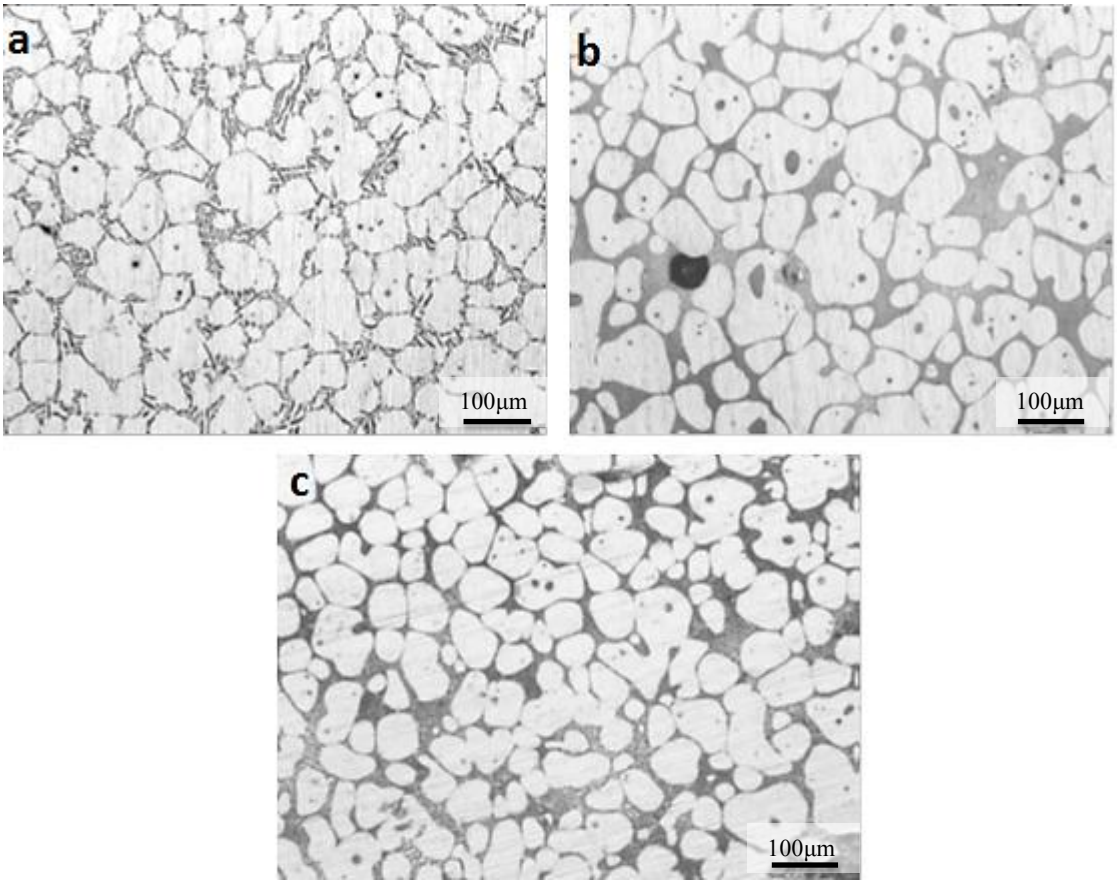

Figure 32: Optical Micrograph of Induction heated A356 billet with 2 minute holding at different semi-solid temperatures of a) 568^{o}C, b) 577^{o}C and c) 583^{o}C

4.2.2 Optical micrographs of induction heated A356/SiC nanocomposite

The nanocomposites after induction heating were quickly quenched in order to freeze the semi-solid microstructure for thixoforging. The effect of induction heating on the microstructure of ultrasonic stir cast nanocomposite billets is shown in Fig. 33. The microstructure of induction heated samples shows solid particles of near globular α (Al) phase surrounded by the eutectic regions. In case of nanocomposites the microstructure contains additional black regions showing presence of SiC agglomerates. Large pores were also seen in samples containing reinforcement and induction heated to solid fraction of 50%.

The effect of SiC reinforcement on the morphology (D_{Eq} and shape factor) of primary phase is shown in Fig. 34. It is observed that with increase in reinforcement content there is definite decrease in the size of the primary phase due the nucleation by SiC particles. Moreover it is observed that the spheroidization of particles increased with decrease in size of primary phase. It is also seen that the size of primary phase is lower in case of samples containing 50% solid fraction compared to samples with solid fraction of 60%. This may be attributed to the partial melting of primary phase at lower semi-solid temperature.

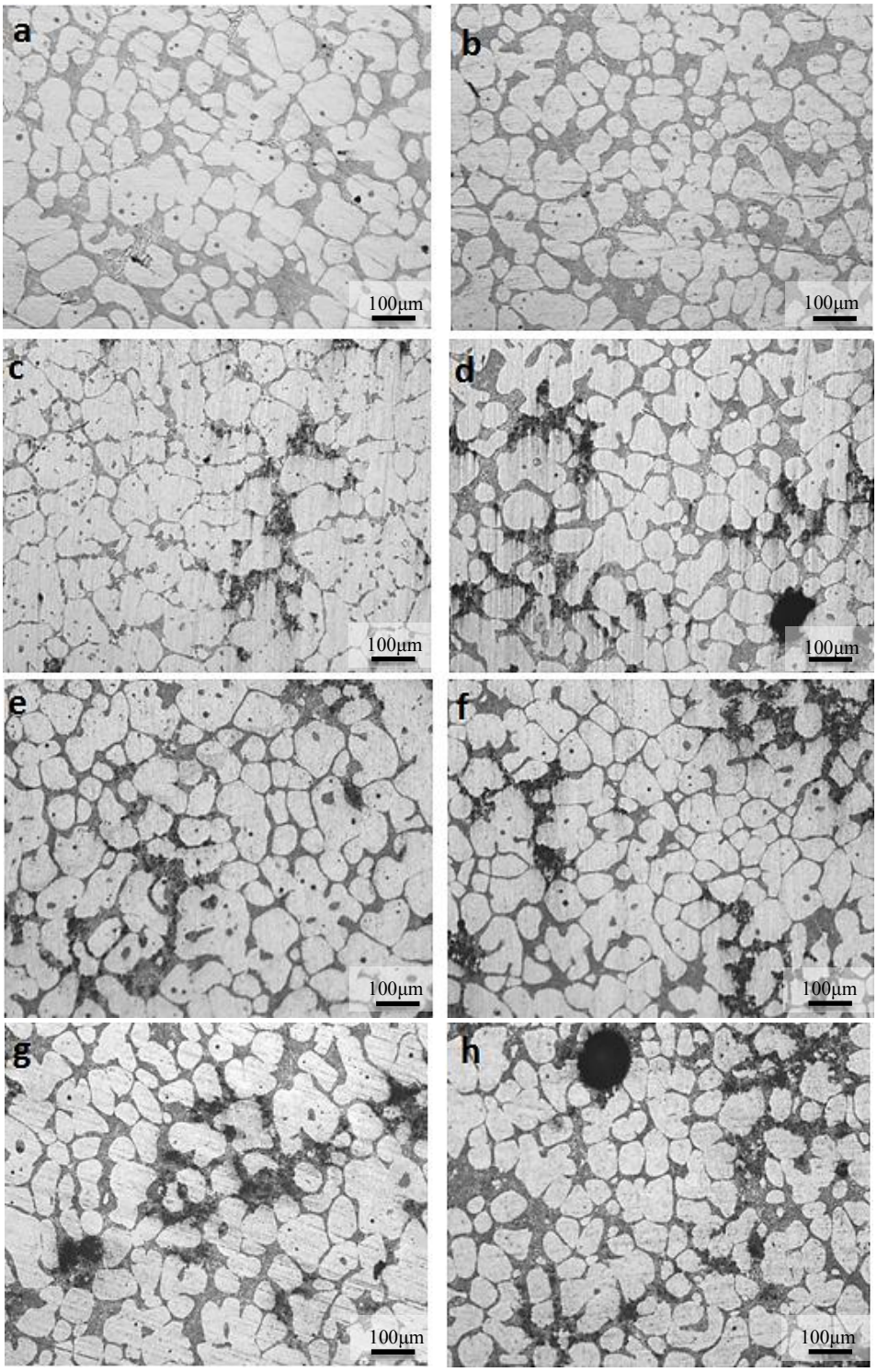

Figure 33: Optical Micrographs of induction heated A356-SiC nanocomposite at different solid fraction of a) A356(f_s=60%), b) A356(f_s=50%), c) A356-1%SiC(f_s=60%), d) A356-1%SiC(f_s=50%), e) A356-2%SiC(f_s=60%), f) A356-2%SiC(f_s=50%), g) A356-3%SiC(f_s=60%) and h) A356-3%SiC(f_s=50%)

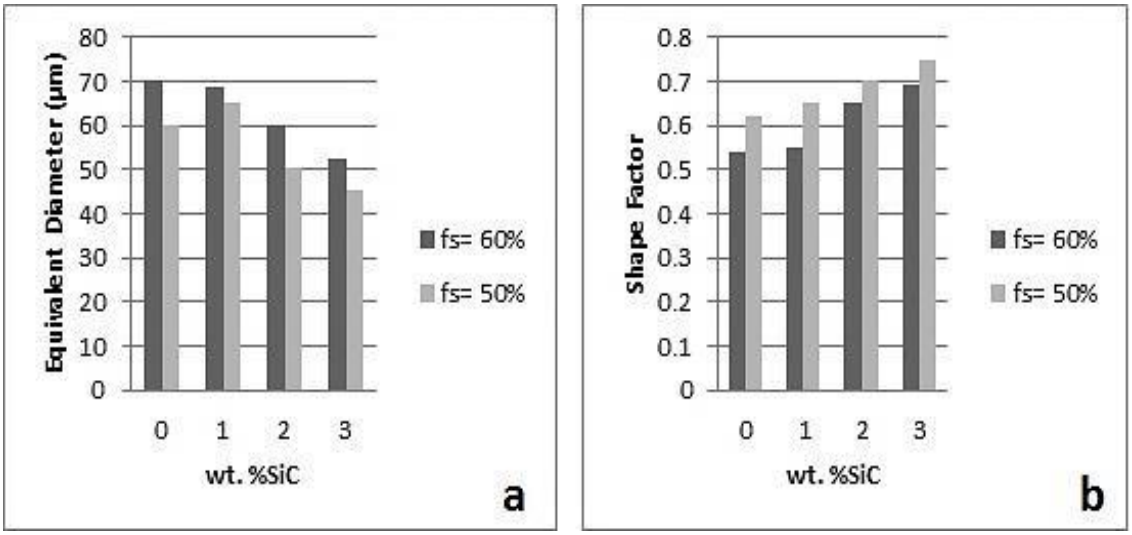

Figure 34: a) Globule size and b) Shape factor in the induction heated samples at different solid fractions

4.2.3 Porosity and hardness of induction heated A356/SiC nanocomposite

The samples quenched after induction heating were sectioned to analyze porosity and hardness. It was observed that sectioned samples containing reinforcement particles were showing large number of pores. These pores were enlarged and developed from the micro pores formed through stir casting of nanocomposites. The pores were also formed by evolution of microstructure during induction heating and because of quenching the billet in the semi-solid state. The densification data in Table 13 quantifies the amount of porosity. The hardness of the nanocomposite followed the same increasing trend with SiC content. It is also observed that the hardness of sample containing 50% solid fraction is more compared to samples with 60% solid fraction. This is attributed to the refined microstructure and presence of more hard secondary phases in these samples (Table 14).

Table 13: Densification of Induction heated samples containing 0, 1, 2 and 3wt. % SiC at different solid fractions for A356/SiC nanocomposite

Sample SiC wt.%	Number of samples	Densification (%)			
		f_s = 60%		f_s = 50%	
		Average	S.D	Average	S.D
0	3	98.8	0.17	98	0.13
1	3	98.6	0.43	97.6	0.33
2	3	97.9	1.86	96.3	0.11
3	3	97.1	1.53	95	0.15

Table 14: Hardness of Induction heated samples containing 0, 1, 2 and 3wt. % SiC at different solid fractions for A356/SiC nanocomposite

Sample SiC wt.%	Number of samples	Vickers Hardness (H_V)			
		f_s = 60%		f_s = 50%	
		Average	S.D	Average	S.D
0	3	67.3	1.96	69	2.34
1	3	71	3.28	72.6	3.40
2	3	76.2	3.22	78.4	3.73
3	3	80.1	4.43	82.3	5.17

4.2.4 Tensile test results of induction heated A356/SiC nanocomposite

The tensile response of induction heated nanocomposite showed similar results as that of stir cast samples. As seen in Table 15 and 16, the tensile properties decreased with increase in SiC content. However it is observed that samples with 50% solid fraction showed more tensile strength and elongation compared to samples with 60% solid fraction. This is attributed to more amount of eutectic and consequently fine microstructure of samples induction heated to higher semi-solid temperature. The tensile properties of nanocomposite at higher reinforcement content deteriorated due to large number of pores formed after induction heating.

Table 15: Tensile Test Results for Induction heated A356/SiC nanocomposite with 60% solid fraction

Sample	Number of samples	UTS (MPa)		Yield Strength (MPa)		Elongation (%)	
Wt.% SiC	-	Average	SD	Average	SD	Average	SD
0	2	197.7	20.53	114	8.06	7.71	2.15
1	2	173.8	6.81	102.8	14.14	4.62	0.13
2	2	156.8	1.24	101.28	6.92	4.05	0.18
3	2	123.8	14.25	90.8	4.48	2.53	0.62

Table 16: Tensile Test Results for Induction heated A356/SiC nanocomposite with 50% solid fraction

Sample	Number of samples	UTS (MPa)		Yield Strength (MPa)		Elongation (%)	
Wt.% SiC	-	Average	SD	Average	SD	Average	SD
0	2	225.3	4.18	124	2.5	11.4	0.15
1	2	194.5	5.19	111.2	2.8	5.56	0.22
2	2	173.6	10.46	101.6	0.23	4.82	1.12
3	2	144.7	12.57	92.08	0.24	3.5	0.83

4.3 Thixoforged A356/SiC Nanocomposites

4.3.1 Optical micrographs of A356/SiC nanocomposite samples

The optical micrographs of the samples from the thixoforged nanocomposite part are taken at center and at the edge (away from the canter). Different magnification is used to analyze and characterize the distribution of secondary phases and size/shape of primary phase in the nanocomposite in different regions of the thixoformed part.

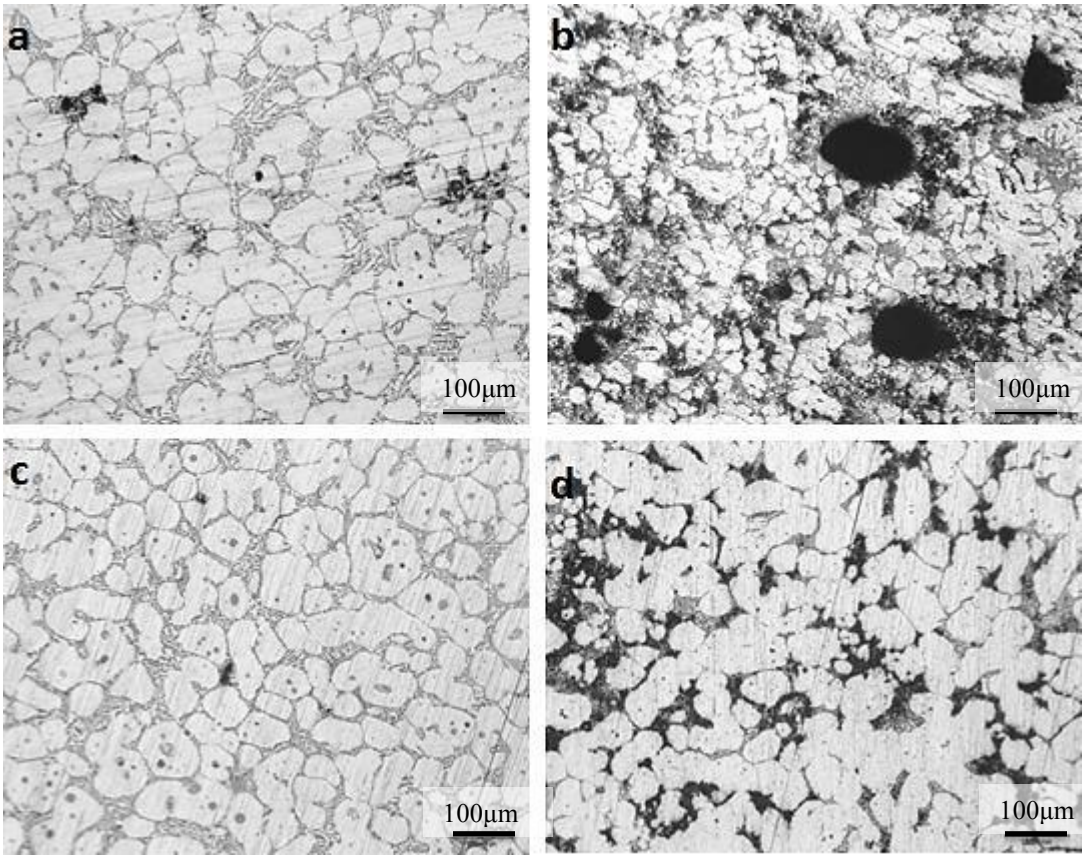

Figure 35: Optical micrographs at the edge of thixoforged part of a)A356(1min.) b)A356-3%SiC(1min.) c)A356-1%SiC(2min.) and d)A356-3%SiC(2min) reheated to fs= 60%

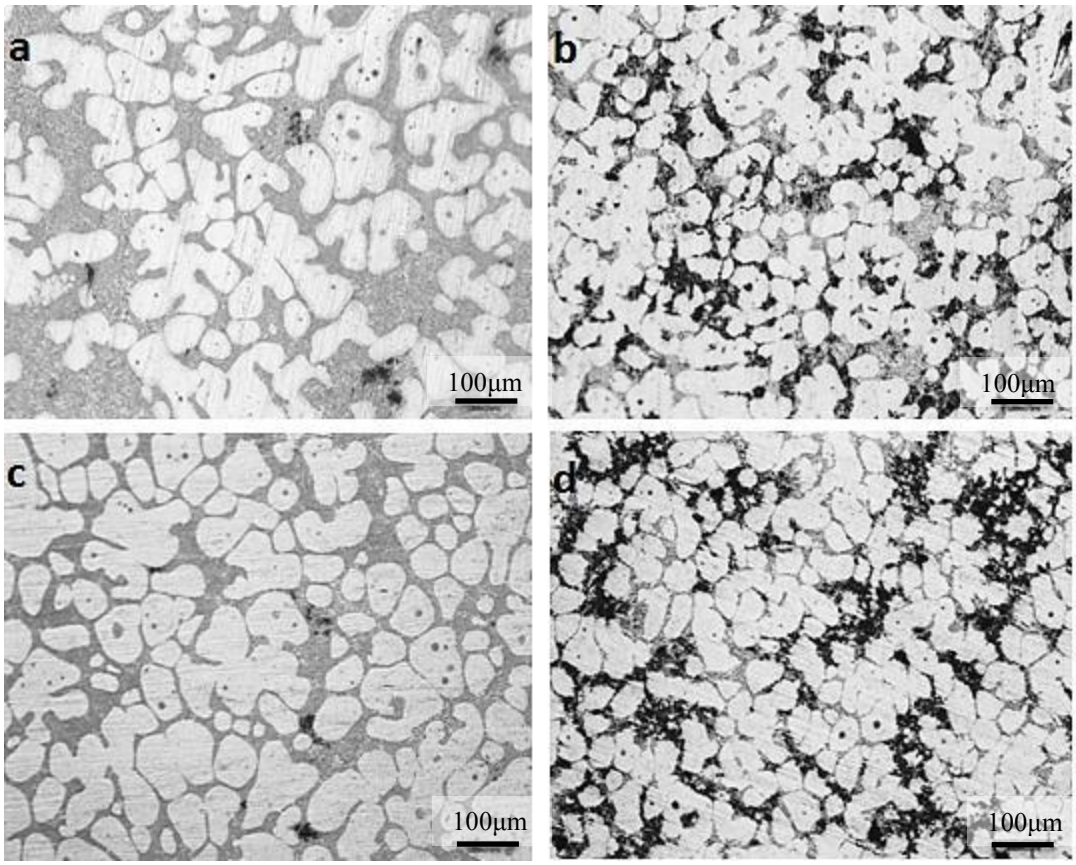

Figure 36: Optical micrographs at the edge of thixoforged part of a)A356(1min.) b)A356-2%SiC(1min.) c)A356(2min.) and d)A356-2%SiC(2min) reheated to fs=50%

The micrograph after thixoforging shows rosette and globular nature of alpha phases surrounded by eutectic phases. The dark region show agglomerated particles lying in the liquid phase which increases with increase in SiC content. Also it is observed that the tendency of globularization is more in case of samples containing reinforcement and thixoforged at higher semi-solid temperature and holding time. The effect of solid fraction and holding time on the microstructure of thixoformed sample can be seen in Fig. 37 and 38. It is observed that with increase in holding time and semi-solid temperature the size of the primary phase is reduced with increase in shape factor.

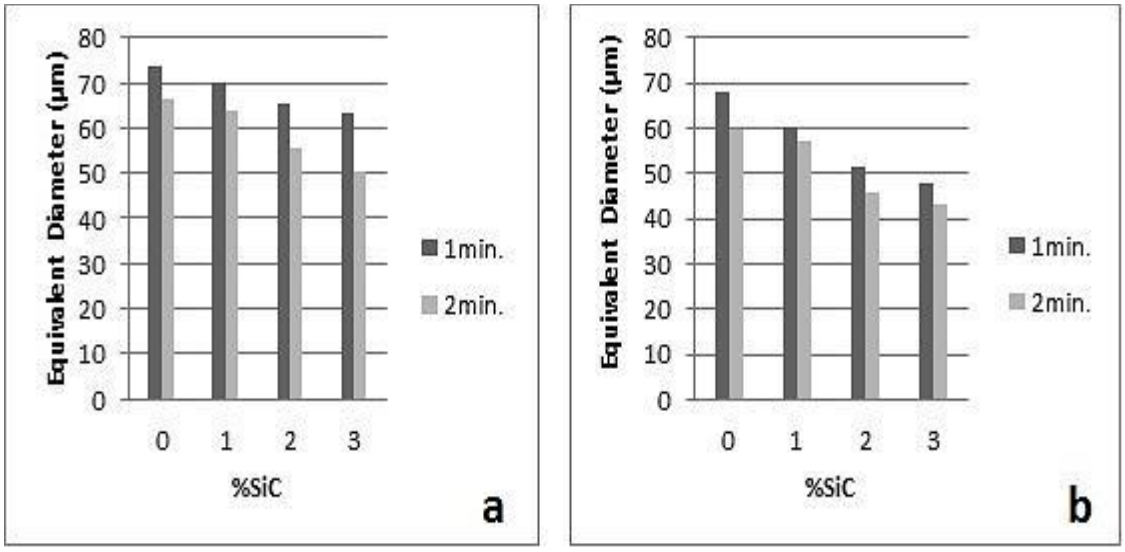

Figure 37: Globule size of primary phase in A356/SiC nanocomposite at a) fs=60% and b) fs=50%

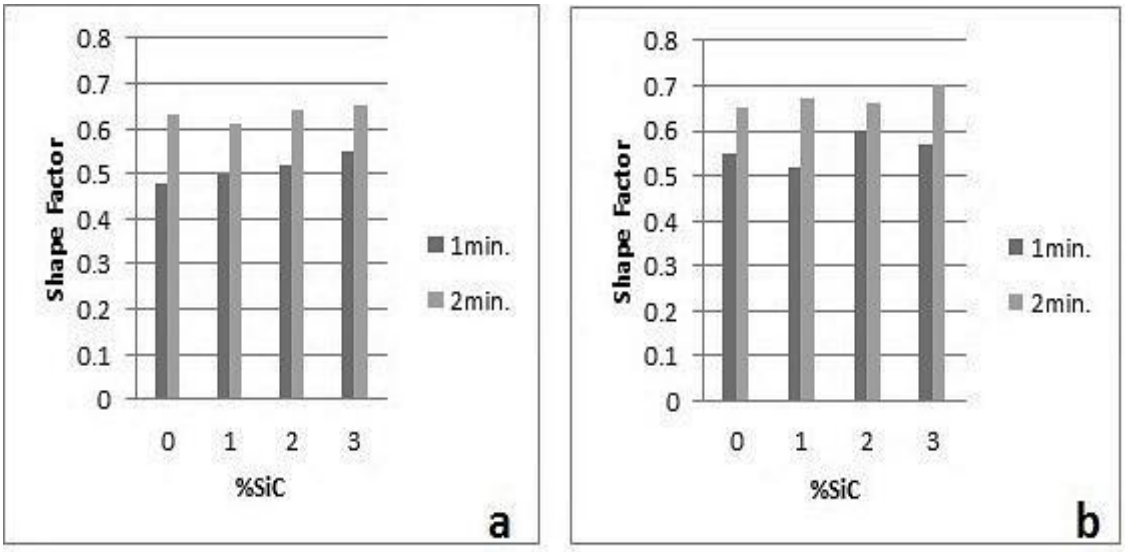

Figure 38: Shape factor of primary phase in A356/SiC nanocomposite at a) fs=60% and b) fs=50%

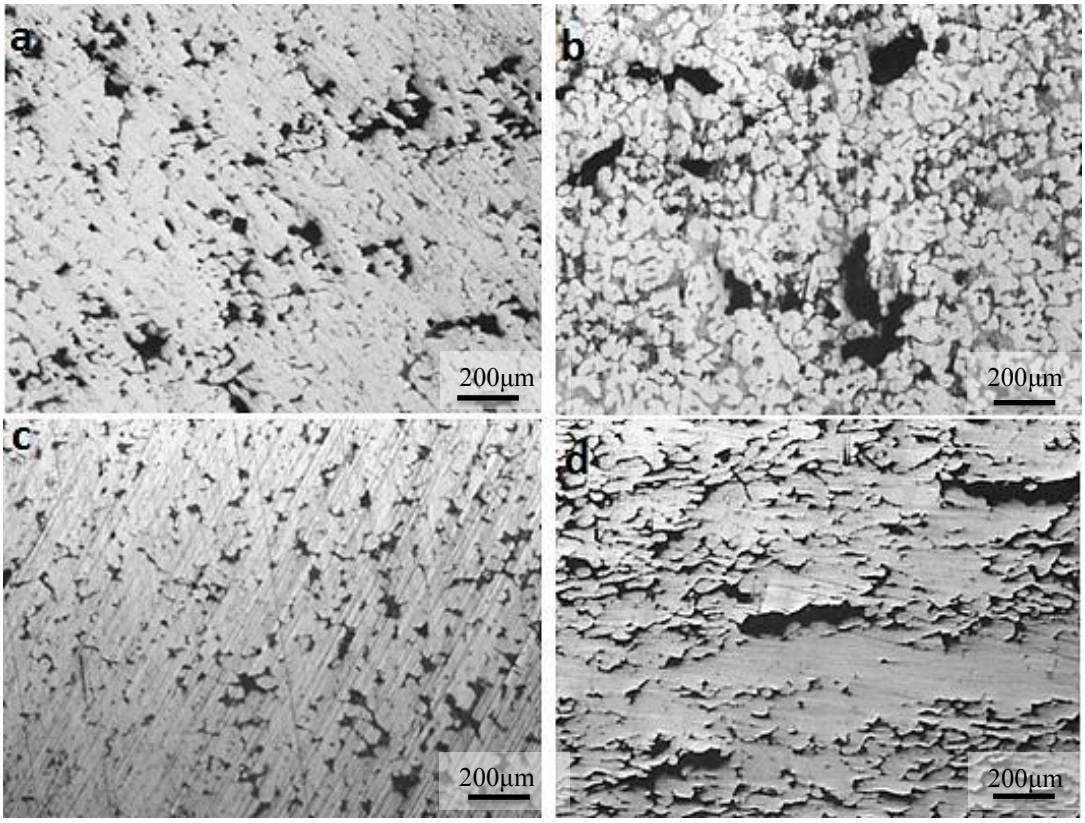

Figure 39: Optical micrographs at the center of thixoforged part of a)A356(1min.) b)A356-3%SiC(1min.) c)A356(2min.) and d)A356-3%SiC(2min.)

The optical micrographs at cross-section of thixoforged samples shows solid phase clustered in the direction of load thereby increasing the density of grains. Less liquid phase is observed entrapped by the moving solid phase during forging operation. As shown in Fig. 39, more cavities are observed in samples reheated with 1min. holding time and containing 3 wt. % SiC compared to 2min. holding sample due to less spheroidization (no globular morphology) of primary phase during thixoforging.

4.3.2 SEM micrographs of thixoforged A356/SiC nanocomposite

SEM analysis is performed on the samples representing the center and the edge (20mm away from center) of the thixoforged part to analyze the distribution of different phases in these regions. Figure 40 and 41 shows SEM micrographs of samples thixoforged at two different semi-solid temperatures corresponding to solid fractions of 60% and 50% respectively. It was observed that in the regions close to the center of the thixoforged part, primary phase was more predominant. Most of the eutectic phase was shifted away from the center during thixoforging. The reinforcement particles were seen lying along the eutectic regions away from the center. As seen in Fig. 41d, the sample thixoforged with 60% solid fraction showed cavities present due to incomplete die filling which is also confirmed by the densification data. The distribution of SiC particles are also shown in Fig. 40d and 41d.

The distribution of different phases is also verified using EDS analysis and mapping Aluminum, Silicon and Carbon elements in different regions of A356/SiC nanocomposite. As seen in Fig. 42 and 43, the EDS spectrum showed fewer amounts of silicon element at the center of thixoforged part compared to the EDS spectrum in regions away from center. Moreover the EDS mapping in Fig. 44 and 45 also depict the distribution of SiC particles in the center and edge regions. It is worth mentioning that the SiC particles as seen earlier in stir casting solidification theory favors the eutectic regions in case of thixoforging.

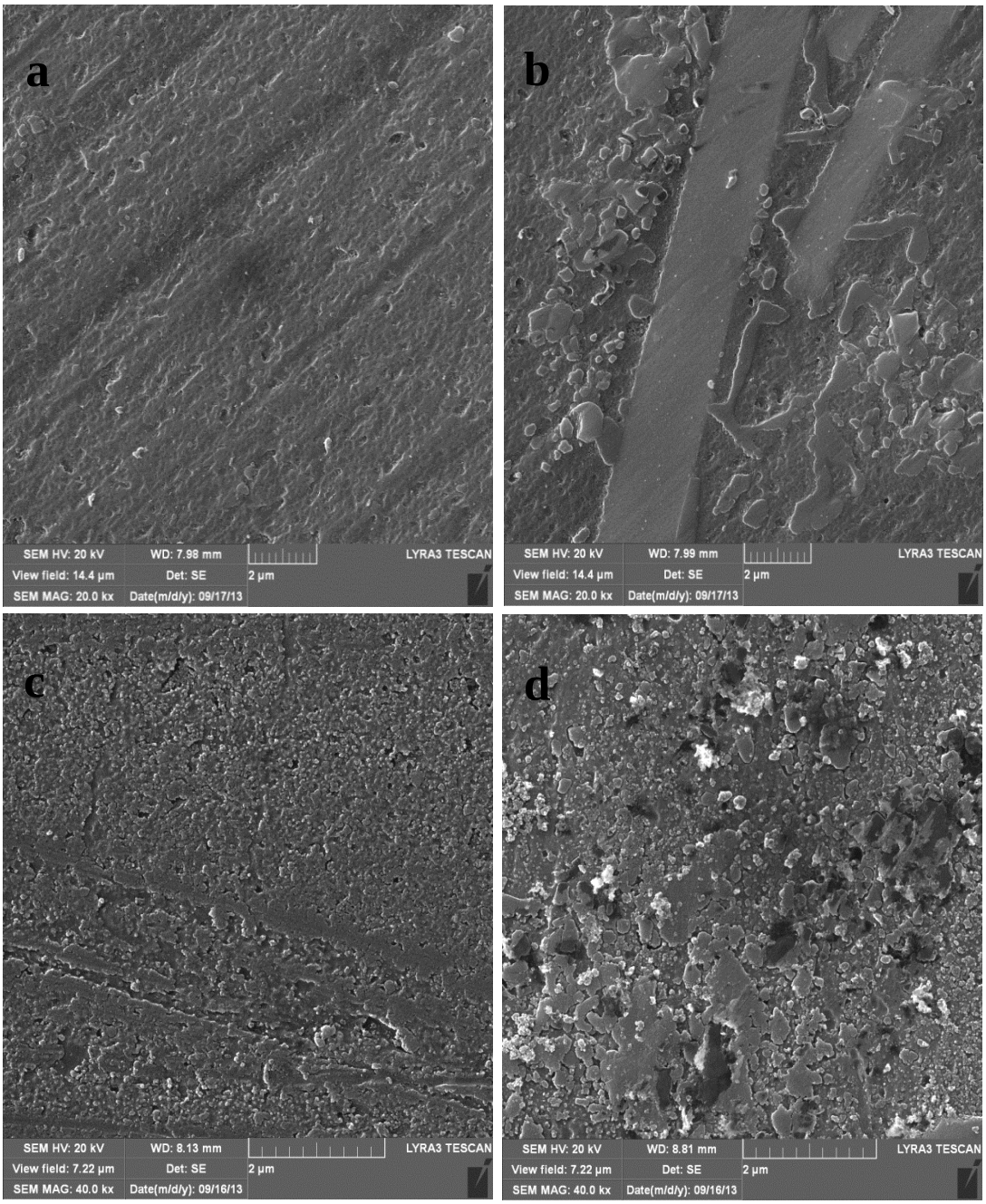

Figure 40: SEM micrographs of A356/SiC nanocomposite thixoforged at fs=50%, containing a) 0wt. %SiC (center), b) 0wt. %SiC (edge), c) 3wt. %SiC (center) and d) 3wt. %SiC (edge)

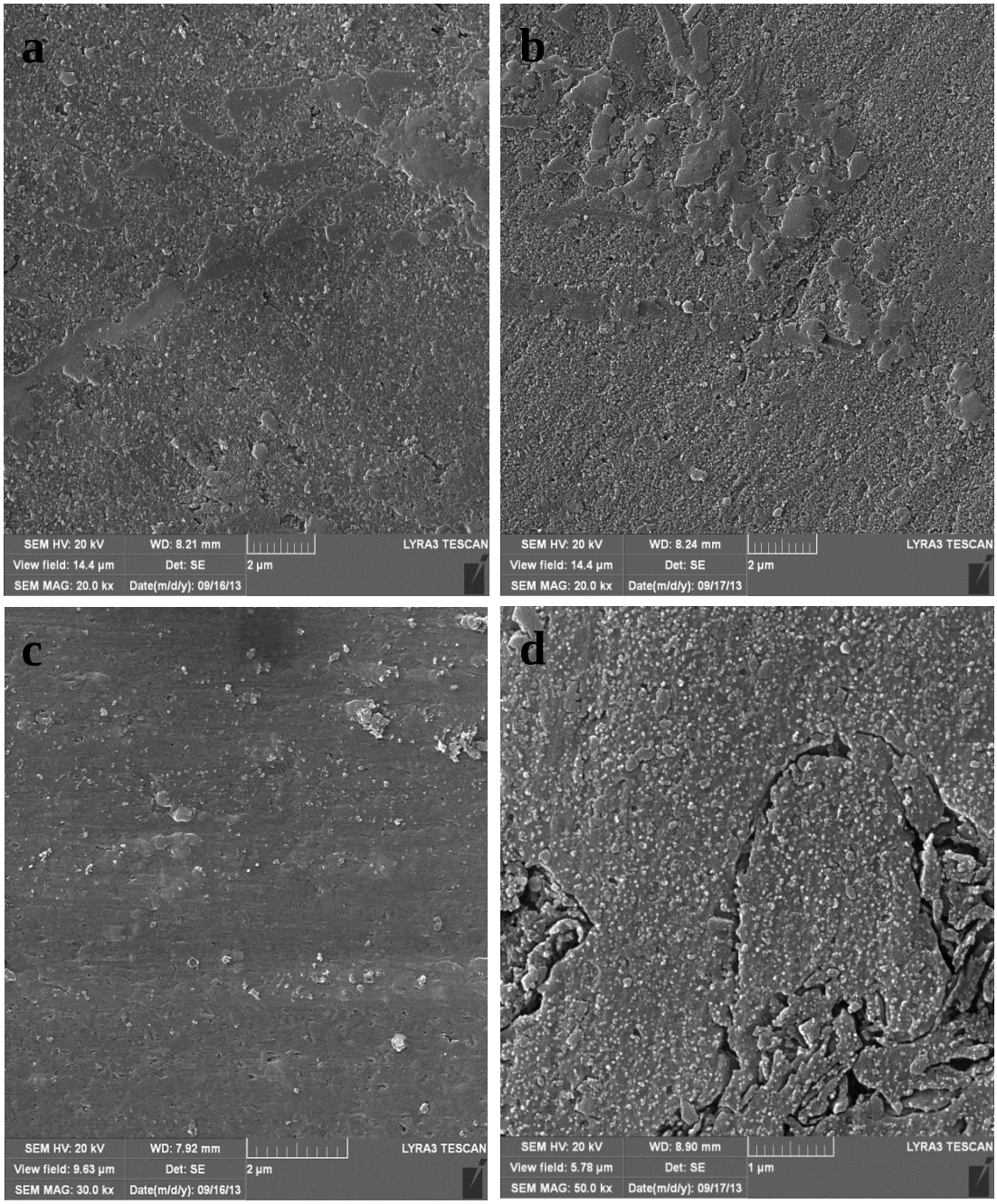

Figure 41: SEM micrographs of A356/SiC nanocomposite thixoforged at fs=60%, containing a) 0wt. %SiC (center), b) 0wt. %SiC (edge), c) 3wt. %SiC (center) and d) 3wt. %SiC (edge)

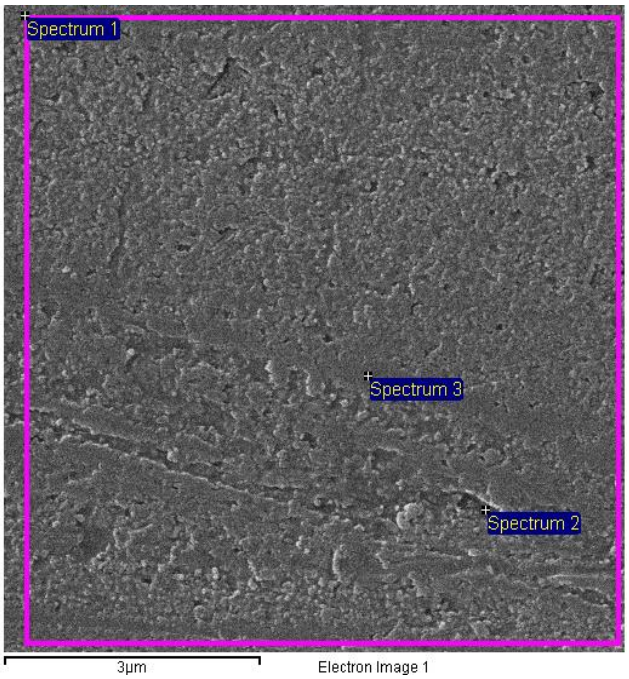

Spectrum	C	O	Al	Si
Spectrum 1	19.02	2.56	77.97	0.45
Spectrum 2	21.76	0.99	77.12	0.13
Spectrum 3	22.09	1.39	76.32	0.21

Figure 42: EDS analysis for A356-3 wt. % SiC nanocomposite at the center of thixoforged part

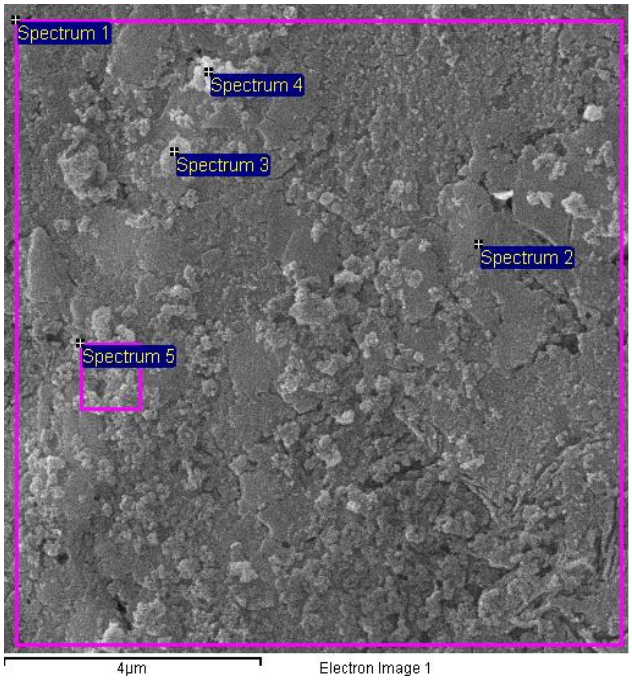

Spectrum	C	O	Al	Si
Spectrum 1	16.16	5.86	64.23	13.75
Spectrum 2	18.32	5.63	54.69	21.36
Spectrum 3	16.28	10.03	51.77	21.92
Spectrum 4	30.85	4.75	47.93	16.47
Spectrum 5	21.86	6.72	48.91	22.5

Figure 43: EDS analysis for A356-3 wt. % SiC nanocomposite at the edge of thixoforged part

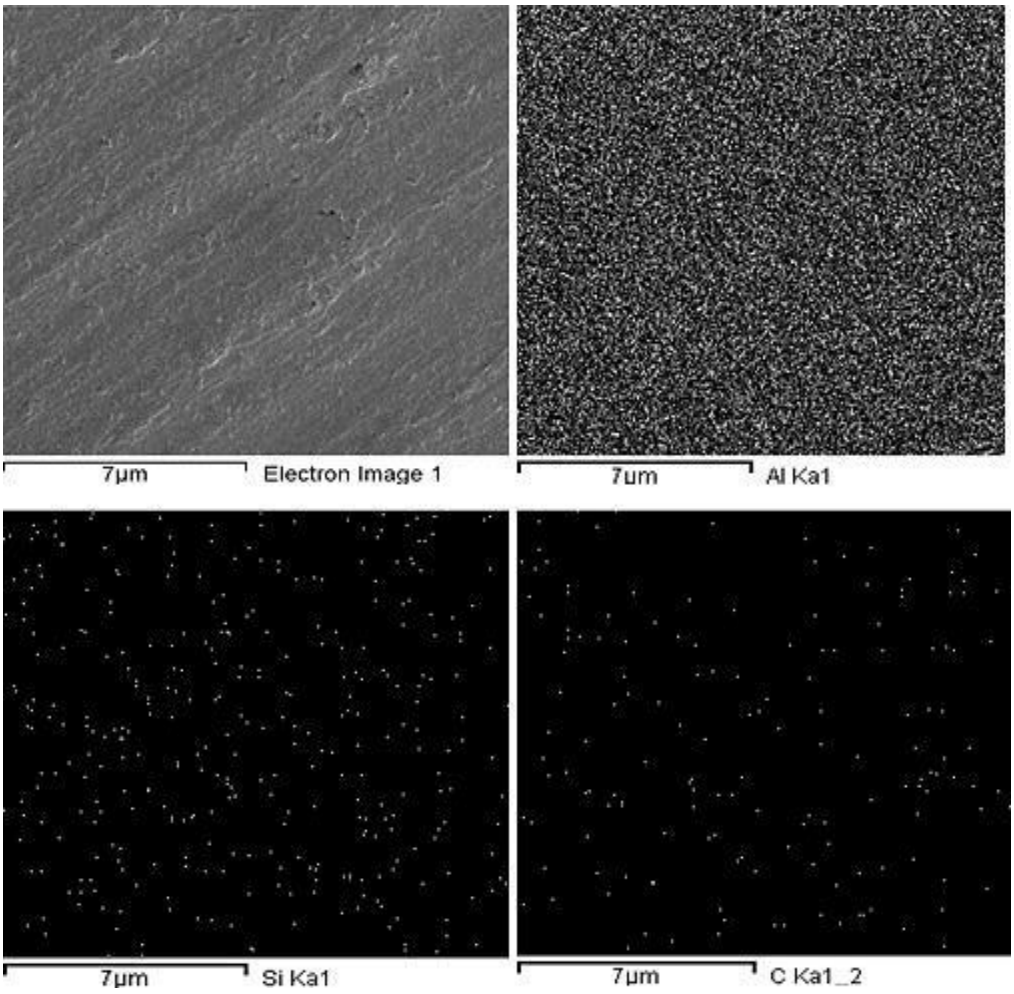

Figure 44: SEM micrograph of A356/2wt%SiC nanocomposite at the center of thixoforged part showing EDX mapping of Aluminum, Silicon and Carbon elements

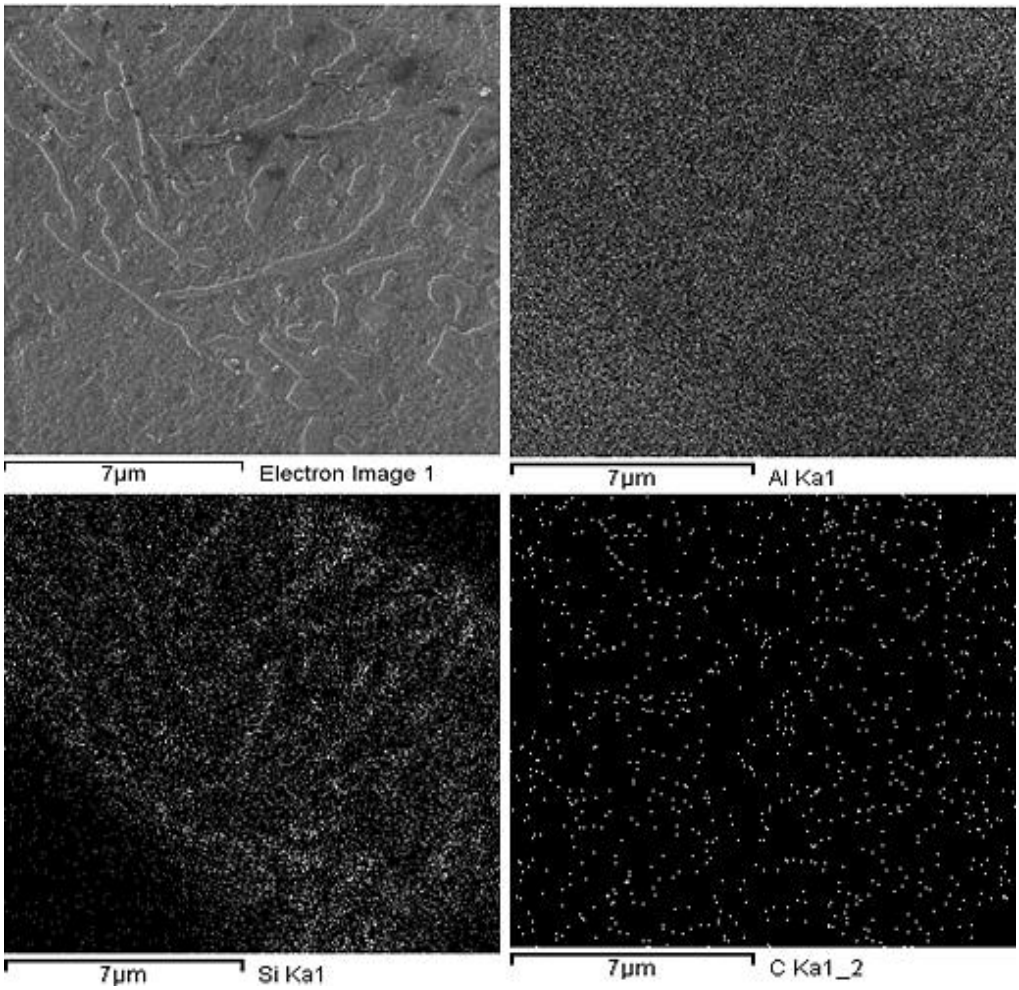

Figure 45: SEM micrograph of A356/2wt%SiC nanocomposite at the edge of thixoforged part showing EDX mapping of Aluminum, Silicon and Carbon elements

4.3.3 Densification of thixoforged A356/SiC nanocomposite component

The porosity of thixoforged component is measured at the center and at the edge 20mm away from the center as shown in Fig. 46 and 47. The densification of regions directly under the line of load is more compared to regions away from the center. Moreover the SiC particles moving away from the center also contributed to the formation of pores in the later part of the solidification inside the die.

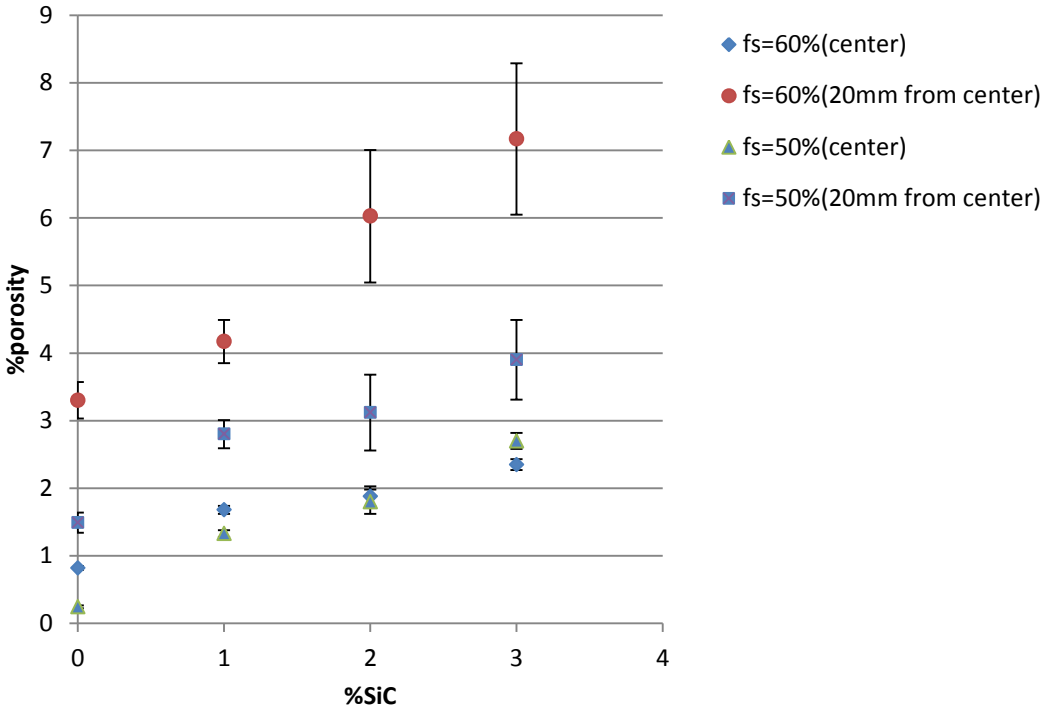

Figure 46: Percentage porosity in thixoforged samples held for 1minute in the reheating condition

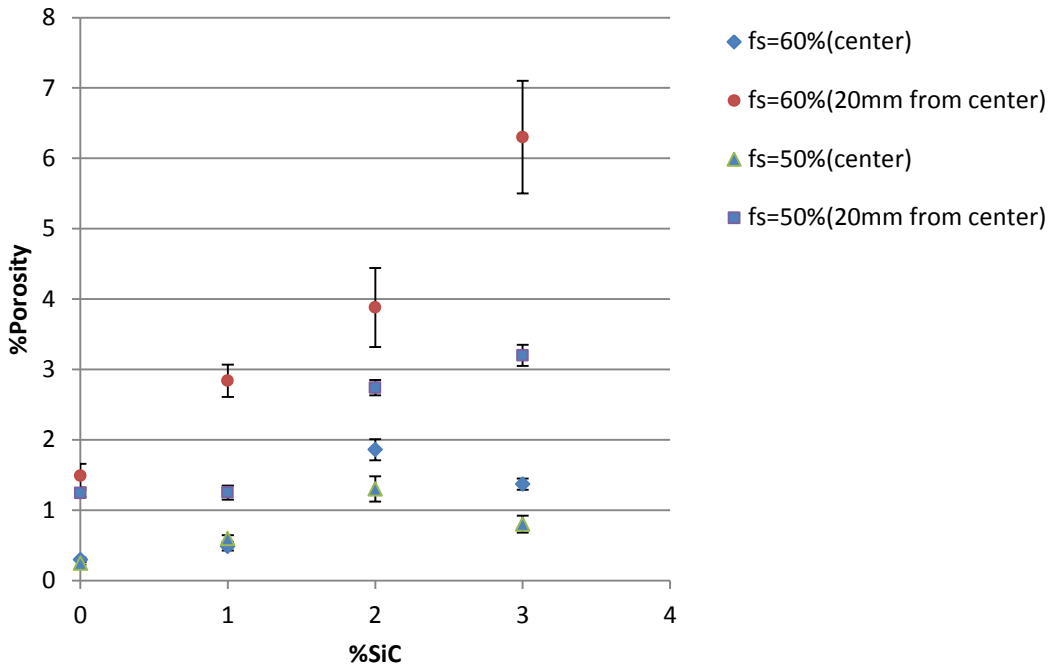

Figure 47: Percentage porosity in thixoforged samples held for 2minute in the reheating condition

4.3.4 Hardness and tensile test results

The measured hardness of thixoforged part at the center and on the edge 20mm away from center of the thixoforged sample is shown in Fig. 48 and 49. As depicted in the microstructure study, the fewer amount of eutectic silicon phase and consequently less amounts of SiC reinforcement present at the center of the thixoforged part resulted in moderate hardness values in this region. However the hardness away from center shows considerable increase with increase in the reinforcement content.

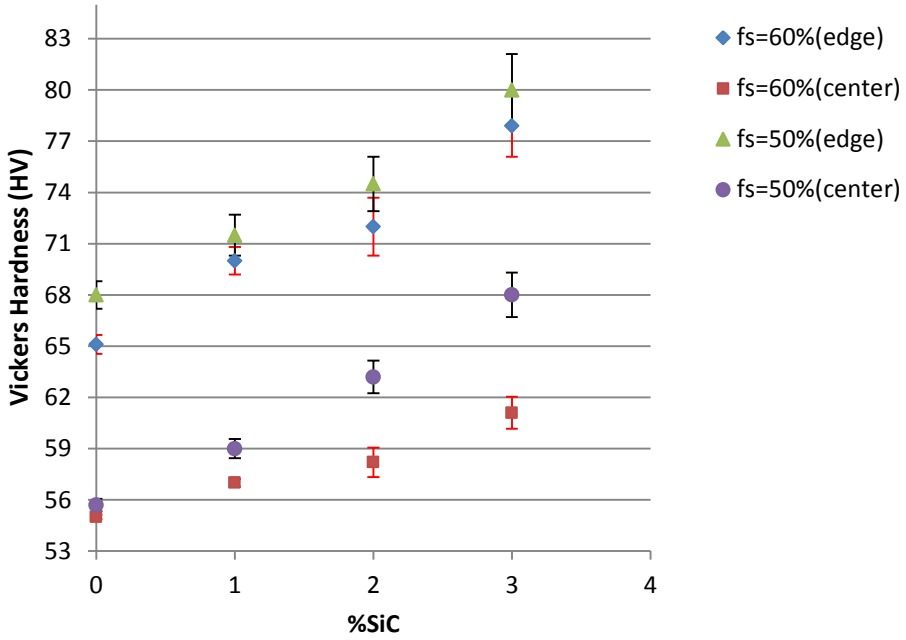

Figure 48: Hardness of thixoforged samples held for 1minute in the reheating condition

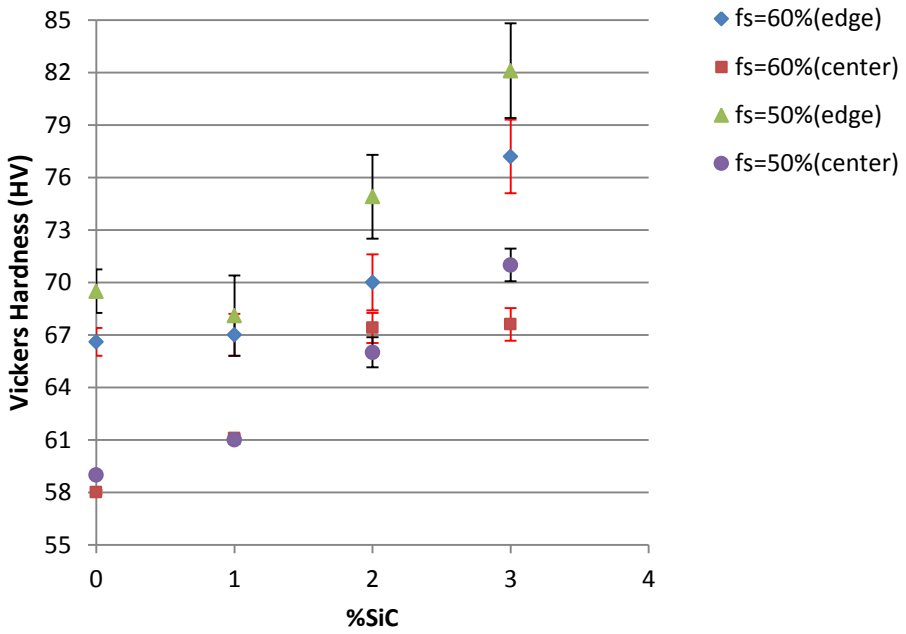

Figure 49: Hardness of thixoforged samples held for 2minute in the reheating condition

The tensile behavior of nanocomposite after thixoforging operation showed increase in ductility with some reduction in yield strength. Figure 50 and 51 shows tensile curves of thixoforged nanocomposite at different solid fractions. It is observed that the tensile strength obtained in case of nanocomposite with 1wt. % SiC is high compared to its monolithic alloy when thixoforged at higher solid fraction, but in case of 50% solid fraction the maximum tensile strength obtained is for the monolithic alloy. Also seen in Table 17, 18, 19 and 20 are the tensile properties of thixoforged nanocomposite, the ductility of samples thixoforged at solid fraction of 50% is higher than samples with solid fraction of 60%. Similar trend is obtained with reheating time of 1 and 2 minutes. But samples reheated with 2min. holding time showed higher tensile results compared to samples reheated with 1 min. holding. This may be attributed to better densification in samples reheated to 2min. holding time.

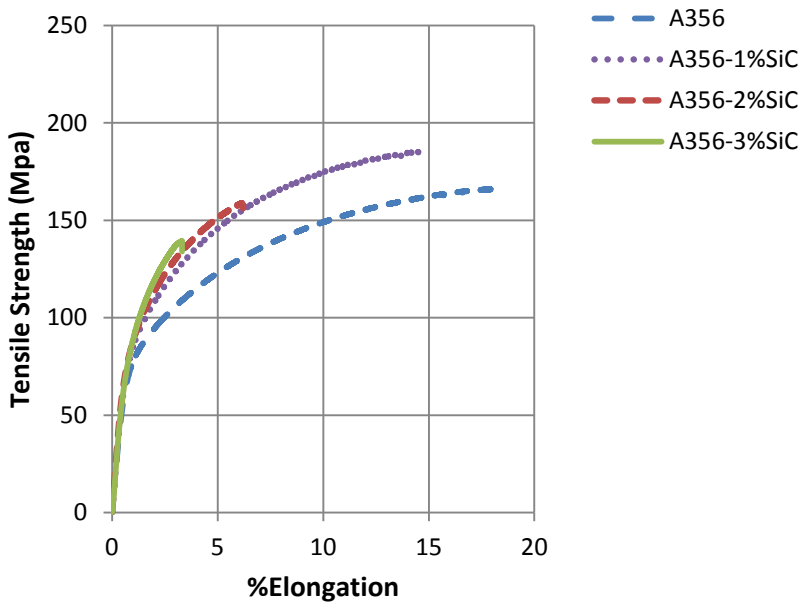

Figure 50: Stress-strain curves of A356-SiC nanocomposite at a) fs=60% with 2minute holding time in the reheating condition

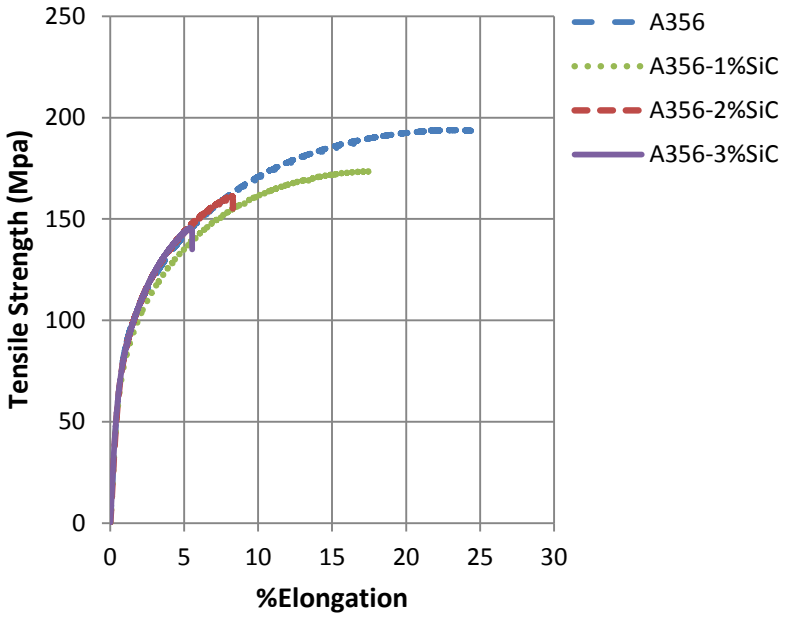

Figure 51: Stress-strain curves of A356-SiC nanocomposite at a) fs=50% with 2minute holding time in the reheating condition

Table 17: Tensile Test Results for Induction heated A356/SiC nanocomposite with holding time of 1min. and solid fraction of 60%

Sample	Number of samples	UTS (MPa)		Yield Strength (MPa)		Elongation (%)	
Wt.% SiC	-	Average	SD	Average	SD	Average	SD
0	2	172.4	2.95	100.9	0.5	12.68	0.98
1	2	184.2	1.05	115.3	1.05	10.7	0.38
2	2	143.3	15.02	96.2	20.8	3.5	0.4
3	2	138.9	0.53	90.9	5.930	3.05	0.37

Table 18: Tensile Test Results for Induction heated A356/SiC nanocomposite with holding time of 1min. and solid fraction of 50%

Sample	Number of Samples	UTS (MPa)		Yield Strength (MPa)		Elongation (%)	
Wt.% SiC	-	Average	SD	Average	SD	Average	SD
0	3	178.46	4.64	99.85	1.35	22.34	2.54
1	3	175.14	2.72	103.35	5.85	12.48	0.78
2	2	149.4	3.9	91.52	4.78	4.94	1.4
3	2	131.68	3.41	75.35	0.05	3.85	0.68

Table 19: Tensile Test Results for Induction heated A356/SiC nanocomposite with holding time of 2min. and solid fraction of 60%

Sample	Number of Samples	UTS (MPa)		Yield Strength (MPa)		Elongation (%)	
Wt.% SiC	-	Average	SD	Average	SD	Average	SD
0	2	175.65	9.55	101.35	6.75	18.12	2.41
1	2	202.85	17.65	110.8	11.4	13.8	1.38
2	2	174.86	8.15	97.04	3.41	6.18	0.03
3	2	139.06	0.39	84.93	0.03	3.49	0.04

Table 20: Tensile Test Results for Induction heated A356/SiC nanocomposite with holding time of 2min. and solid fraction of 50%

Sample	Number of Samples	UTS (MPa)		Yield Strength (MPa)		Elongation (%)	
Wt.% SiC	-	Average	SD	Average	SD	Average	SD
0	2	184.75	9.14	100.5	0.95	27.83	0.86
1	3	179.38	5.82	99.65	1.55	16.84	1.57
2	3	166.56	5.2	97.58	1.76	9.28	0.99
3	2	152.9	7.44	93.42	6.68	5.78	0.2

The fracture surface of nanocomposites after thixoforging operation shows complex morphologies like cleavages, dimples, voids, segregation, porosities and shrinkages. Figure 52 and 53 shows tensile fracture surface of thixoforged nanocomposite at different solid fractions. It is observed that at higher SiC content the crack initiation is occurring from the porosities and shrinkages existing in the thixoforged part. The monolithic alloy and nanocomposite with 1wt. %SiC reveals ductile fracture mode consisting of dimples. It is also observed from Fig. 52a and 53a that the plane facets and de-cohesion of primary phase on the fracture surfaces shows ductile fracture surface with intergranular morphology. And the crack initiation is attributed to the presence of micro voids and secondary phase inclusions present at the grain boundaries as seen in optical micrographs Fig. 35, 36 and 39.

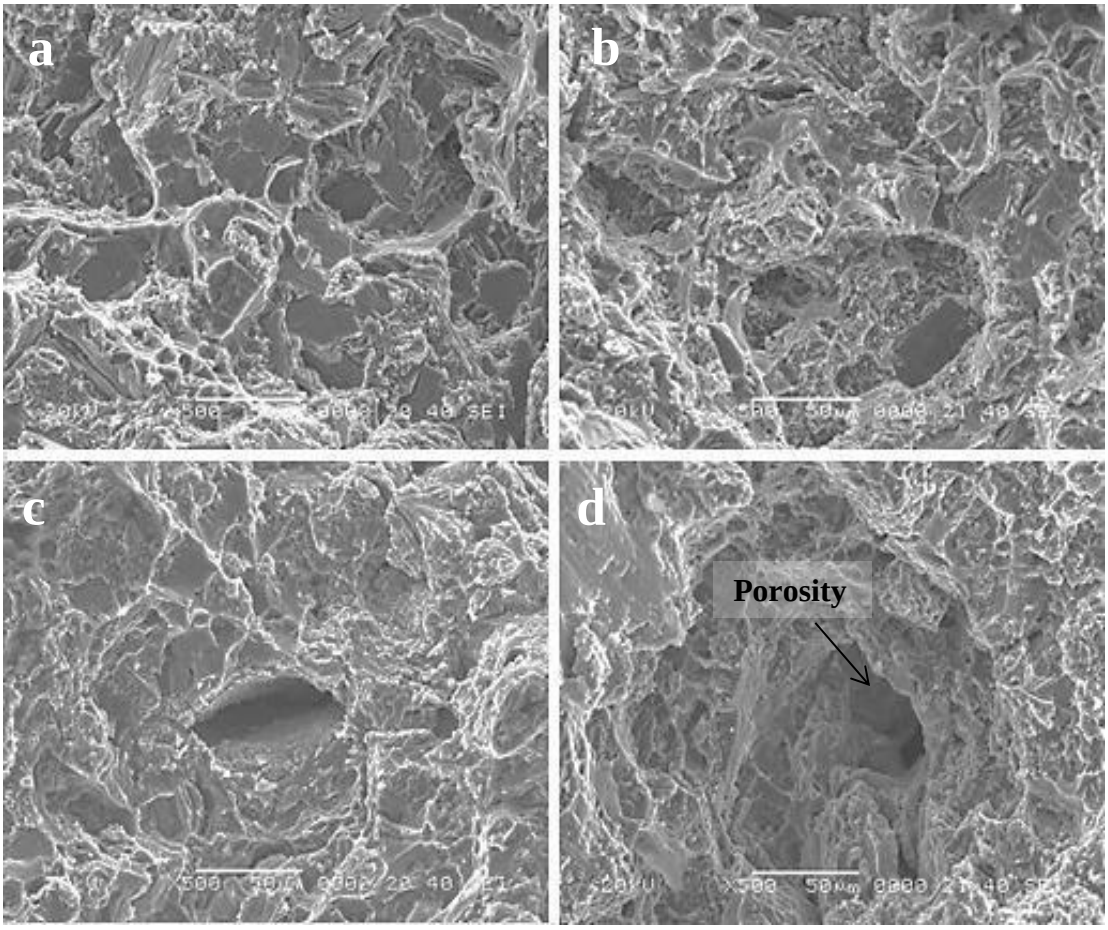

Figure 52: Tensile fracture surface of A356/SiC nanocomposite thixoforged at fs= 60% containing a) 0wt. % SiC, b) 1wt. % SiC (T6), c) 2wt. % SiC, d) 3wt. % SiC

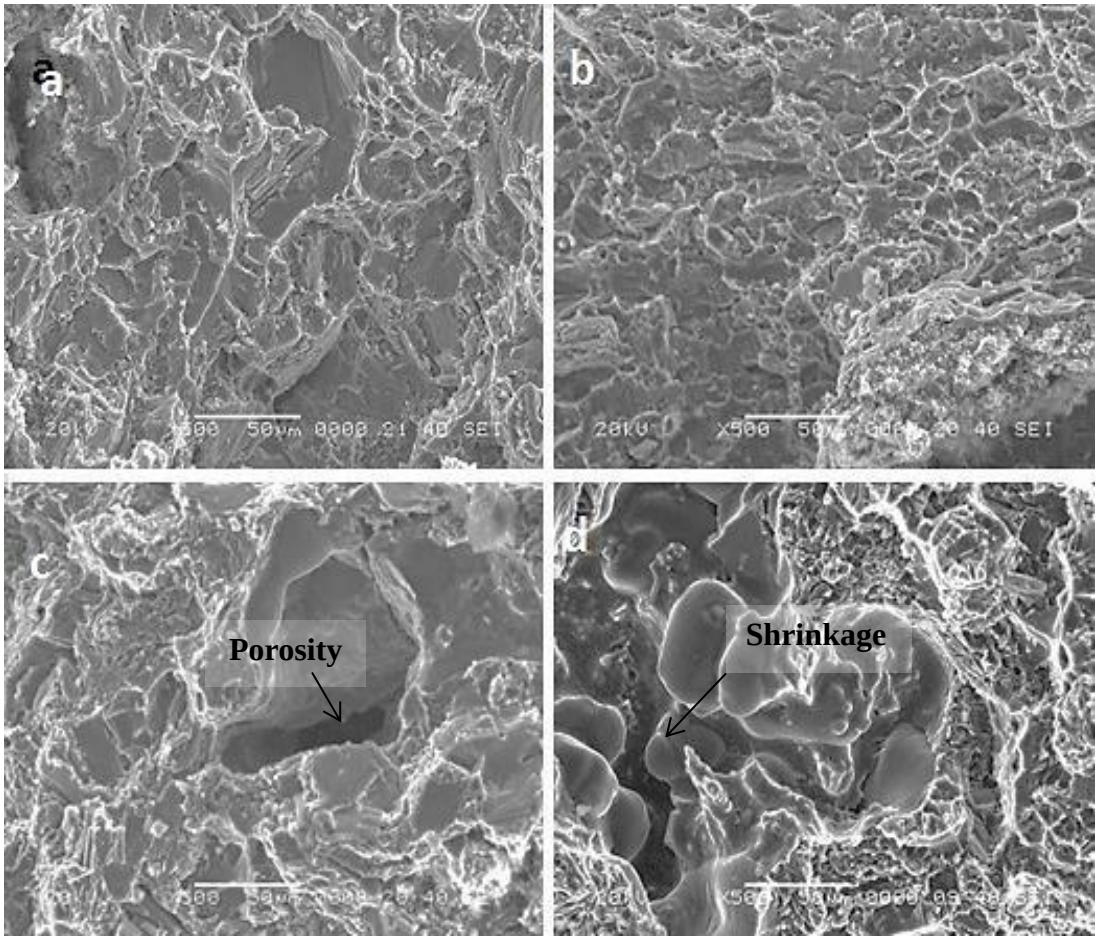

Figure 53: Tensile fracture surface of A356/SiC nanocomposite thixoforged at fs= 50% containing a) 0wt. % SiC, b) 1wt. % SiC (T6), c) 2wt. % SiC, d) 3wt. % SiC

4.3.5 Surface quality of thixoforged part

The images of samples obtained after thixoforging process at two different semi-solid fractions are taken to analyze the quality of sample obtained with ram speed of 12mm/sec. As shown in Fig. 54 the samples thixoforged at 60% solid fraction shows incomplete die filling compared to samples thixoforged at 50% solid fraction. Moreover the tendency of incomplete die filling is more in samples containing SiC nanoparticles at lower semi-solid temperature. This is due to higher solid fraction and faster cooling rate during thixoforging process at lower semi-solid temperature. Surface roughness was also measured using profilometer to quantify the surface quality of the thixoforged part.

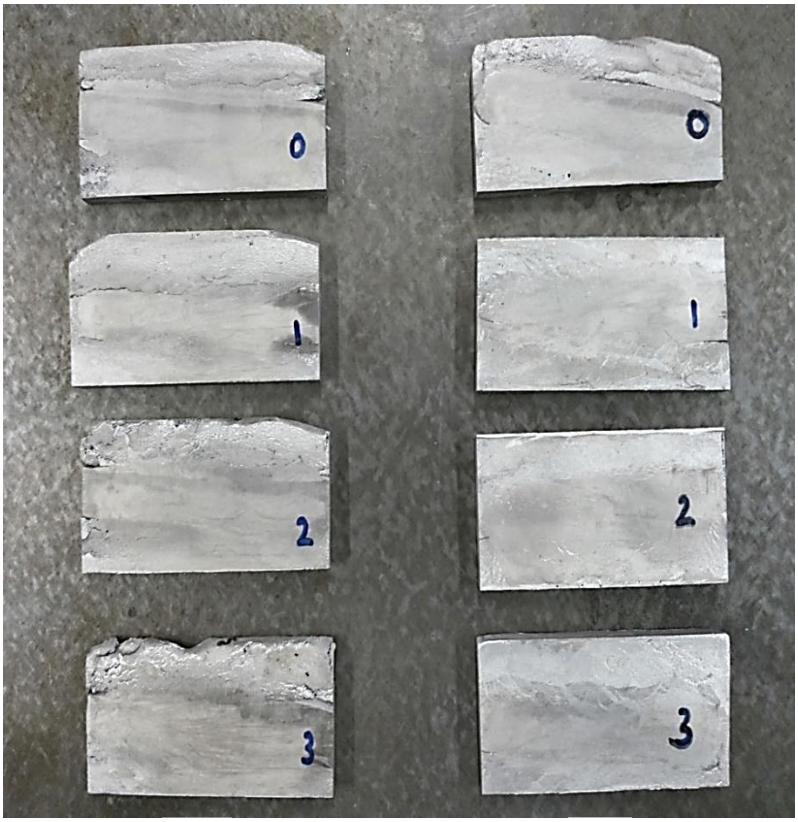

a **b**

Figure 54: Images of thixoforged samples with a) f_s=60% and b) fs=50%, with different wt. %SiC compositions marked on the sample

Figure 55 shows the thixoforged sample of nanocomposite containing 3wt. %SiC, clearly it is seen that due to higher solid fraction and lower ram speed, the material solidifies quickly resulting in defects like porosities, incomplete die filling. On the other hand sample with higher semi solid temperature shows liquid segregation and oxide films with inhomogenous distribution of phases at the edges of the thixoforged part as shown in Fig. 56. The defects lke these in the thixoforged part can be overcome by invariably using higher ram velocity and punch force.

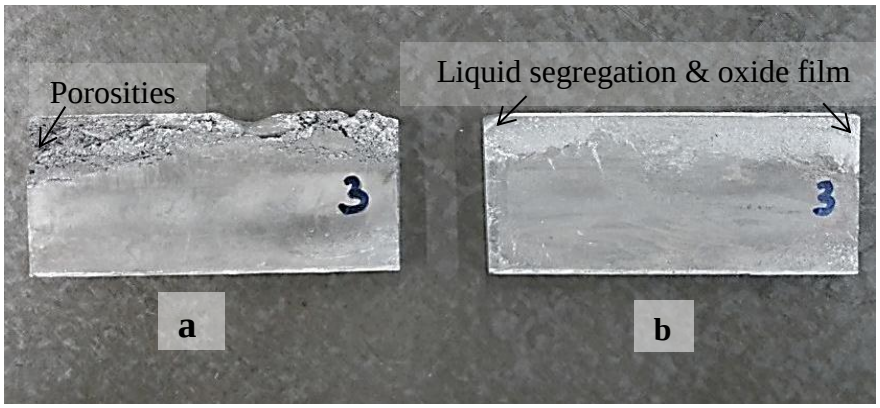

Figure 55: Image of A356-3%SiC composite part thixoforged at a) 60% and b) 50% solid fractions

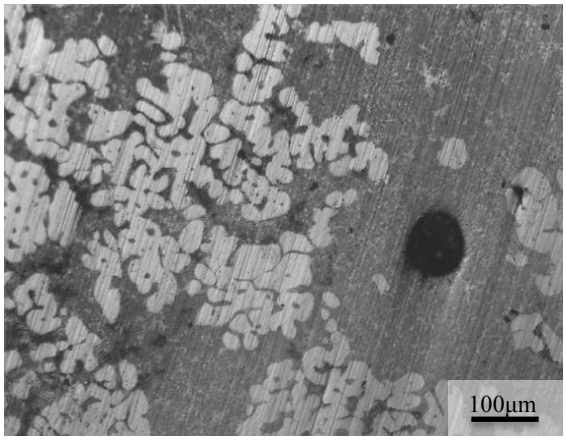

Figure 56: Optical micrograph showing liquid segregation in the edge of thixoforged part containing 3wt. %SiC at 50% solid fraction

Figure 57 shows the surface roughness values for the thixoforged nanocomposite samples at distance 20mm away from the center. Both top and bottom surface of the part is evaluated for roughness. The roughness in case of samples with SiC reinforcement showed higher values due to difference in solidification of the part resulting from nanoparticles. Also the region at the center solidifies faster and is in contact with the die for longer portion compared to regions away from the center. Hence the roughness value of the region at the center is less than the region away from center. The surface roughness values remain constant for the entire sample at the center. However the roughness deteriorated gradually away from center. The increase in roughness with distance can be seen for a thixoforged A356 alloy at different semi-solid temperatures in Fig. 58.

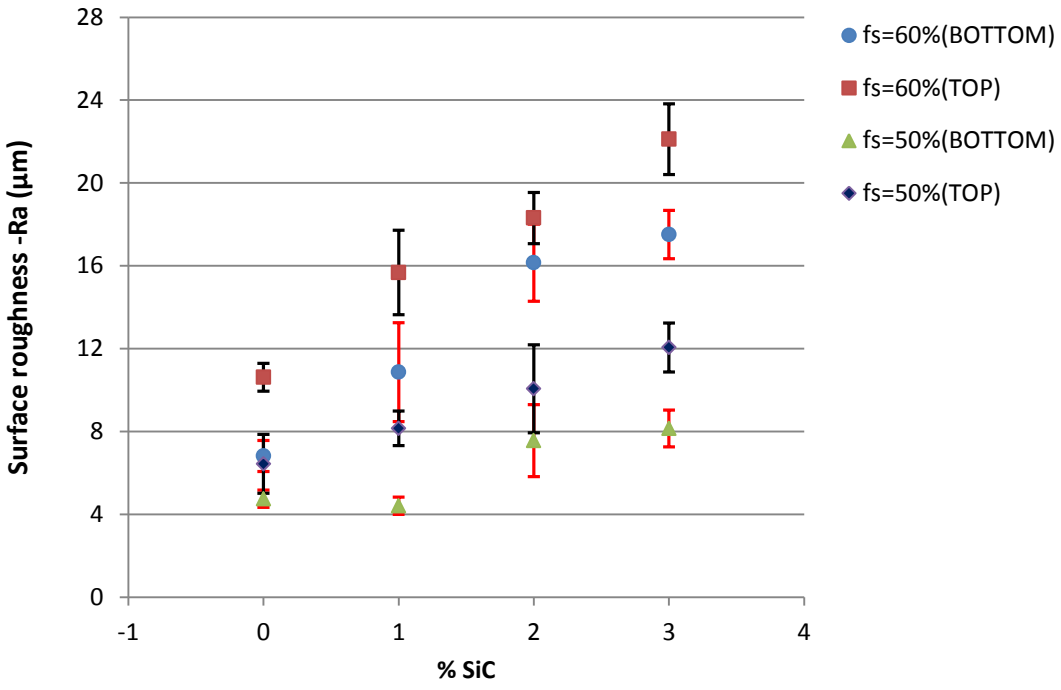

Figure 57: Surface roughness values of aluminum nanocomposite at distance 20mm from the center of thixoforged part

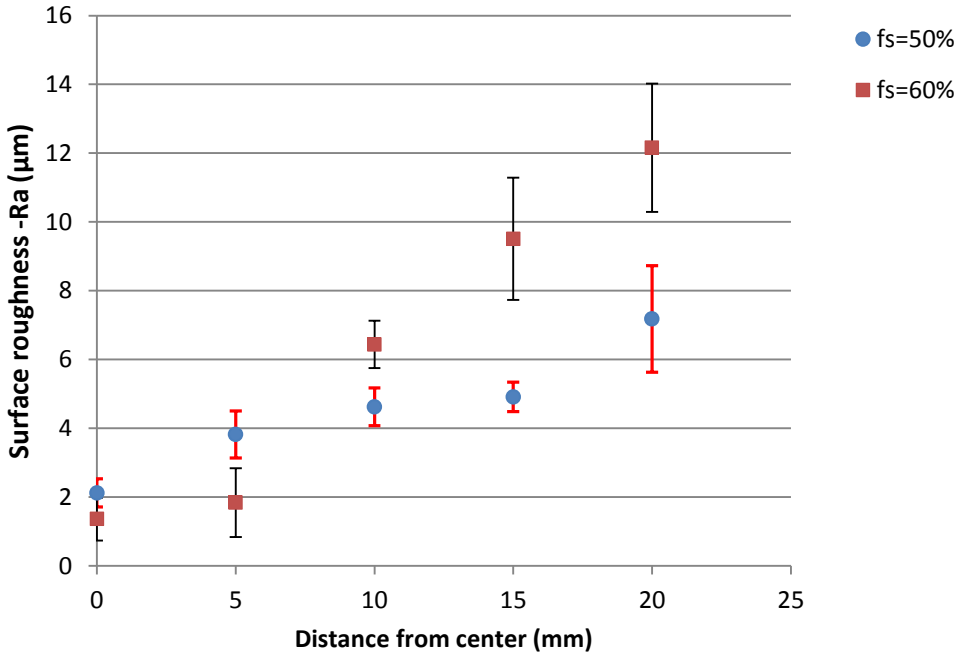

Figure 58: Surface roughness values of thixoforged A356 with distance from the center of the thixoforged part

4.4 General Discussion

Aluminum nanocomposite using aluminum alloy A356 as matrix was synthesized using stir casting technique by ultrasonically dispersing nano sized silicon carbide (SiC_p) at different weight percentages. The ultrasonication of melt was carried at temperature of 700^{o}C for 15 minutes before finally pouring it in a die preheated to 200^{o}C. Incorporation of reinforcement inside the melt was done by preheating the particles to 900^{o}C and adding it in the vortex created by a mechanical stirrer. Furthermore, for thixoforging operation, billets of nanocomposites synthesized from stir casting with ultrasonic treatment were used as a feedstock. Thixoforging is carried by reheating these billets

using induction heating device to semi-solid temperatures corresponding to solid fractions of 60% and 50%. Two heating regimes in the induction heating of billets were utilized with holding time of 1 and 2 minutes. The mushy billet after induction heating was quickly transferred to a die and pressed with ram speed of 12mm/sec and die temperature of 350^{o}C.

It is worth mentioning that in evaluating the results of stir casting, thixoforging and their characterization, all parameters were kept constant to compare between the monolithic alloy and reinforced alloy. Below are some of the observations from the work.

- **Microstructure Characterization**

The microstructure of stir cast A356 and its nanocomposites analyzed from optical study and SEM differed after thixoforging operation. In the stir casting process the monolithic alloy and its nanocomposite unlike typical casting microstructure shows near non-dendritic structure due to the effects of ultrasonication and inclined pouring method which acted as a cooling slope before solidification inside the die. Other studies [55, 62] also obtained similar microstructure using ultrasonic stir casting technique.

Good distribution of SiC particles was obtained in the nanocomposite samples. The SiC particles were incorporated and entrapped into the interdendritic regions or grain boundary interface developed during solidification. At higher SiC content clusters were seen and tendency of particle clustering was directly related to the ultrasonic intensity. Higher ultrasonic intensity of 80W/cm^2 was able to break the SiC clusters efficiently; however with 2wt. % and 3wt. % SiC, clustering was persistent. Therefore it can be stated that with higher SiC content, the intensity of ultrasonication should be increased

more than 80W/cm^2 in order to impart more cavitation effect on the particles. Similar behavior was observed in other studies were clustering was persistent and nanoparticles are entrapped at the grain boundaries [57, 58, 60].

The near non-dendritic microstructure due to ultrasonic effect obtained in the as cast samples aided in the evolution of globular microstructure during induction heating. It is observed that the size of globules/primary phase decreased with increase in SiC content. This is attributed to the grain refinement obtained from the stir cast samples of nanocomposite which aided in the evolution of primary phase to relatively small size compared to its monolithic alloy. Similar hypothesis was made by Wang et.al, [69] where the morphology of microstructure after reheating and isothermal holding was directly related to the microstructure obtained in the prior solidification. The spheroidization of these primary phases also increased with the holding time.

After thixoforging process, the microstructure and distribution of nanoparticles was changed. The process of forging mushy rectangular billet to a flat plate was not performed before; therefore its microstructure cannot be correlated. In this study, it is observed that during thixoforging inside the die the material was severely deformed resulting in inhomogeneous distribution of phases. At the center of thixoforged part primary phase was predominant and consequently most of the secondary phase (eutectic) and SiC particles were moved away from the center. Similar observation was made by Wang et.al [27] during thixoforging of A356/SiC packaging shell. This distribution of phases after thixoforging has to be optimized by invariably using higher ram velocity and punch force.

- **Mechanical Behavior**

The properties of the component formed after thixoforging are dependent on the fraction solid, size, distribution and morphology of solid particles and secondary phases within the liquid matrix. The fraction solid is controlled by the temperature whereas other features are a function of isothermal holding time and flow of slurry inside the forging die. On the other hand the mechanical behavior of nanocomposite is also greatly affected by the reinforcement content, its distribution after stir casting and thixoforging process.

From the hardness results after ultrasonic stir casting, it was observed that as ultrasonic intensity is increased the densification and Vickers's hardness values also increased. This is attributed to the higher cavitation and dispersing effect of ultrasonication. For nanocomposite the hardness is increased with the reinforcement content from 1 to 3wt. % with gradual decrease in densification. The higher degree of defects and micro porosity observed at higher SiC fraction as seen in optical and SEM micrographs is the result of increased amount of interface area. The increment in hardness is attributed to the refined structure and consequently reduced grain size of nanocomposite with increase in SiC content. The SiC particles will also act as obstacles to the motion of dislocation thereby increasing the hardness. Similar trend is observed in the thixoforged samples where the porosity and hardness of nanocomposite part also increased with increase in SiC content. The hardness in samples thixoforged at 50% solid fraction was more compared to 60% due to fine microstructure and more amount of secondary phase. Due to lack of holding time and consequently incomplete globurization, the samples with holding time of 1min. showed lower hardness and higher porosity.

From Tensile results, it is observed that the strength and ductility of nanocomposites is drastically reduced due to the clustering of SiC particles at higher reinforcement content. In case of cast samples, the region for crack growth is eutectic phase; therefore the brittle reinforcement particles agglomerating at these regions will further augment the drop in ductility and strength. The sample containing 1wt. % SiC showed increment in strength and ductility after T6 heat treatment while sample with 2 and 3wt. % SiC showed decrease in tensile properties even after heat treatment. The microscopic responses in the nanocomposite like particle cracking, interface debonding and void formation in the matrix are the main reasons for the brittle fracture and, hence, are responsible for the low strength and ductility of the nanocomposite material.

Higher tensile strength was observed in nanocomposite with 1wt. % SiC at 60% solid fraction after thixoforging due to homogenous distribution of phases relative to 50% solid fraction wherein shrinkage and segregation defects were observed. However at higher SiC content the tensile results remained low due to addition of SiC clustering element. Highest ductility of 27% was achieved for monolithic alloy thixoforged at 50% solid fraction. Increase in ductility was more in samples containing 50% solid fraction and reheated with 2min. holding time, this is attributed to higher shape factor and lower size of primary phase resulting in more dense and homogenous microstructure after thixoforging and consequently due to the transition of fracture mode to intergranular. Similar trend in results were obtained by other studies wherein the increase in holding time and semi-solid temperature resulted in higher tensile properties due to reduction in equivalent diameter of primary phase and increase in the roundness or shape factor [31, 32, 36, 70].

CHAPTER 5

CONCLUSIONS AND RECOMMENDATIONS

5.1 Conclusions

Aluminum alloy matrix reinforced with nanosized SiC particles were synthesized using ultrasonic stir casting technique using two different ultrasonic intensities of 40W/cm^2 and 80W/cm^2. The stir cast billets were induction heated and thixoforged to two different solid fractions of 60%, 50% and with holding time of 1 and 2 minutes. The effect of these processes and secondary phase concentration on the resulting microstructure and mechanical behavior were elucidated. The following specific conclusions can be drawn:

- The incorporation of SiC particles in the molten metal was achieved by preheating the particles and adding them in the vortex created by mechanical stirrer at temperature close to the liquidus before ultrasonication.
- A reasonable dispersion of SiC reinforcement was obtained after stir casting by using 80W/cm^2 ultrasonic intensity. Some agglomeration was observed at the grain boundaries during solidification.
- Induction heating to solid fraction of 50% with intermediate power and holding time of 2 minutes resulted in better reheating condition for thixoforging. The shape factor attained a value of up to 0.8 in some regions.

- The microstructure of nanocomposite evolved from non-dendritic rosette like structure in stir cast samples to near globular morphology after induction heating. The size of these globules decreased with increase in SiC content.
- The microstructure of thixoforged part showed more amount of secondary phases located away from the center and consequently less SiC particles were observed at the center of thixoforged part.
- Thixoforging nanocomposites with solid fraction of 50% and holding time of 2 min. gave complete die filling, high densification and better surface quality in the thixoforged part.
- Increase in hardness was observed with increase in amount of reinforcement content in the stir cast and thixoforged samples. The hardness in the thixoforged part remained low at the center and increased towards the edge.
- Tensile results of nanocomposite showed decrease in tensile properties with SiC content more than 2wt. %. Higher properties were observed in nanocomposite with 1wt. % SiC stir casted with 80W/cm^2 after T6 heat treatment. Similarly in the thixoforged part tensile strength of nanocomposite with 1wt. % SiC was found to be higher at 60% solid fraction.
- The ductility of nanocomposite improved after thixoforging operation. Highest ductility of 27% was obtained for the monolithic alloy samples reheated to solid fraction of 50% and holding time of 2 min. in the reheating condition.

5.2 Recommendations

Some of the beneficial recommendations and scope for future work related to present experiments are highlighted below:

- The ultrasonic stir casting parameters can be thoroughly studied to optimize the process for better dispersion of nanoparticles where agglomeration is still an issue.
- Parametric study related to thixoforging of nanocomposite can be performed to evaluate the effect of nanoparticles on the forging parameters like load, time etc.
- Thixoforging of semi-solid billet with higher solid fraction can be studied with the use of higher ram velocity and forging load.
- Investigation of compressive and tribological behavior of nanocomposite after thixoforging would be useful as this process is used for making intricate components in structural applications.
- Computer simulations would be helpful in predicting the die filling behavior of semi-solid billet in the forging die and optimizing the thixoforging process.

References

[1] T.W. Clyne, P.J. Withers, "An Introduction to Metal Matrix Composites", Cambridge University Press, Cambridge, UK, 1995

[2] K.U. Kainer, "Metal Matrix Composites: Custom-made Materials for Automotive and Aerospace Engineering', Wiley-VCH, 2006.

[3] W. . Miller, L. Zhuang, J. Bottema, a. . Wittebrood, P. De Smet, a Haszler, and a Vieregge, "Recent development in aluminium alloys for the automotive industry," Materials Science and Engineering: A, vol. 280, no. 1, pp. 37–49, Mar. 2000.

[4] N. Al-Aqeeli, G. Mendoza-Suarez, C. Suryanarayana, R.A.L. Drew, "Development of new Al-based nanocomposites by mechanical alloying". Materials Science and Engineering: A, Volume 480, Issues 1-2, pages 392-396 و 15 May 2008.

[5] R. K. and R. A. R. P. V. Evans, "Squeeze casting of aluminium alloys for near net shape manufacturing," Materials and Design, vol. 17, pp. 7–9, 1993.

[6] C. Y. CHEN, "Thixoforging of Aluminum Alloys," Materials Science and Engineering, vol. 40, pp. 265–272, 1979.

[7] A. Wolf and D. J. Baur, "Thixoforging." pp. 1–24, 2001.

[8] H. V. A. Sinan Kandemir, "Production of Aluminum Matrix Nanocomposite feedstock for Thixoforming by an Ultrasonic Method," Key Engineering Materials, vol. 504–506, no. 2012, pp. 339–344, 2012.

[9] T. Moons, P. Ratchev, P. De Smet, B. Verlinden, P. Van Houtte, "A comparative study of two Al---Mg---Si alloys for automotive applications". Scripta Materia, Volume 35, Issue 8, pages 939-945, 15 October 1996.

[10] Hirt, G., R. Cremer, T. Witulski and H.C. Tinius, "Lightweight Near Net Shape Components Produced by Thixoforming", Materials & Design, Vol. 18, pp. 315-321, 1997.

[11] M. S. Salleh, M. Z. Omar, J. Syarif, and M. N. Mohammed, "An Overview of Semisolid Processing of Aluminium Alloys," ISRN Materials Science, vol. 2013, pp. 1–9, 2013.

[12] J. Baur, "Recent developments in thixoforging," in Proceedings of ICEME, pp. 1– 8, 2000.

[13] R. Kopp, D. Neudenberger, and G. Winning, “Different concepts of thixoforging and experiments for rheological data,” Journal of Materials Processing Technology, vol. 111, no. 1–3, pp. 48–52, Apr. 2001.

[14] Kapranos, P., P.J. Ward, H.V. Atkinson and D.H. Kirkwood, “Near Net Shaping by Semi-solid Metal Processing”, Materials and Design, Vol. 21, pp. 387-394, 2000.

[15] H. Jiang, T. H. Nguyen, and M. Prud’homme, “Optimal control of induction heating for semi-solid aluminum alloy forming,” Journal of Materials Processing Technology, vol. 189, no. 1–3, pp. 182–191, Jul. 2007.

[16] H. Jung, “The induction heating process of semi-solid aluminium alloys for thixoforming and their microstructure evaluation,” Journal of Materials Processing Technology, vol. 105, no. 1–2, pp. 176–190, Sep. 2000.

[17] T.W. Clyne, P.J. Withers, “An Introduction to Metal Matrix Composites”, Cambridge University Press, Cambridge, UK, 1995.

[18] J. Hashim, L. Looney, and M. S. . Hashmi, “Metal matrix composites: production by the stir casting method,” Journal of Materials Processing Technology, vol. 92–93, pp. 1–7, Aug. 1999.

[19] G. I. Eskin, “Broad prospects for commercial application of the ultrasonic (cavitation) melt treatment of light alloys.,” Ultrasonics sonochemistry, vol. 8, no. 3, pp. 319–25, Jul. 2001.

[20] X. Li and Y. Yang, “Theoretical and experimental study on ultrasonic dispersion of nanoparticles for strengthening cast Aluminum Alloy A356,” Metall Sci Technol, vol. 26, 2008.

[21] Y. Saberi, S.M. Zebarjad, G.H. Akbari, ‘On the role of nano-size SiC on lattice strain and grain size of Al/SiC nanocomposite‘, Journal of Alloys and Compounds, Volume 484, Issues 1-2, pages 637-640, 18 September 2009.

[22] N. Zhao, P. Nash, X. Yang, _The effect of mechanical alloying on SiC distribution and the properties of 6061 aluminum composite‘. Journal of Materials Processing Technology, Volume 170, Issue 3, 30 December 2005, Pages 586-592.

[23] A. Mazahery and M. O. Shabani, “Characterization of cast A356 alloy reinforced with nano SiC composites,” Transactions of Nonferrous Metals Society of China, vol. 22, no. 2, pp. 275–280, Feb. 2012.

[24] Wang, Zhirui, Zhang, Ruby J, “Mechanical Behavior of Cast Particulate SiC / AI (A356) Metal Matrix Composites,” Metallurgical Transactions, vol. 22A, pp. 1585-1593, July 1991.

[25] Kenney, M.P., J.A. Courtois, R.D. Evans, G.M. Farrior, C.P. Kyonka, A.A. Koch and K.P. Young, "Semisolid Metal Casting and Forging", Metals Handbook,Ninth Edition, Vol.15, pp. 327-338, 1998.

[26] Fan, Z., "Semi-solid Metal Processing", International Materials Reviews, Vol. 47, No. 2, pp. 49-85, 2002

[27] Kirkwood, D. H., "Semi-solid Metal Processing", International Materials Reviews,Vol.39, No. 5, pp. 173-189, 1994

[28] David H. Kirkwood, "Semi-solid Processing of Alloys", Springer series in material science, 2010

[29} Kopp, R., T. Bremer, H.P. Mertens, D. Neudenberger and G. Winning, "Thixoforging of Aluminum Alloys with a Hydraulic Forging Press", Proceedings ofInternational Conference on Competitive Advantages by Near-Net-Shape Manufacturing, 1997, http://www.rwthaachen.de/sfb289/Wv/ pdf/pub_ibf_ nearnetshape97.pdf

[30] K. Wang, Y. Kang, P. Song, F. Xu, and X. Li, "Preparation of SiCp/A356 electronic packaging materials and its thixo-forging," Transactions of Nonferrous Metals Society of China, vol. 20, pp. s988–s992, Sep. 2010.

[31] W Cho and C. Kang, "Mechanical properties and their microstructure evaluation in the thixoforming process of semi-solid aluminum alloys," Journal of Materials Processing Technology, vol. 105, no. 3, pp. 269–277, Sep. 2000.

[32] E. R. De Freitas, E. G. Ferracini Júnior, V. P. Piffer, and M. Ferrante, "Microstructure, material flow and tensile properties of A356 alloy thixoformed parts," Materials Research, vol. 7, no. 4, pp. 595–603, Dec. 2004.

[33] G. Vaneetveld, A. Rassili, J. C. Pierret, and J. Lecomte-Beckers, "Improvement in Thixoforging of 7075 Aluminium Alloys at High Solid Fraction," Solid State Phenomena, vol. 141–143, pp. 707–712, 2008.

[34] C. Kang and H. Jung, "A study on solutions for avoiding liquid segregation phenomena in thixoforming process: Part II. Net shape manufacturing of automotive scroll component," Metallurgical and Materials Transactions B, vol. 32, February, pp. 129–136, 2001

[35] S. Chayong, H. V. Atkinson, and P. Kapranos, "Thixoforming 7075 aluminium alloys," Materials Science and Engineering: A, vol. 390, no. 1–2, pp. 3–12, Jan. 2005.

[36] S. Tahamtan and a. Fadavi Boostani, “Microstructural characteristics of thixoforged A356 alloy in mushy state,” Transactions of Nonferrous Metals Society of China, vol. 20, no. May, pp. 781–787, Sep. 2010.

[37] Kapranos, P., R. C. Gibson, D. H. Kirkwood and C. M. Sellars, “Induction Heating and Partial Melting of High Melting Point Thixoformable Alloys”, Proceedings of the 4th International Conference on Semi-solid Processing Alloys and Composites, 1996.

[38] H.Jung, “The induction heating process of semi-solid aluminium alloys for thixoforming and their microstructure evaluation,” Journal of Materials Processing Technology, vol. 105, no. 1–2, pp. 176–190, Sep. 2000.

[39] H. Jung and C. Kang, “Induction heating process of an Al–Si aluminum alloy for semi- solid die casting and its resulting microstructure,” Journal of Materials Processing Technology, vol. 120, no. 1–3, pp. 355–364, Jan. 2002.

[40] J. Choi, H. Park, and B. Kim, “The influence of induction heating on the microstructure of A356 for semi-solid forging,” Journal of Materials Processing Technology, vol. 87, pp. 46–52, 1999.

[41] H. Lakshmi, M. C. Vinay Kumar, P. Kumar, V. Ramanarayanan, K. S. S. Murthy, and P. Dutta, “Induction reheating of A356.2 aluminum alloy and thixocasting as automobile component,” Transactions of Nonferrous Metals Society of China, vol. 20, pp. s961–s967, Sep. 2010.

[42] S. Zinn and S. L. Semiatin, “Elements of Induction Heating: Design, control and applications,” ASM International, 1988

[43] Y. P. Jeon and C. G. Kang, “Reheating process for thixoforging of metal matrix composites fabricated by induction heating and the,” Proc. Instn Mech. Engrs, vol. 217 Part B, pp. 1383–1391, 2003.

[44] C. Kang and S. Youn, “Mechanical properties of particulate reinforced metal matrix composites by electromagnetic and mechanical stirring and reheating process for thixoforming,” Journal of Materials Processing Technology, vol. 147, no. 1, pp. 10–22, Mar. 2004.

[45] C.Kang and S.Youn, “Mechanical properties of particulate reinforced metal matrix composites by electromagnetic and mechanical stirring and reheating process for thixoforming,” Journal of Materials Processing Technology, vol. 147, no. 1, pp. 10–22, Mar. 2004.

[46] N. Haghdadi,A.Zarei-Hanzaki,S.Heshmati-Manesh,H.R.Abedi , S.B.Hassas-Irani, “The semisolid microstructural evolution of a severely deformed A356 aluminum alloy,” Materials and Design, vol. 49, page no. 878–887, 2013

[47] Tzimas, E. and A. Zavaliangos, "A Comparative Characterization of Near-equiaxedMicrostructures as Produced by Spray Casting, Magnetohydrodynamic Casting andthe Stress Induced, Melt Activated Process", Materials Science and Engineering, Vol.A289, pp. 217-227, 2000.

[48] Haga, T. and S. Suzuki, "Casting of Aluminium Alloy Ingots for Thixoforming Using a Cooling Slope", Journal of Materials Processing Technology, Vol. 118, pp.169-172, 2001.

[49] S. Zhang, Y. Zhao, X. Cheng, G. Chen, and Q. Dai, "High-energy ultrasonic field effects on the microstructure and mechanical behaviors of A356 alloy," Journal of Alloys and Compounds, vol. 470, no. 1–2, pp. 168–172, Feb. 2009.

[50] G. I. Eskin, "Broad prospects for commercial application of the ultrasonic (cavitation) melt treatment of light alloys." Ultrasonics sonochemistry, vol. 8, no. 3, pp. 319–25, July. 2001.

[51] G. Eskin, "Cavitation mechanism of ultrasonic melt degassing," Ultrasonics Sonochemistry, vol. 2, no. 2, pp. S137–S141, Jan. 1995.

.

[52] H. Xu, X. Jian, T. T. Meek, and Q. Han, "Degassing of molten aluminum A356 alloy using ultrasonic vibration," Materials Letters, vol. 58, no. 29, pp. 3669–3673, Nov. 2004.

[53] G. Eskin, "Principles of ultrasonic treatment: Application for light alloys melts," Advanced Performance Materials, vol. 232, pp. 223–232, 1997

[54] X. Jian, T. T. Meek, and Q. Han, "Refinement of eutectic silicon phase of aluminum A356 alloy using high-intensity ultrasonic vibration," Scripta Materialia, vol. 54, no. 5, pp. 893–896, Mar. 2006.

[55] X. Jian, H. Xu, Q. Han, "Effect of power ultrasound on solidification of aluminum A356 alloy," Materials Letters, Vol. 59, page no. 190– 193, 2005

[56] Z. Zhou, W and Xu, "Casting of SiC reinforced metal matrix composites," Journal of materials processing technology, vol. 63, no. 1997, pp. 358–363, 1997.

[57] K. B. Nie, X. J. Wang, K. Wu, L. Xu, M. Y. Zheng, and X. S. Hu, "Processing, microstructure and mechanical properties of magnesium matrix nanocomposites fabricated by semisolid stirring assisted ultrasonic vibration," Journal of Alloys and Compounds, vol. 509, no. 35, pp. 8664–8669, Sep. 2011.

[58] Y. Yang, J. Lan, and X. Li, "Study on bulk aluminum matrix nano-composite fabricated by ultrasonic dispersion of nano-sized SiC particles in molten aluminum alloy," Materials Science and Engineering: A, vol. 380, no. 1–2, pp. 378–383, Aug. 2004.

[59] X. Li and Y. Yang, "Theoretical and experimental study on ultrasonic dispersion of nanoparticles for strengthening cast Aluminum Alloy A356," Metall Sci Technol, vol. 26, 2008.

[60] S. Donthamsetty, N. Damera, and P. Jain, "Ultrasonic Cavitation Assisted Fabrication and Characterization of A356 Metal Matrix Nanocomposite Reiforced with Sic, B4C, CNTs," aijstpme.kmutnb.ac.th, vol. 2, pp. 27–34, 2009

[61] W. Z. Li, S. Y. Liu, Q. Y. Zhang, and X. Zhu, "Untrasonic-Assisted Fabrication of SiC Nanoparticles Reinforced Aluminum Matrix Composites," Materials Science Forum, vol. 654–656, pp. 990–993, Jun. 2010.

[62] H. V. Atkinson. Sinan Kandemir,"Production of Aluminum Matrix Nanocomposite feedstock for Thixoforming by an Ultrasonic Method," Key Engineering Materials, vol. 504–506, no. 2012, pp. 339–344, 2013.

[63] J. Hashim, L. Looney, and M. S. . Hashmi, "Metal matrix composites: production by the stir casting method," Journal of Materials Processing Technology, vol. 92–93, pp. 1–7, Aug. 1999.

[64] J. Hashim, L. Looney, and M. S. J. Hashmi, "The wettability of SiC particles by molten aluminium alloy," Journal of Materials Processing Technology, vol. 119, no. 1–3, pp. 324–328, Dec. 2001.

[65] Subhranshu Chatterjee, and Amitava Basu Mallick, "Challenges in manufacturing aluminium based metal matrix nanocomposites via stir casting route", Materials Science Forum Vol. 736, pp 72-80, 2013.

[66] ASTM E-8M-04 Standard, "Standard Test Methods for Tension Testing of Metallic Materials", 2004.

[67] ASTM B-917M-01 Standard, "Standard Practice for Heat Treatment of Aluminum Alloy Castings from All Processes", 2001.

[68] D. B. Spencer; PhD thesis, MIT, Cambridge, MA, 1971.

[69] H. Wang, C.J. Davidson and D.H. St John "Semisolid microstructural evolution of AlSi7Mg alloy during partial remelting", Materials Science and Engineering A368, pp. 159–167, 2004

[70] C.G. Kang, S.W. Youn, and P.K. Seo, "The Effect of Globular MicrostructureSize on the Mechanical Properties in Reheating Process of Aluminum Alloys" ASM International, JMEPEG ,13:172-184, 2004

Vitae

Name	Mohammed Abdul Azeem
Nationality	Hyderabad, INDIA
Date of Birth	13-12-1988
Email	abdulazeem4640@gmail.com
Academic Background	M.S (Mechanical Engineering) December 2013
	Specialization in Applied Materials and Manufacturing
	King Fahd University of Petroleum and Minerals, Dhahran, Saudi Arabia
	B.E (Mechanical Engineering) September 2010
	Osmania University, Hyderabad, India